NASA/TM–20240012679
NESC-RP-21-01639

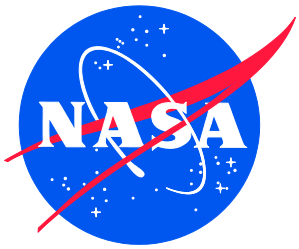

NESC Ceramic Oxygen Generator (COG) Technology Development

John C. Graf
Johnson Space Center, Houston, Texas

Jeffry W. Stevenson
Pacific Northwest National Lab (retired), Richland, Washington

October 2024

NASA STI Program Report Series

Since its founding, NASA has been dedicated to the advancement of aeronautics and space science. The NASA scientific and technical information (STI) program plays a key part in helping NASA maintain this important role.

The NASA STI program operates under the auspices of the Agency Chief Information Officer. It collects, organizes, provides for archiving, and disseminates NASA's STI. The NASA STI program provides access to the NTRS Registered and its public interface, the NASA Technical Reports Server, thus providing one of the largest collections of aeronautical and space science STI in the world. Results are published in both non-NASA channels and by NASA in the NASA STI Report Series, which includes the following report types:

- TECHNICAL PUBLICATION. Reports of completed research or a major significant phase of research that present the results of NASA Programs and include extensive data or theoretical analysis. Includes compilations of significant scientific and technical data and information deemed to be of continuing reference value. NASA counterpart of peer-reviewed formal professional papers but has less stringent limitations on manuscript length and extent of graphic presentations.

- TECHNICAL MEMORANDUM. Scientific and technical findings that are preliminary or of specialized interest, e.g., quick release reports, working papers, and bibliographies that contain minimal annotation. Does not contain extensive analysis.

- CONTRACTOR REPORT. Scientific and technical findings by NASA-sponsored contractors and grantees.

- CONFERENCE PUBLICATION. Collected papers from scientific and technical conferences, symposia, seminars, or other meetings sponsored or co-sponsored by NASA.

- SPECIAL PUBLICATION. Scientific, technical, or historical information from NASA programs, projects, and missions, often concerned with subjects having substantial public interest.

- TECHNICAL TRANSLATION. English-language translations of foreign scientific and technical material pertinent to NASA's mission.

Specialized services also include organizing and publishing research results, distributing specialized research announcements and feeds, providing information desk and personal search support, and enabling data exchange services.

For more information about the NASA STI program, see the following:

- Access the NASA STI program home page at http://www.sti.nasa.gov

- Help desk contact information:

https://www.sti.nasa.gov/sti-contact-form/
and select the "General" help request type.

NASA/TM–20240012679
NESC-RP-21-01639

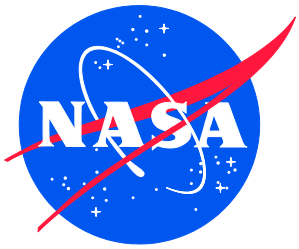

NESC Ceramic Oxygen Generator (COG) Technology Development

John C. Graf
Johnson Space Center, Houston, Texas

Jeffry W. Stevenson
Pacific Northwest National Lab (retired), Richland, Washington

National Aeronautics and
Space Administration

Langley Research Center
Hampton, Virginia 23681-2199

October 2024

Acknowledgments

The NESC assessment team acknowledges the peer reviewers of this report, including Morgan Abney, Timothy Brady, Steven Gentz, Gregory Harrigan, Bryan McEnerney, and Joel Sills. The technical material included in the appendices was provided by Steven Hornung (White Sands Test Facility (WSTF)) and Dale Taylor (American Oxygen).

Available from:

NASA STI Program / Mail Stop 050
NASA Langley Research Center
Hampton, VA 23681-2199

NASA Engineering and Safety Center (NESC)
Technical Assessment Final Report

NESC Ceramic Oxygen Generator (COG)
Technology Development

TI-21-01639

July 9, 2024

Report Approval and Revision History

NOTE: This document was submitted to the NESC Director for out-of-board approval on July 9, 2024, for configuration control.

Approved: Timmy Wilson Digitally signed by Timmy Wilson Date: 2024.09.17 11:25:49 -04'00'

NESC Director

Version	Description of Revision	Office of Primary Responsibility	Effective Date
1.0	Initial Release	Jon P. Haas, NESC Principal Engineer, WSTF	7/9/2024

Table of Contents

List of Figures

List of Tables

List of Appendices

Technical Assessment Report

1.0 Notification and Authorization

The NASA Engineering and Safety Center (NESC) was asked to support development and advancement of ceramic oxygen generator (COG) technology for NASA and COVID[1]-related medical use (i.e., medical-COG (M-COG)). NASA's Advanced Exploration Systems Program has previously sponsored COG technology development activities for spacesuit oxygen tank recharge. The intent of this assessment was to accelerate the pace of technology development, assess the use of NASA technology for medical applications, and validate manufacturing techniques. Under this assessment, the M-COG project developed and tested five full-scale (i.e., 30-wafer) cell stacks and performed testing via a prototype unit.

Mr. Clinton Cragg (retired) was selected to lead this assessment, with Mr. Jon Haas as deputy co-lead, and Mr. John Graf as the technical lead. The key stakeholders included NASA's Chief Medical Officer; the Bureau of Global Health under the United States Agency for International Development (USAID); the NASA Extravehicular Activity (EVA) Office, and the Johnson Space Center (JSC) Engineering Directorate.

[1] COVID-19, the 2019 novel coronavirus, causes severe acute respiratory syndrome 2, or SARS-CoV-2. For the purposes of this report, COVID-19 will be referred to as COVID.

2.0 Signatures

Submitted by: NESC Lead

JON HAAS Digitally signed by JON HAAS Date: 2024.07.23 08:56:35 -06'00'

Mr. Jon P. Haas

Concurrence:

Morgan Abney Digitally signed by Morgan Abney Date: 2024.07.19 13:32:40 -05'00'

Dr. Morgan B. Abney, NASA Technical Fellow for Environmental Control and Life Support Systems

Bryan McEnerney Digitally signed by Bryan McEnerney Date: 2024.07.19 09:46:36 -07'00'

Dr. Bryan W. McEnerney, NASA Technical Fellow for Materials

Significant Contributors:

John Graf Digitally signed by John Graf Date: 2024.07.19 11:20:37 -05'00'

Dr. John C. Graf

Email concurrence attached, 7/19/2024

Dr. Jeffry W. Stevenson

Signatories declare the findings, observations, and NESC recommendations compiled in the report are factually based from data extracted from program/project documents, contractor reports, and open literature, and/or generated from independently conducted tests, analyses, and inspections.

3.0 Team Members

Name	Discipline	Organization
Core Team		
Clint Cragg	NESC Lead, retired	LaRC
Jon Haas	NESC Co-lead	WSTF
John Graf	Technical Lead	JSC
Bryan McEnerney	NESC Lead, Final Report Preparation, 2024	LaRC
Michael Casteel	System Engineer	JSC/Jacobs Technology
Steve Fitzgerald	Thermal Fluids Analyst	Principium Plus Solution
Damir Ljubanovic	Electrical Engineer	GRC
Fred Lutfy	Mechanical Engineer	JSC/Jacobs Technology
Fernando Pellerano	Chief Engineer	GSFC
Dan Rybicki	Materials and Processes Engineer	JSC/Jacobs Technology
Marta Shelton	Electrical/Systems Engineer	WFF
Jeff Stevenson	Electrochemical Ceramics	Pacific Northwest National Laboratory (retired)
Jonathan Tylka	O_2 Systems/Test Engineer	WSTF
Virginia Ward	O_2 Systems/Test Engineer	WSTF
Mark Weislogel	Thermal Fluids Analyst	IRPI LLC
Jason Bermudez	Oxygen Generation/Manufacture	American Oxygen LLC
Joseph Fellows	Oxygen Generation/Manufacture	American Oxygen LLC
Kenny Ho	Oxygen Generation/Manufacture	American Oxygen LLC
Ziyang Jiang	Oxygen Generation/Manufacture	American Oxygen LLC
Chad Lee	Oxygen Generation/Manufacture	American Oxygen LLC
Zhipeng Nan	Oxygen Generation/Manufacture	American Oxygen LLC
Dale Taylor	Oxygen Generation/Manufacture	American Oxygen LLC
Tom Taylor	Oxygen Generation/Manufacture	American Oxygen LLC
True Thatcher	Oxygen Generation/Manufacture	American Oxygen LLC
Thomas Tyler	Oxygen Generation/Manufacture	American Oxygen LLC
Forrest Erickson	Control Systems	Public Invention
Lawrence Kincheloe	Control Systems	Public Invention
Geoff Mulligan	Control Systems	Public Invention
Robert Read	Control Systems	Public Invention
Consultants		
Catherine Christiansen	Food and Drug Administration (FDA) Certification	JPL
Christopher Yahnker	Group Supervisor	JPL
Business Management		
Michelle Bamford	Program Analyst	LaRC/MTSO
Assessment Support		
Betty Trebaol	Project Coordinator	LaRC/AMA
Linda Burgess	Planning and Control Analyst	LaRC/AMA
Jonay Campbell	Technical Editor	LaRC/AS&M

3.1 Acknowledgments

The NESC assessment team acknowledges the peer reviewers of this report, including Morgan Abney, Timothy Brady, Steven Gentz, Gregory Harrigan, Bryan McEnerney, and Joel Sills. The technical material included in the appendices was provided by Steven Hornung (White Sands Test Facility (WSTF)) and Dale Taylor (American Oxygen).

4.0 Executive Summary

The Medical Ceramic Oxygen Generator (M-COG) extracts oxygen from air, producing high-purity (>99.9%) oxygen. This report provides background on the initial technology development and describes NASA's efforts for spacesuit application [ref. 1] and, more recently, the NASA Engineering and Safety Center's (NESC's) effort to accelerate the development of M-COG technology as a contributing solution to the medical oxygen shortage during the COVID pandemic.

At the start of the NESC M-COG assessment, oxygen generation using ion transport membranes was restricted to low technology readiness level (TRL) research and development (R&D) efforts. The technology, at that time, did not include the manufacturing capability to build cell stacks at the production scale needed for medical oxygen, and ion transport membranes could not produce oxygen at the delivery pressure needed for spacesuit oxygen tank recharge. Over the course of the M-COG assessment, full-scale cell stacks were manufactured and tested. New methods of thermal management were prototyped and tested, demonstrating substantial improvements in energy efficiency, and high-pressure oxygen generation was achieved. The net result of the effort was an advancement in the TRL.

The M-COG assessment team designed, developed, and tested systems purely for ground testing; these systems were not optimized for crewed flight and will require additional testing to ensure safe operation in flight. The M-COG high-pressure prototype system operates at low production rates, but the key technical issues of cell stack pressure integrity and pressure vessel integration were addressed via testing. The M-COG prototype systems are small scale compared with medical oxygen needs, and the prototypes are not certified for medical use, thus are not currently suitable for use in hospitals. The key technical issues of manufacturing capability and power efficiency were addressed through direct demonstration. The assessment team developed prototype systems that can be loaned to health organizations for hospital field testing.

Conclusions and NESC Recommendations

The M-COG produced oxygen at a production rate of 4.5 standard liters per minute (slpm) from a single cell stack, where no previous ion transport membrane cell stack has produced more than 2.0 slpm. M-COG had a specific energy use of 87 watts (W) per slpm, where no previous ion transport membrane system has used less than 200 W per slpm. The M-COG assessment team developed a system capable of steady-state operations without heater power.

M-COG produced 20.7 megapascals (MPa) (3000 pounds per square inch gauge (psig)) of oxygen [ref. 2]. M-COG extracted oxygen from ambient air, transported the oxygen across two ion transport membranes, and electrochemically pumped oxygen ions across a 20.7-MPa (3000-psig) pressure difference. The 20.7-MPa (3000-psig) technology demonstrator is large and heavy, and production rates are too low to meet human spaceflight mission needs. Thus, additional development work is needed before the M-COG can be qualified for flight.

Additional testing in a hospital environment is needed before M-COG can be certified for medical use, but M-COG prototype testing has demonstrated the ability to produce high-purity (>99.9%) pressurized oxygen with specific energy use <100 W per slpm. However, the M-COG prototypes do not currently produce sufficient quantities of oxygen to be useful for medical applications and are not certified for medical use.

5.0 Assessment Plan

The medical oxygen supply chain was stretched during the pandemic. NASA, working through the NESC and NASA's Chief Health and Medical Officer, supported efforts to identify additional sources of medical oxygen to meet the increasing oxygen needs. The NESC-sponsored M-COG assessment started in the early days of the COVID pandemic. The NESC initially supported a series of emergency response activities, including a Jet Propulsion Laboratory (JPL)-led ventilator development project (NESC assessment TI-19-01523, Hardware Development for COVID Applications).

A Human Exploration and Operations Mission Directorate (HEOMD)-sponsored technology development activity led by JSC researchers was considered a potential additional source of medical oxygen [ref. 1]. COGs using ceramic ion transport membranes were under development for recharge of spacesuit oxygen tanks, as extended EVA operations beyond low Earth orbit will require a safe, effective, and reliable method of oxygen recharge. COG technology is solid state, the COG oxygen separation process does not involve hydrogen, and the oxygen product reliably meets EVA purity requirements [ref. 2].

This NESC M-COG assessment had the following objectives:

- Reduce cell stack manufacturing risks with development wafer and cell stack hardware.
- Demonstrate large-scale medical grade oxygen generation, specifically, at least 1,200 L/hour (hr) of oxygen at 99.999% purity.
- Demonstrate a (scaled) power efficiency of <100 W/kgO_2 comparable to or better than commercially available systems.

As the assessment progressed, evaluating medical certification processes was added to the assessment scope (see Appendix E). Additionally, high pressure development and testing was conducted as a concurrent goal with an active Advanced Exploration Systems Life Support Systems project task. The task sought to develop a COG design capable of maintaining mechanical integrity while producing pressurized oxygen up to 24.8 MPa (3600 pounds per square inch absolute (psia)).

6.0 Background and Description of M-COG Technology

M-COG uses ceramic ion transport membrane technology to extract oxygen from an ambient air source, often atmospheric air. The United States Air Force (USAF) sponsored a significant R&D effort between 2000 and 2010, which demonstrated that a solid-state device could produce high-purity oxygen, but delivery rates were too low and energy consumption was too high to practically meet medical oxygen demands [ref. 3]. NASA sponsored R&D efforts performed by JSC Engineering between 2010 and 2020 to use ion transport membranes to recharge spacesuit oxygen tanks with high-pressure, high-purity oxygen [ref. 1]. These efforts focused on technology development but not on the development of cost-effective manufacturing processes for widespread commercial use.

The NESC sponsored the M-COG project in the early days of the COVID pandemic as part of an effort to identify additional sources of medical oxygen to meet the surging needs of patients (NESC assessment TI-19-01523, Hardware Development for COVID Applications). The NESC-sponsored efforts focused on increasing the pace of technology maturation, developing a manufacturing capability, and demonstrating energy-efficient oxygen production systems.

This section provides a general overview of the M-COG technology and describes the interfaces, key components, and configuration. The core of an M-COG system is the cell stack, where oxygen is extracted from air and delivered through a piping system. The central element of a cell stack is the wafer. The component within the wafer that handles the oxygen separation is the ceramic ion transport membrane. The ion transport membrane, wafer, and cell stack are described in this section, and the system configuration and balance of plant components are discussed.

6.1 General Overview

Figure 6.1-1 identifies the main components of an M-COG system. M-COG systems have two sections: one that operates at ambient temperature and another that operates at an elevated temperature. The ambient temperature section contains the power distribution electronics and control systems (the left side of Figure 6.1-1). The high-temperature insulated section (the right side of Figure 6.1-1) has a process air stream with a process air inlet, blower, heat exchanger, heater, cell stack, and process air vent.

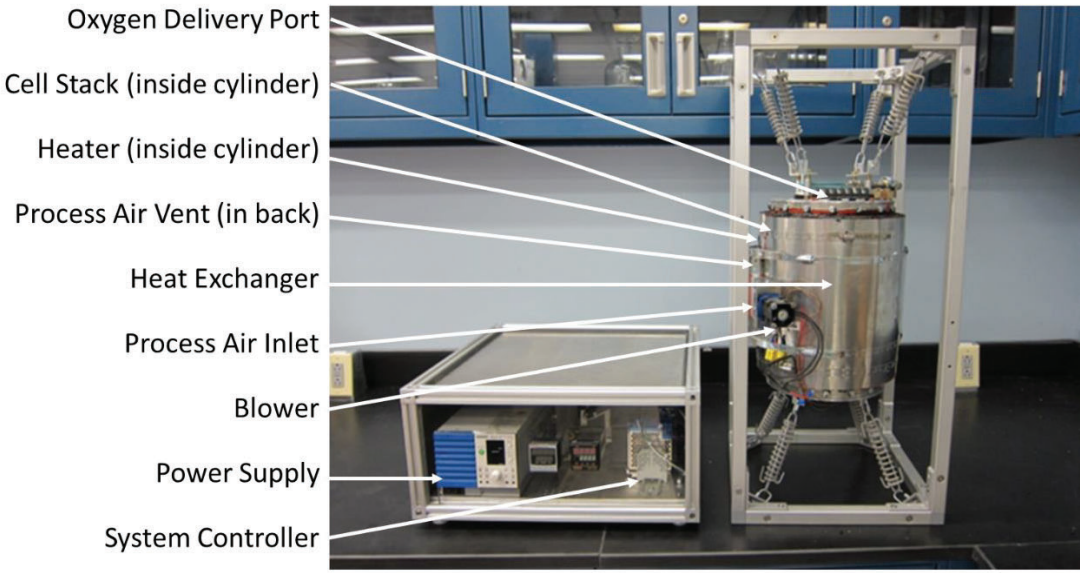

Figure 6.1-1. M-COG System with Main Components Identified (Control systems are located on the left, physically isolated from the elevated temperature components (600 to 800 °C (1112 to 1472 °F).)

Figure 6.1-2 shows a process schematic of an M-COG system, describing the configuration of the main components and illustrating the progression of air as it flows through the process air stream. Ambient air enters the M-COG through the process air inlet and is drawn through the system by the blower. Because the process air flow path is open and unrestricted, the blower requirements are minimal. The performance specifications for the blower are similar to those of ventilation blowers used in residential settings: ~0.424 cubic meters per minute (m^3/min) (15 cubic feet per minute (cfm)). The operating temperature for the cell stack is nominally 700 degrees Celsius (°C) (1292 degrees Fahrenheit (°F)). A dual-purpose heat exchanger simultaneously preheats the incoming air stream while cooling the heated process air prior to venting. This arrangement reduces energy consumption and simplifies venting requirements by reducing the temperature of the exhaust products. Process air heaters are located between the

heat exchanger and the cell stack. The heaters provide a large amount of heating during transient system startup and operate under reduced loads in steady-state operation (see Appendix C).

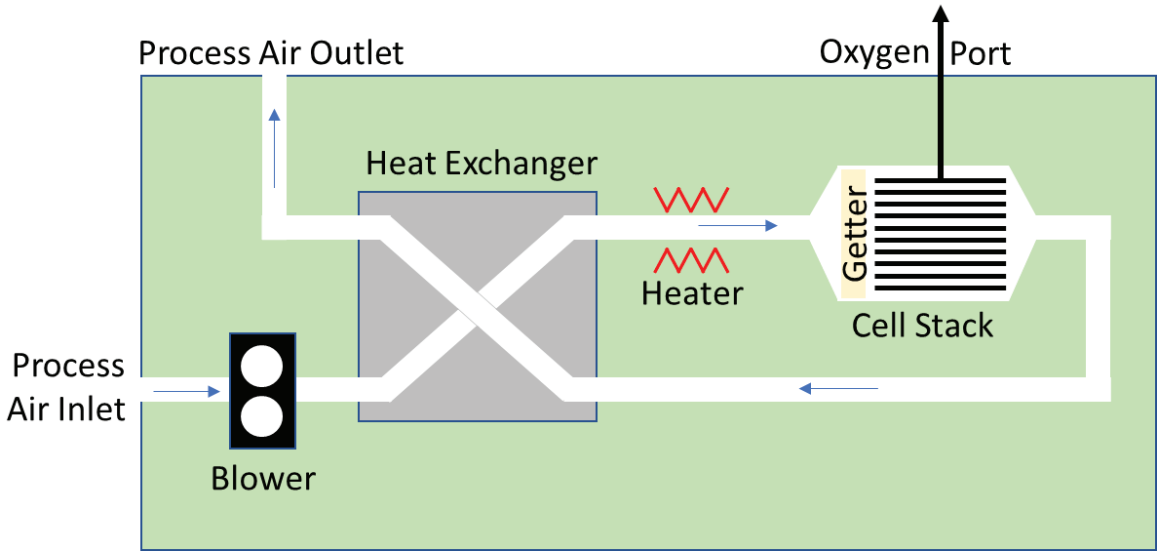

Figure 6.1-2. Process Schematic of M-COG System

The cell stack is an ion transport mechanism that extracts oxygen from the process air stream, produces oxygen delivered through a central pipe, and adds heat to the process air stream (i.e., the ion transport process, which transports oxygen across the ceramic, produces waste heat). Downstream of the cell stack, the process air temperature is elevated, and the oxygen concentration is ~19.5% because some of the oxygen has been extracted; the minimum safe oxygen content, per eCFR §1910.146, is 19.5 volume percent (vol. %). The oxygen-depleted elevated-temperature air is sent through the heat exchanger, cooled, and vented. The blower, heater, and cell stack use electrical power.

The system interfaces are comparable to pressure swing adsorption (PSA) oxygen generation systems. The M-COG device assembly is placed in a vented location and connected to a source of electricity. The M-COG uses ambient air, which serves as the source of oxygen and regulates internal temperatures. Particle filtration and dehumidification may not be required and were demonstrated in limited field service (see Section 7.16). The as-reacted process gas is an oxygen-depleted (~19.5% nominal) 150 °C air stream.

M-COG process air flow is steady state and continuous (see Appendix C). There are no air selector valves and no mechanical movement other than the blower fan blades. The blower operates continuously when the system is running. Heaters bring the system to temperature during startup and then maintain a uniform and consistent temperature during operation (see Appendix C). The cell stack is powered when oxygen is needed and is otherwise placed in a standby mode.

The concept of operations for an M-COG system is to install the system in a ventilated location, connect it to a power source, and connect it to an oxygen delivery piping system. The M-COG will maintain a supply of pressurized oxygen ready for delivery through a distribution pipe when oxygen is needed. The schedule for regular maintenance is expected to be once every 2 years (see Section 7.16). The predicted maintenance tasks (i.e., replacing the blower and replacing thermocouples) are projected to be low in complexity based upon experience with the test units.

6.2 M-COG Oxygen Separation Element: The Ion Transport Membrane

The heart of M-COG technology is the ceramic ion transport membrane, which extracts oxygen from air, transports the oxygen across an impermeable, dense, monolithic ceramic structure. The ion transport membrane is solid (i.e., the oxygen separation process is solid state).

Certain ceramic materials are capable of transporting oxygen ions through their structure if supplied with an electrical potential. These materials do not conduct electricity (i.e., do not transport electrons), but if supplied with an electric potential they can transport oxygen ions (i.e., are ionically conductive). The ion transport membranes are made from ion-conducting ceramic oxides, which are insensitive to elevated temperature oxygen service. These ceramic oxide materials can be formed into dense structures, and when constructed into an operational device, they take the shape of a membrane that is gas impermeable. When the ion transport membrane is connected to a "strongback" structure (e.g., the M-COG wafer assembly), the ion transport membrane forms a hermetic seal with the inlet air on one side and oxygen on the other.

Gases cannot permeate an ion transport membrane, but oxygen ions can be electrically transported provided they are given a direct current (DC) electrical potential. The ion transport membrane material has an oxide lattice structure that has atomic-scale holes [refs. 4-6]. These holes can contain and transport an oxygen ion under an applied electrical potential, as the oxygen ions can migrate through the membrane by moving from one hole to another across the thickness of the membrane.

The other constituents of air (e.g., nitrogen, argon, carbon dioxide, and excess oxygen) are unaffected by the ion transport membrane. Some of the oxygen is electrochemically dissociated into oxygen ions, and the oxygen ions are electrochemically pumped across the ion transport membrane. The rate of oxygen ion transport is set by the current passing through the membrane. The current/oxygen flow relationship is linear (i.e., increasing the current by 10% increases the flow of oxygen by 10%).

Ion transport membranes are not used commercially for medical oxygen generation, but ion transport membranes are used as automotive oxygen sensors. Sensors referred to as "zirconia O_2 sensors" measure the air-to-fuel ratio in automotive combustion environments. Like the M-COG ion transport membrane, zirconia sensors use a ceramic ion transport membrane that is dense and impermeable to gas flow and operates at elevated temperatures [ref. 7]. The automotive oxygen sensor market is mature, with a developed manufacturing base. The global automotive oxygen sensor market was valued at 30 billion United States dollars (USD) in 2021 [ref. 8].

Figure 6.2-1 shows a functional schematic of an ion transport membrane. At the center of the ion transport membrane is a dense, monolithic ceramic electrolyte. The electrical resistance of ion transport membranes is essentially infinite at room temperature, but as the temperature increases, the electrical resistance decreases. Effective ion transport membranes capable of transporting meaningful amounts of oxygen operate in the 600 to 800 °C temperature range to reduce electrical resistance. Increasing the surface area increases the amount of allowable oxygen transport. Electrical resistance increases as the electrolyte thickness increases, so effective ion transport membranes require a minimum thickness for effective mechanical strength, assumed to be defect free. Excess thickness should be avoided to minimize energy input for oxygen transport. Ion transport membranes operate in environments as hot as practically possible to reduce electrical resistance and improve power efficiency.

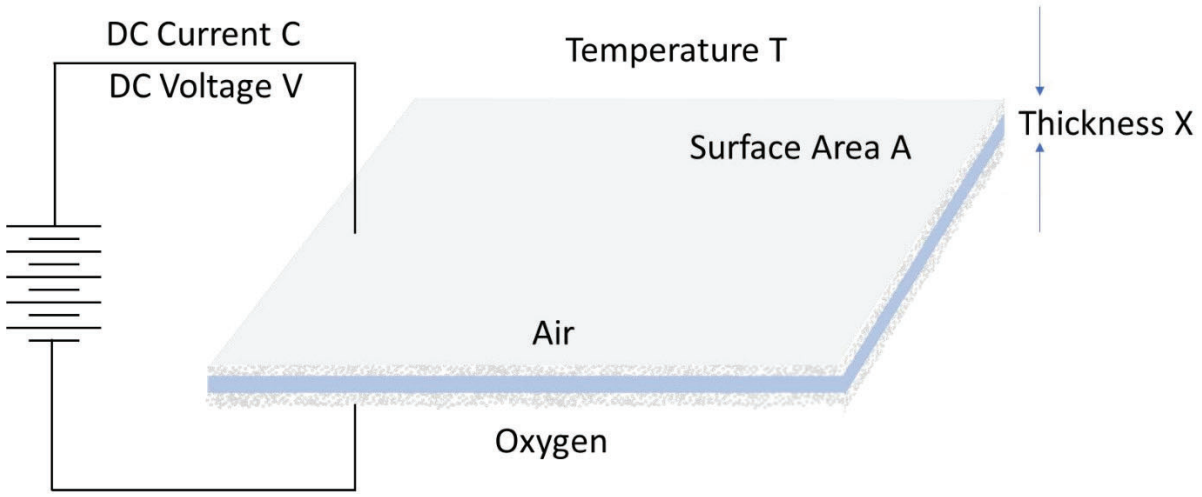

Figure 6.2-1. Functional Schematic of Ion Transport Membrane

Each surface of the electrolyte supports a transition zone, bridging the interface between free gas and solid electrolyte. The air-facing surface of the electrolyte must receive electrons from the external power supply, ionize molecular oxygen into oxygen ions, and deliver the oxygen ions to the electrolyte surface. Electrochemically, the air-facing surface of the electrolyte acts as the cathode. Cathode materials are porous to maximize surface area and increase the contact area between the air and the solid cathode surface. The cathode is referred to as a "mixed ionic conductor" because it is capable of transporting electrons and oxygen ions.

The anode side of the electrolyte has a porous layer made from materials with mixed ionic conductor properties. At the anode, oxygen ions reform into molecular oxygen. This process releases an electron. The anode collects the electrons and transports them to the rest of the DC current loop, completing the DC circuit.

Figure 6.2-2 provides a detailed cross section of an ion transport membrane and maps the electrochemical configuration, physical configuration, and electron/oxygen ion charge-carrying properties. Note that the cathode is on the air-facing side, and the anode is where oxygen is collected and generated. Anode and cathode structures are porous ceramic oxides, with as much surface area as possible to improve the kinetics of electrochemical processes occurring at the solid/gas interface. The electrolyte is solid and impervious to gas flow, even at pressure differences up to 1 MPa (145 pounds per square inch (psi)) [ref. 9].

Cathode	Air	Porous	Carries electrons and O^- ions
Electrolyte	No Free Gas	Solid	Carries only O^- ions
Anode	Oxygen	Porous	Carries electrons and O^- ions

Figure 6.2-2. Cross-sectional View of Ion Transport Membrane, with Mapping of Electrochemical Components, Physical Configuration, and Ion Transport Properties

Figure 6.2-3 shows a cross section of a scanning electron microscope (SEM) image of an ion transport membrane. Note that the ceramic electrolyte layer is fully dense, and the cathode and anode structures are porous. The right-hand side of Figure 6.2-3 shows an electrochemical

schematic of the DC circuit that drives the process. Note the location of electron transfer and oxygen ion transport across the electrolyte and the direction of oxygen ion transport.

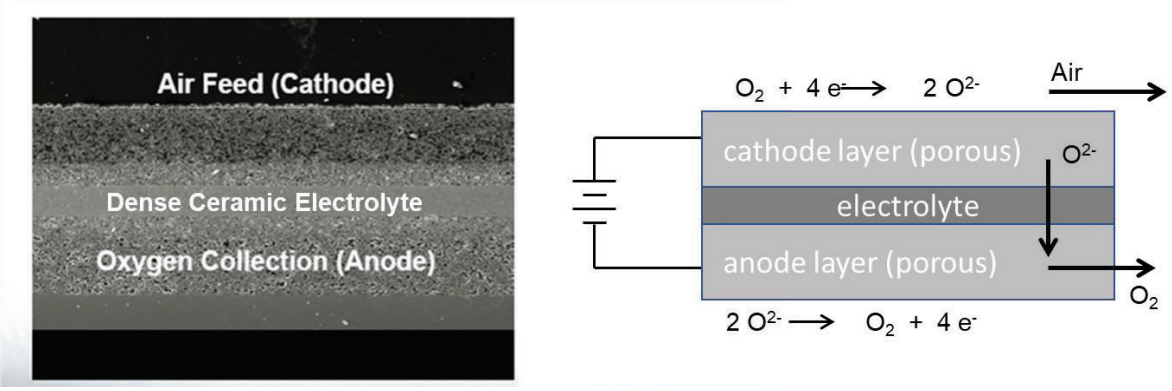

Figure 6.2-3. Cross Section of M-COG Ion Transport Membrane with Electrical Circuit, Electron Transfer, and Oxygen Ion Movement

6.3 Primary M-COG Component: The Wafer

Ion transport membranes are operated at elevated temperatures to reduce electrical resistance and at a thickness that is optimized to provide an acceptable level of mechanical strength with minimized electrical resistivity. Researchers have used unsupported ion transport membranes for decades [ref. 10]. It is easier to fabricate a "simple" ion transport membrane consisting of three layers (i.e., cathode, anode, and electrolyte) than it is to fabricate a more complex structure with sealed edges. These three-layer structures are placed in an external support frame to enable testing. The frames are prone to leakage; pressurized oxygen is likely to leak around the support frame and flow into the air side of the assembly. If not properly designed, these frames exert mechanical forces, causing the hot, thin, brittle ion transport membrane to fracture. It is difficult to structurally support the ion transport membrane and allow free flow of gases on both sides of the membrane. It is especially difficult to do this at elevated temperatures because the external frames are frequently made of materials with different coefficients of thermal expansion (CTEs). Small CTE mismatches can cause significant structural loads when a test article is cycled between 20 and 700 °C. The target CTE for the wafer is 12.5 ± 0.5 parts per million (ppm) per kelvin (K).

M-COG ion transport membranes are structurally supported through bonding to a strong structural support layer. The structural supports are made from ceramic materials with matched CTEs, which have been shown to support and protect the ion transport membrane against targeted, intentional thermal excursions. Additional thermostructural testing of the assembled cell stack structure is future work. The sealed enclosure for the oxygen is designed to be hermetic.

Figure 6.3-1 shows an M-COG wafer and some of its main elements and illustrates the configuration of the ion transport membrane structural support. The ion transport membrane, consisting of anode, cathode, and electrolyte, is bonded to the top surface of a strong, thick, dense, gas-impermeable structural support layer referred to as the strongback. Each layer in the structure (i.e., strongback, anode, electrolyte, and cathode) has a hole to feed gas to the oxygen port. The strongback accounts for >90% of the total mass of the wafer.

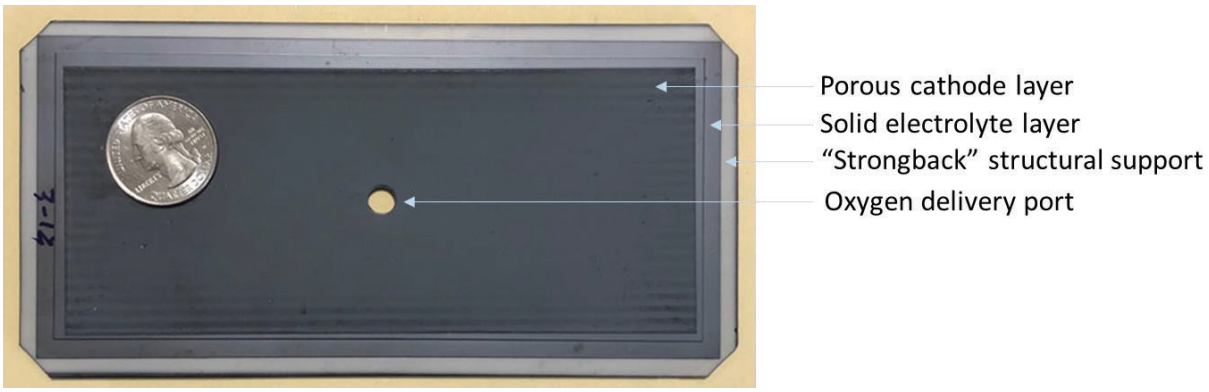

Figure 6.3-1. M-COG Wafer (top view) with Main Elements Identified

The fabrication of a strongback-supported wafer with a hermetic seal between the air and oxygen in this effort represents a significant improvement in manufacturing capability over previous work by the USAF [ref. 3]. Testing at Tinker Air Force Base demonstrated that thin unsupported wafers could not withstand thermal shock caused by system restart after a power outage. The M-COG wafer shown in Figure 6.3-1 has been exposed to thermal shock conditions caused by loss of power. Independent testing conducted at JSC demonstrated that M-COG wafers withstand worst-case thermal shock conditions (Appendix C). Additional testing that would be required for spaceflight (e.g., mechanical shock and vibration testing) was not performed.

Figure 6.3-2 shows a simplified illustration of the wafer, ribs, washer seal, and oxygen port in cross section. The dimensions of the components are not to scale and demonstrate the relative geometry. The strongback is joined to the ion transport membrane surface continuously along the surface of the ion transport membrane. Additionally, the wafer structure has a hermetic seal that separates the "oxygen pocket" that forms in the pores of the anode layer from the air that surrounds the outside of the wafer.

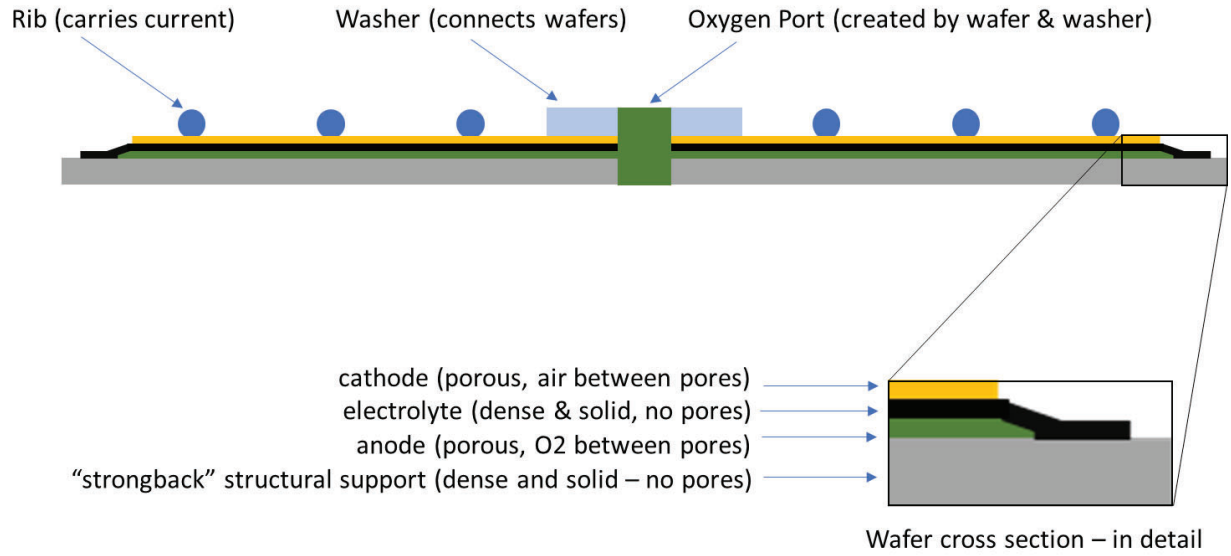

Figure 6.3-2. Graphical Cross Section of Wafer, Ribs, Washer Seal, and Oxygen Port (image is not to scale)

Oxygen is electrochemically pumped from outside the wafer into the porous region inside the wafer (i.e., to the anode). The porous anode region is sealed along the outside edges of the wafer, but there is an open path to the oxygen port located in the center of the wafer. As oxygen migrates into the porous anode region, internal pressure rises. This pressure drives the flow of oxygen to the oxygen port. A ring-shaped washer is attached to the top of the wafer, surrounding the oxygen port. This washer creates a "chimney" for oxygen transport. A set of ribs is attached to the top of each wafer, providing structural support for the stacked assembly of wafers. These ribs carry current from one wafer to the next.

When attached to a strongback and formed into a wafer, the ion transport membrane can withstand pressure loads greater than 1.38 MPa (200 psig). For verification and validation, M-COG wafers are subjected to a cold pressure decay and structural challenge test during which the wafer is placed in a test fixture, sealed, and pressurized to 1.38 MPa (200 psig). More than 2000 wafers have been tested, with ~10% of the wafer-washer assemblies suffering from leakage rates greater than specification A, B, or C (see Table 6.3-1) [ref. 9]. Leak rate tests result in each individual wafer receiving a quality grade. Grade criteria also are listed in Table 6.3-1.

Table 6.3-1. Definitions of Wafer Grades per Cold Pressure Decay Leak Tests

Grade	Cold Pressure Decay Rate	Absolute Leak Rate (standard cubic centimeters per minute)
A	>200 minutes	<0.013
B	100–200 minutes	0.013–0.026
C	50–100 minutes	0.026–0.052
F	<50 minutes	>0.052

Cold pressure decay rate is the time in minutes for pressure to drop from 200 psi to 100 psi. Note that none of the developmental wafer-washer assemblies have fractured or failed due to testing.

Figure 6.3-3 provides an isometric view of a stack of six wafers. Each wafer has a washer and a set of ribs. The washer thickness sets the wafer spacing. Each wafer is ~2 millimeters (mm) thick, and the gap between each wafer is ~2 mm. The configuration of the wafer allows pressurized oxygen to accumulate inside a sealed pocket within the wafer. The configuration of the wafer/washer/rib assembly allows oxygen from multiple wafers to be routed to a single oxygen port.

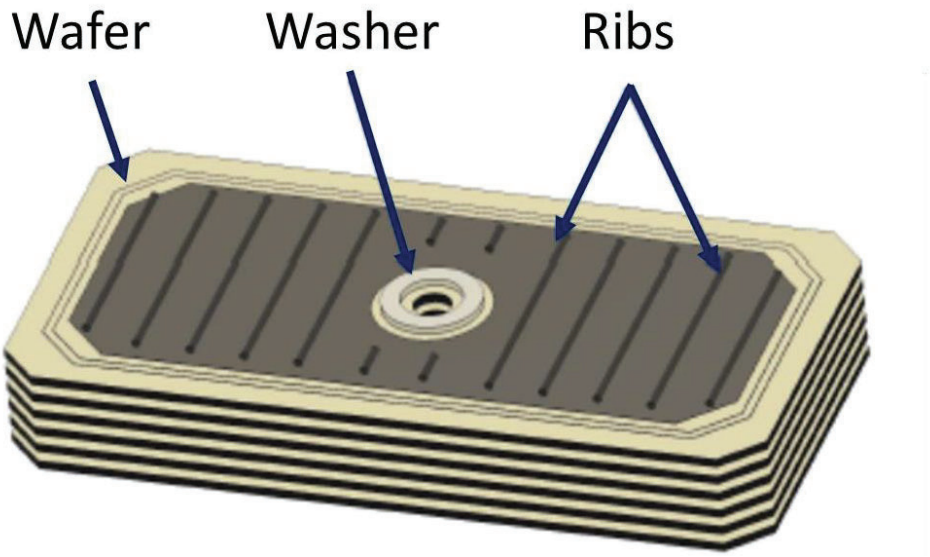

Figure 6.3-3. Isometric View of Stack of Six Wafers (each wafer has a washer and a set of ribs)

6.4 Primary M-COG Subassembly: The Cell Stack

Oxygen production rates are limited by the total amount of ion transport membrane surface area. Larger areas can generate oxygen at faster rates, but manufacturing limitations (e.g., mechanical warping of larger parts due to shrinkage stresses) restrict the maximum size of a wafer to ~20 centimeters in length. Larger wafers are more prone to warping during high-temperature sintering. The current wafer geometry is limited to less than 200 milliliters (mL)/min of oxygen production per wafer. M-COG system designers use a planar stack configuration to generate more surface area/system volume to achieve higher, total oxygen generation rates.

Figure 6.4-1 provides a schematic of a cell stack assembly of four wafers in cross section and identifies the main components of a cell stack assembly. An M-COG device stack consists of 30 wafers. The oxygen ports are aligned and combined with the washers to form a central chimney that allows the oxygen produced by the cell stack to be delivered through a single port. The gap is approximately the thickness of a wafer, allowing uniform airflow to sweep across the wafers. The process air sweep removes waste heat and ensures a uniform temperature across the wafer surface.

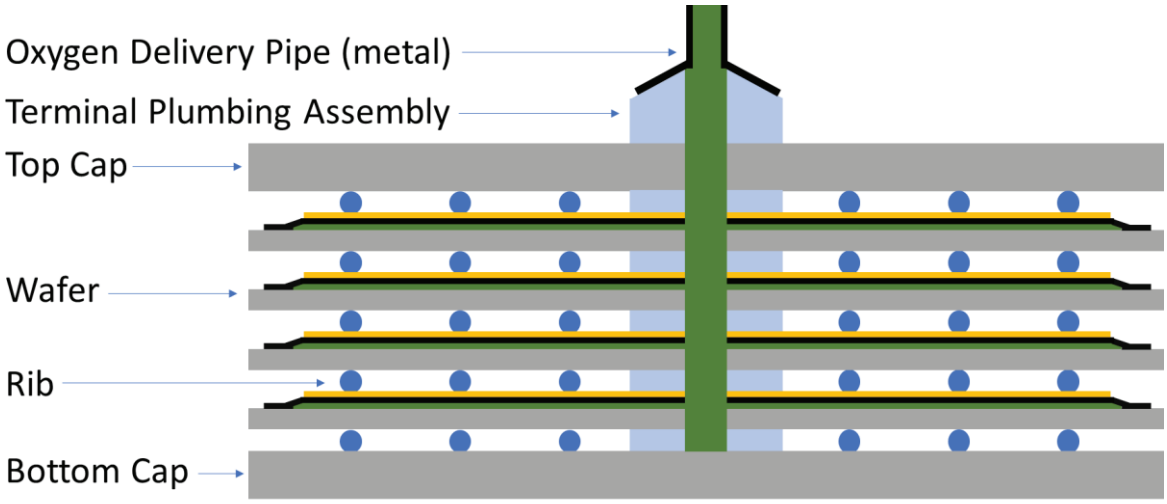

Figure 6.4-1. Schematic of Cell Stack Assembly Cross Section (image is not to scale)

The cell stack is manufactured using high-temperature joining processes. The oxygen from each cell stack is ported using a single piece of stainless-steel tubing (SAE 304). The ceramic/metal interface is referred to as the terminal plumbing assembly (TPA), which accommodates the mismatch in CTE between metals and ceramics.

The ceramic cell stack is connected to power leads, surrounded by non-conducting insulation, and encased inside a metal housing to facilitate installation of the cell stack into the process air stream. The top and bottom caps have several functions, including structurally protecting the cell stack, providing a place to connect power leads, and facilitating electrical isolation. The caps are approximately four times thicker than the wafer for structural capability as rigid mechanical backing.

Figure 6.4-2 shows the ceramic elements of a development cell stack. The wafers are not in perfect alignment due to uneven shrinkage during densification at high temperatures. The ceramic cell stack needs a connection to electrical leads, uniform air flow across the wafers without flow bypassing, and consistent outside dimensions to facilitate installation into the process air flow duct. To facilitate connection of electrical leads and provide consistent dimensions, the ceramic elements are enclosed in a stainless-steel structure.

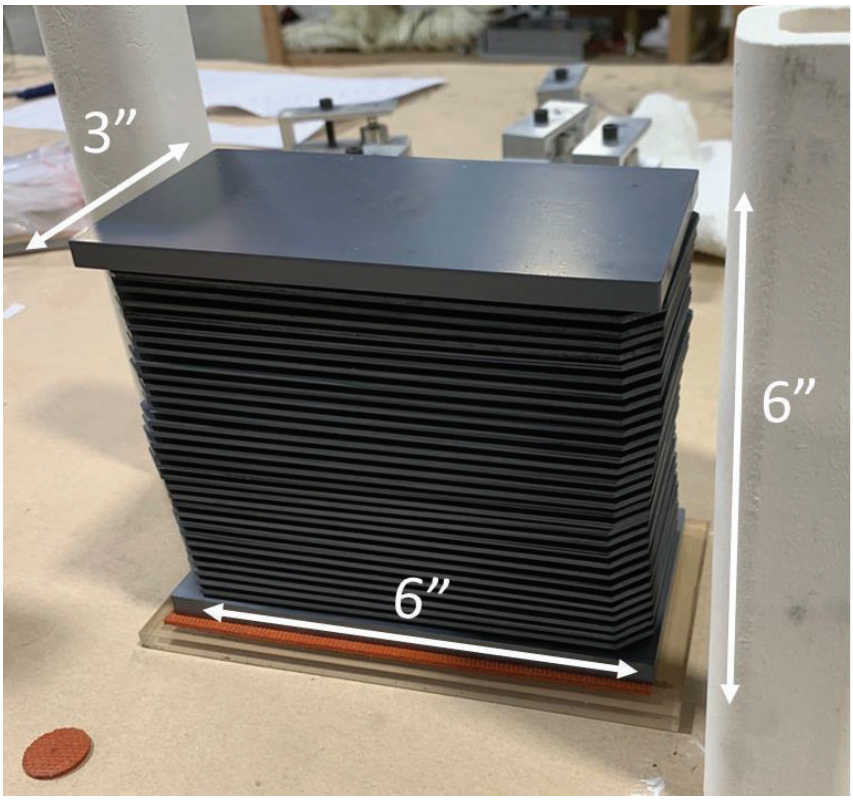

Figure 6.4-2. Ceramic Elements of Cell Stack (6 inches = 152.4 mm)

Figure 6.4-3 shows the M-COG boxed stack in exploded view. Process air can flow freely and uniformly through the spaces between the wafers without bypass flow around the ceramic cell stack. The ceramic cell stack is electrically isolated. The entire cell stack can be energized with a single cathode power lead and a single anode power lead. Oxygen is delivered through a single stainless-steel tube that is connected to the TPA. The outside dimensions of the boxed stack meet manufacturing tolerances (±5 mm) for repeatable assembly of the M-COG system. Figure 6.4-4 provides an image of an assembled M-COG boxed stack. This boxed stack is the building block of the M-COG technology. Oxygen production depends on the specific design details, but for first-order sizing purposes, each boxed cell stack can be thought of as a device capable of producing 4 to 5 slpm of oxygen, which is roughly what a single patient requiring supplemental oxygen would require [ref. 11].

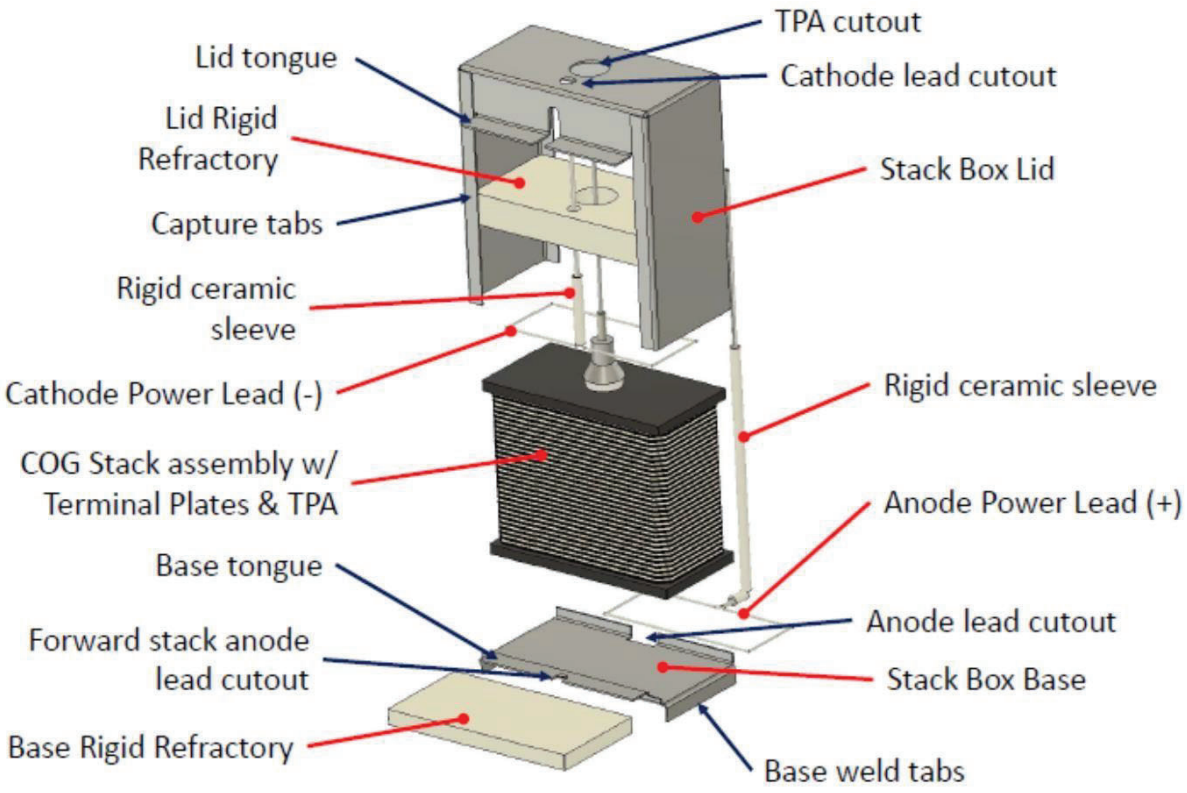

Figure 6.4-3. Configuration of M-COG Boxed Stack in Exploded View

Figure 6.4-4. Fully Assembled M-COG Boxed Stack with Sixpack of 500-mL Beverages for Scale

6.5 M-COG Configuration and Balance of Plant

Figure 6.5-1 shows an M-COG schematic demonstrating the flow of process air through the device. Note the sequence for process air flow through the system.

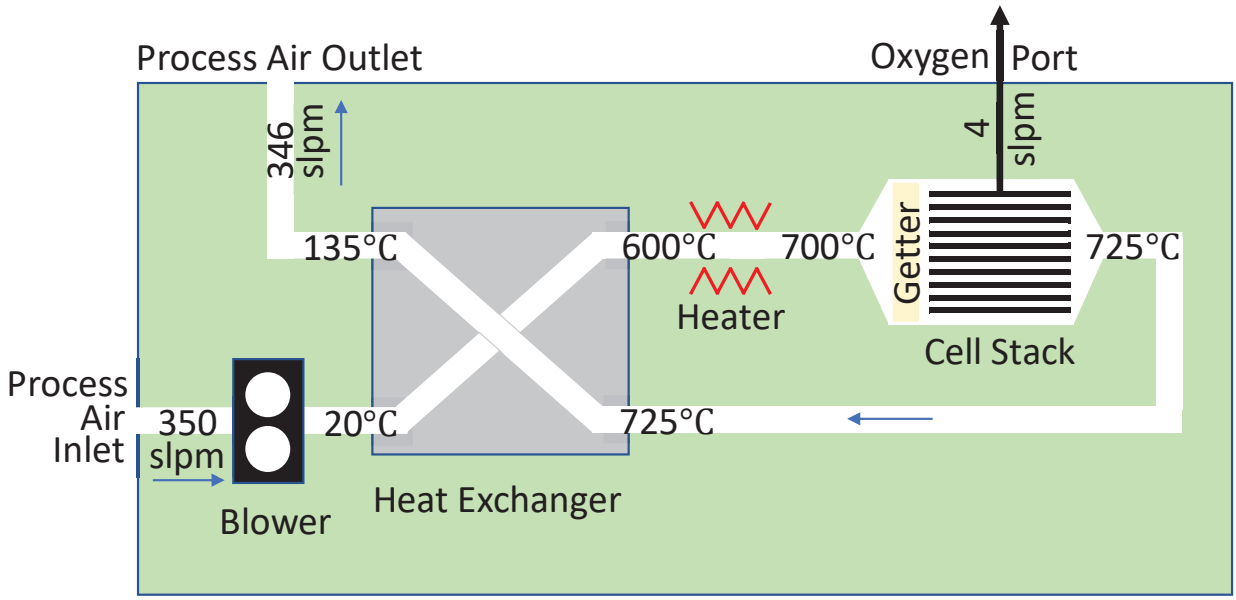

Figure 6.5-1. M-COG Schematic with Notional Values for a Single Value

The cell stack does not require air filtration or dehumidification since particulate and humidity cannot diffuse across the membrane; however, system filtration must be determined by the tolerance of balance of plant and the environmental conditions of the inlet process air. Gross contamination of the inlet air can cause secondary system problems that will not manifest in the cell stack. The blower used in this testing was commercially available off the shelf. Different blowers can be used for different M-COG prototypes, as systems with more cell stacks require additional air flow. The current designs do not require inches of water column (IWC) pressure above 0.49 kilopascals (kPa) (0.072 psi). Important blower specifications include maximum flow (with no pressure drop), maximum pressure drop (with no flow), power draw, and rated mean time between failure. The purchase price for the blower shown in Figure 6.5-2, when purchased as a single device for developmental use, was ~$43. The performance attributes for this blower are given in Table 6.5-1.

Table 6.5-1. Performance Attributes

Maximum flow (with no pressure drop)	33.8 m^3/hr (20 ft^3/min)
Maximum pressure drop (with no flow)	2 IWC or 0.49 kPa (0.072 psi)
Power use	20 W
Mean time between failure*	70,000 hr (8 years continuous use)

* Claim per manufacturer's documentation. Not validated in this test campaign.

Figure 6.5-2. Blower used in CFC M-COG

There are two main designs for M-COG systems, each using a different type of heat exchanger. The M-COG design referred to as the T-configuration uses a box-shaped heat exchanger with a counterflow design (see Figure 6.5-3). A single septum separates the two counterflow air streams. The second M-COG design, referred to as the crossflow cylinder (CFC) configuration, has a cylindrical shape and two nested airflow paths with two counterflow spiral flow paths (Figure 6.5-4). The CFC heat exchanger is made from SAE 304 stainless steel sheet material and manufactured using a process that involves rolling and welding. This heat exchanger was manufactured at American Oxygen facilities.

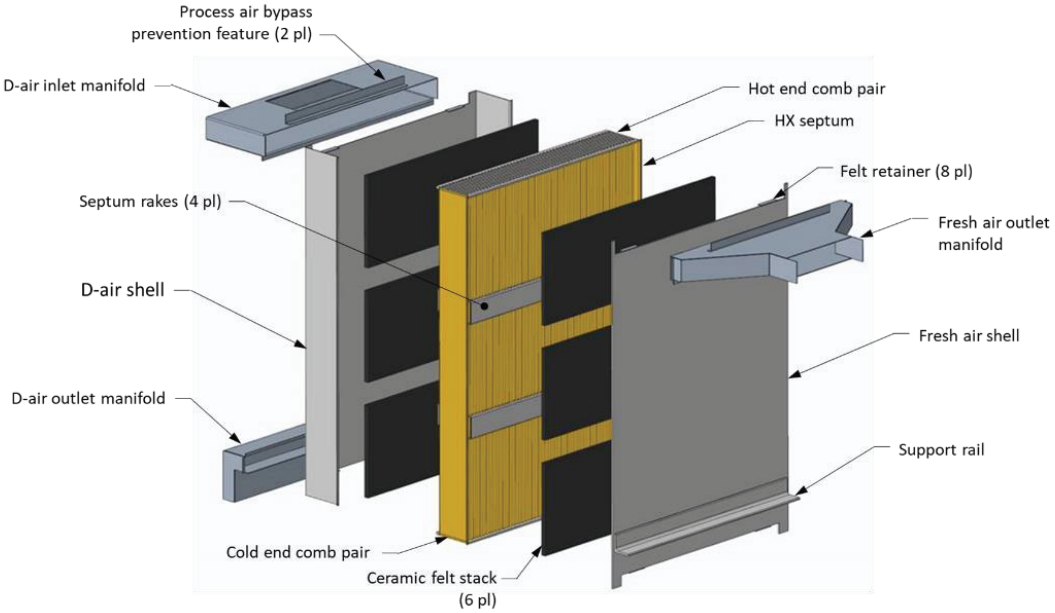

Figure 6.5-3. Exploded View of Counterflow Heat Exchanger used in T Configuration M-COG

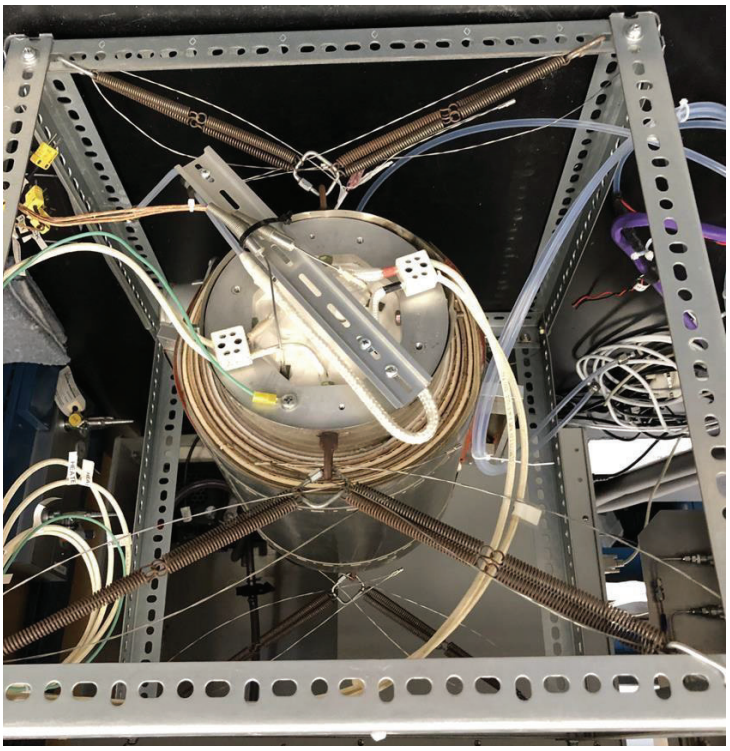

Figure 6.5-4. CFC Configuration M-COG (spiral-wound heat exchanger is outermost cylinder)

The key attributes that drive M-COG thermal management system design are the preheat start time, total power use, fault tolerance, and service life, as predicted by commercial component mean time between failure. Startup times are conservatively selected to be 6 hr for a system starting at 25 °C, which is intended to minimize the thermal stresses on the wafer. Startup time and total system power-use limitations set the maximum power levels applied to process air heaters. During steady-state operations, system heat is largely supplied by heat generated by the cell stack. During startup, cell stacks do not operate; system heating is provided by the process air heaters. Best practices recommend using multiple heater elements to ensure system performance when one heater element fails [ref. 12]. The M-COG Chassis 2 configuration (see Section 7.2) uses four heaters, and the M-COG CFC configuration uses two heaters. Mean-time-between-failure service life ratings are inversely proportional to power use (i.e., heaters burn out more quickly when they are operated at their maximum power rating and last longer when they are operated with less load). Because of system startup heating requirements and fault tolerance requirements, nominal heating power during steady-state operations is less than 10% of the maximum power rating for the cases evaluated for this assessment.

M-COG designers developed two configurations for cell stack alignment and thermal management:

- Configuration 1 used the T configuration (see Figure 6.5-5). The T configuration takes its name from the orientation of the heat exchanger and the cell stacks. The heat exchanger is perpendicular to the cell stacks, with the hot end near the cell stacks and the cool end as far from the cell stacks as practically possible. This orientation results in improved thermal efficiency, but the overall size of the system is relatively large. The system shown in Figure 6.5-5 can hold eight cell stacks in series.

- Configuration 2 used the CFC configuration. CFC systems have fewer cell stacks, with the example shown in Figure 6.5-6 having only one cell stack. Other CFC configurations are capable of housing two, three, or four cell stacks, with four being the current limit for this design configuration. CFC systems are easier to manufacture. The thermal management system for this configuration is currently at a preliminary design review level of maturation.

Current operational concepts for M-COG oxygen generators for global health involve a suite of CFC systems, colocated in an insulated housing. This concept allows for oxygen generation with reduced energy needs and lower manufacturing costs, at the trade of increased thermal losses.

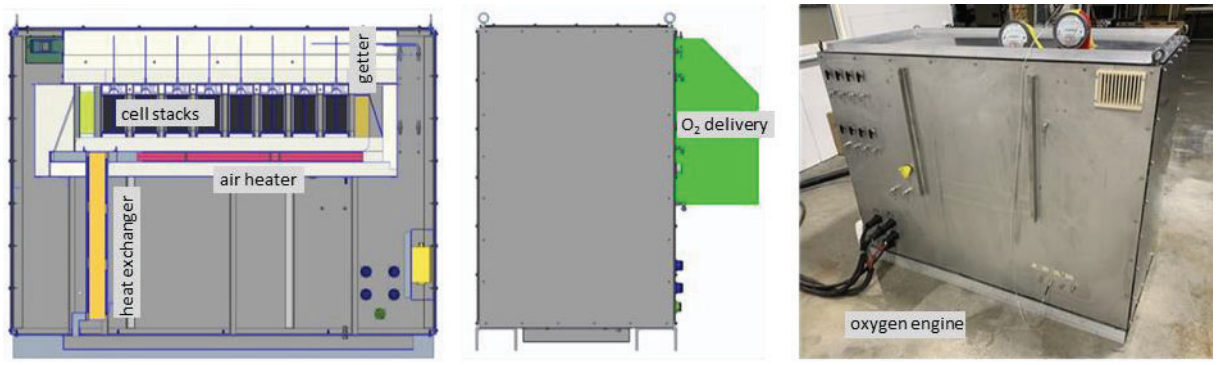

Figure 6.5-5. Cross-sectional View, Side View, and T Configuration Image

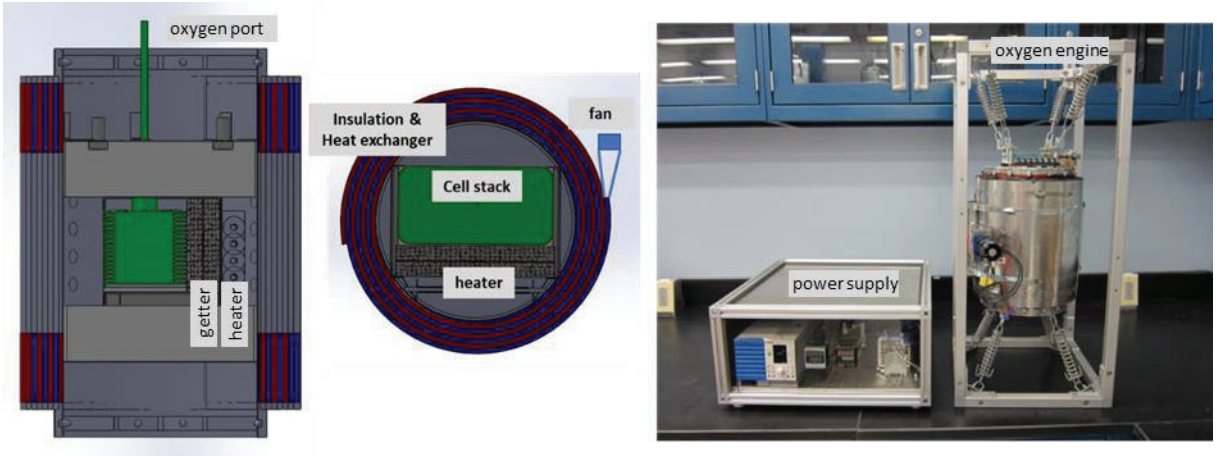

Figure 6.5-6. Cross-sectional View, Side View, and CFC M-COG Configuration Image

While the T configuration has improved power efficiency, the manufacturing costs are greater, the system size is larger, and protection from shock and vibration loads is more difficult. After building and testing both designs, the manufacturing benefits of the CFC configuration appear to outweigh the energy efficiency benefits of the T configuration. Thermal models suggest that groups of CFCs will heat each other, and overall power efficiency for CFCs will improve if they are used as part of a larger system. Direct measurement of power use for a set of CFCs grouped in an insulated structure is beyond the scope of this M-COG assessment.

7.0 Test Results

This section describes key attributes of the M-COG systems [ref. 2].

7.1 Performance Test of Chassis 1

Chassis 1 was a step in the development of the T configuration. Chassis 1 was the first complete prototype system capable of producing oxygen with a series-segmented arrangement of cell stacks. Different cell stacks operated at different temperatures, which was new to ion transport membrane oxygen generators. The structural frame of Chassis 1 was capable of supporting eight cell stacks, but because the quantity of available cell stacks was limited at the time of testing, four cell stacks were installed into Chassis 1, with four cell stack surrogates. The cell stack surrogates matched the thermal and pressure drop properties of a cell stack but did not produce oxygen. An air-to-air heat exchanger was installed in Chassis 1 to preheat the incoming process air and cool the oxygen-depleted process air that passed through the cell stacks. For packaging reasons, the orientation of airflow in the heat exchanger was parallel to the orientation of airflow in the wafer stack.

Tests were conducted at the WSTF in August 2021. Sample purity measurements were taken by a direct injection of the inline oxygen product into Fourier transform infrared spectroscopy (FTIR), gas chromatography (GC) with an argon carrier gas, and GC with a nitrogen carrier gas, respectively.

The primary objectives of the test series were:

1. Demonstrate the production of oxygen in an independent test facility unaffiliated with American Oxygen.
2. Measure oxygen purity.
3. Demonstrate system-level performance when cell stacks were placed in a series-segmented configuration.

Key test results and findings are:

1. Chassis 1 was capable of producing oxygen, and system performance was demonstrated.
2. The purity of the generated oxygen was 99.97%.
3. The integrated oxygen generation system successfully produced oxygen when each of the cell stacks was activity controlled to operate at a different temperature. The series-segmented configuration was able to improve energy efficiency without causing a system control failure.
4. The orientation of the heat exchanger improved packaging efficiency but reduced thermal performance. A counterflow heat exchanger has a “hot” and a “cold” side. The horizontal placement of the heat exchanger put the cold side close to the cell stacks, which lowered heat exchanger performance. Chassis 1 test results caused a realignment of the heat exchanger in Chassis 2.

Operating Chassis 1 at WSTF demonstrated that M-COG could be transported. Testing in a new location formalized interfaces and interface control. As an independent third-party test facility, WSTF measurements have a special credibility.

Measurement of the purity of oxygen produced by Chassis 1 was the main objective of this test series. WSTF developed a standard method for measuring the purity of the oxygen produced by Chassis 2. Nitrogen was measured using gas chromatography with an argon carrier gas. Argon

was measured using gas chromatography with a nitrogen carrier gas. Water vapor and trace organics were measured using Fourier-transform infrared spectroscopy. Using three different techniques, a comprehensive measurement of oxygen purity can be made. Resulting measurements indicated the oxygen purity was 99.97%.

Purity and performance tests of COG systems previously have been conducted at WSTF. These earlier tests were of systems consisting of one cell stack. This 2021 test series marked the first time an oxygen generator using more than one cell stack was tested.

Limitations to the testing included:

1. Full-scale 30-wafer cell stacks were not available. In August 2021, at the time of Chassis 1 testing, manufacturing processes to construct 30-wafer cell stacks had not been developed. Chassis 1 testing was restricted to six-wafer cell stacks.
2. Pressurized oxygen could not be demonstrated. Wafers were pressure tested at 1.38 MPa (200 psig), but the ceramic-metal connection that joins the cell stack to the metal piping system had not been fully developed. Chassis 1 testing was restricted to delivery pressures of <0.02 MPa (<3 psig).
3. Production rates were limited to <0.5 L/m for each six-wafer cell stack.

A more detailed description of the test configuration and methods of measuring product purity is provided in Appendix A.

7.2 Performance Test of Chassis 2

Chassis 2 was the second step in the development of the T configuration. Chassis 2 was the first M-COG prototype with production-ready, 30-wafer cell stacks. The structural frame of Chassis 2 was capable of supporting eight 30-wafer cell stacks, but because the quantity of available cell stacks was limited at the time of testing, four 30-wafer cell stacks were installed into Chassis 2, with four cell stack surrogates. The cell stack surrogates matched the thermal and pressure drop properties of a cell stack but did not produce oxygen. This configuration implemented a lesson learned from the Chassis 1 testing, such that the air-to-air heat exchanger in Chassis 2 was configured with a flow direction perpendicular to the flow direction through the cell stacks.

Tests were conducted at WSTF in December 2022. Sample purity measurements were taken by a direct injection of the inline oxygen product into FTIR, GC with an argon carrier gas, and GC with a nitrogen carrier gas, respectively.

The primary objectives of the test were:

1. Demonstrate the production of oxygen in an independent test facility unaffiliated with American Oxygen.
2. Measure oxygen purity.
3. Test the performance of a full-scale, 30-wafer cell stack.
4. Measure total system power use.
5. Demonstrate the ability to operate an M-COG system without the use of supplemental heaters to preheat incoming air.

Operating Chassis 2 at WSTF demonstrated that M-COG could be transported. Testing in a new location formalized interfaces and interface control, as well as validated data at an independent, third-party test facility.

Measurement of the purity of oxygen produced by Chassis 2 was the main objective of this test series. Using the WSTF-developed standard method for measuring the purity of oxygen, measurements showed the oxygen purity produced by Chassis 2 was 99.995%.

The Chassis 2 testing marked the first occasion to test a full-scale 30-wafer M-COG cell stack. WSTF testing started with relatively low oxygen production rates of 2 slpm for each cell stack. Production rate for one of the cell stacks was increased, in 0.5-slpm increments, until a production rate of 4.5 slpm was achieved.

Total power consumption of Chassis 2 was measured. One objective of the Chassis 2 design was increased power efficiency, as multiple cell stacks in series are capable of sufficiently heating the process air to temperatures that allow for process air heaters to be turned off. The Chassis 2 system was tested initially at relatively low oxygen production rates of 2.0 slpm (where supplemental heat from process heaters was required). Cell stack power and heater power were measured and tracked as oxygen production rates were increased in 0.5-slpm increments.

One of the Chassis 2 test objectives was to demonstrate that at sufficiently high oxygen production rates, cell stack heat could maintain system temperature without the use of process air heaters. This technical goal was demonstrated when oxygen production rate reached 12.5 slpm. At the 12.5-slpm production rate, the process heaters could be turned down until they consumed <5% of the total system power.

Key test results and findings are:

1. Chassis 2 was capable of producing oxygen, and system performance was demonstrated.
2. The purity of the generated oxygen was 99.995%.
3. Full-scale, 30-wafer cell stacks performed in accordance with their specifications for production rate (i.e., ≥4 slpm), delivery pressure (i.e., ≥0.344 MPa (≥50 psig)), and power consumption (i.e., ≤450 W) [ref. 13]. No changes to the 30-wafer cell stack are required.
4. A 30-wafer cell stack was capable of producing 4.5 slpm of oxygen at 0.552 MPa (80 psig) with a power use of 400 W.
5. Series-segmented thermal management was demonstrated. The Chassis 2 system operated without the need of supplemental heaters.

Limitations to the testing included:

1. Only one cell stack at a time was operated at 100% power/100% production rate. This was performed out of an abundance of caution, as operating one cell stack at full power while the other cell stacks operated at partial power allowed one cell stack to be tested under maximum design power conditions, for specific review of the cell stack under test. The test plan took a "crawl, then walk, then run" approach.
2. Total oxygen production was limited to 12.5 slpm. Four of the cell stacks were surrogates that did not produce oxygen. Three of the four oxygen-producing cell stacks were operated at reduced power. As a result, even though Chassis 2 was designed to produce 34 slpm, oxygen production was limited to 12.5 slpm.
3. Maximum delivery pressure was 0.552 MPa (80 psig). Every element of the system was proof tested to 1.379 MPa (200 psig), but because Chassis 2 was located in the WSTF Chemistry Lab, which had test safety restrictions on maximum pressure, the maximum pressure of oxygen generated during Chassis 2 testing was 0.552 MPa (80 psig).

A more detailed description of the test configuration and methods of measuring product purity is provided in Appendix B.

7.3 Performance Testing of the "Mule"

The M-COG prototype referred to as the *Mule* was subjected to long-duration (~1200 hr) testing in the summer of 2023. The test article contained one full-scale 30-wafer cell stack, which was packaged inside a spiral counter flow air-to-air heat exchanger (i.e., the CFC configuration). A CFC configuration M-COG is small compared with Chassis 2 and does not produce as much oxygen (i.e., 4 slpm maximum flow under steady state, 4.5 slpm under temporary surge conditions). Smaller systems with just one cell stack are less energy efficient. When the CFC produces 4 slpm, cell stack power is 340 W, heater power is 480 W, blower power is 20 W, total power is 840 W, and specific energy use is 210 W/slpm (Appendix C). The CFC configuration M-COG is suited for long-term testing.

Tests were conducted at the American Oxygen facility in Salt Lake City, Utah, in the summer of 2023.

The primary objectives of the test were:

1. Understand the interactions between cell stack operating power (i.e., DC voltage and current), nominal operating temperature, heater power, and volume air flow rate.
2. Measure vertical and lateral temperature distribution in the stack as a function of operating parameters.
3. Collect the maximum run time practically possible.
4. Characterize the thermal performance of a single-cell CFC.
5. Integrate and check out the instrumentation/control system with production configuration thermocouples and automated control software.
6. Understand system response to electrical power loss.

Mule testing characterized the effects of operating parameters on system temperature by systematically changing one operating parameter at a time. The operating parameters tested included cell stack current, inlet process air temperature, and volumetric process air flow rate.

The Mule was outfitted with additional thermocouples, and the locations of these thermocouples could be adjusted. Temperatures at the trailing edge of the cell stack were measured in nine locations, and the resulting temperature maps were used to assess uniformity of process air flow and cell stack thermal stresses. Cell stack inlet temperatures ranged from 650 to 750 °C in 25-degree increments. Production rates ranged from 1.0 to 4.0 slpm in 0.5-slpm increments, and process air flow rates ranged from 100 to 200 slpm in 25-slpm increments.

Mule testing included untended and overnight testing to maximize total run time. Cell stack voltage/current ratios were compared each month to check for changes in cell stack performance.

The trailing edge of an oxygen generator with a single cell has a relatively uniform radiative environment. Oxygen generators with two or more cell stacks in series have more complicated thermal environments. By measuring the lateral and vertical temperature distributions of a single-cell-stack system, cell-stack heating can be directly measured without confounding effects from downstream cell stacks.

The Mule used two thermocouples as inputs for system control and three additional thermocouples for thermal characterization. Operating the Mule under a wide range of conditions (e.g., varying cell stack temperature, process air flow, and oxygen production rate) can test the stability of system control.

As is the case for many long-duration tests, the most instructive test was unintentional. A loss of system power placed the cell stack in a more severe thermal stress environment than any planned test condition. After the loss of power event, the unit's performance was re-characterized by repeating a set of test conditions. The loss of power event did not change system performance.

Key test results and findings are:

1. Cell stack performance was evaluated over a variety of operating conditions. In general, the system response matched pretest analysis. Specifically, more process air flow was needed to remove waste heat produced by the cell stack than the process air flow rates used in Chassis 2.
2. After a change of spacing between the cell stack and heater in the CFC structure, the vertical and lateral temperature variations matched pretest analysis.
3. The system was operated for >1200 hr, with no hardware failures at a variety of process conditions.
4. Thermal characterization of a CFC was completed. Because of the thermal characterization tests, operational techniques can be developed to decrease preheat time. To date, the data show that heating at a rate of 5 °C/min does not cause structural damage. Faster heating requires a greater energy density into the system and can increase thermal stresses.
5. Laboratory-setting control systems were checked out and shown to operate within the limits of testing. A test of the software nominal operations and fault detection was completed. The developed control and fault detection logic was shown to reliably and safety control the blower, heater, and cell stack for laboratory operations.
6. The system was shown to be robust (i.e., no fracture or mechanical failure) at a cooling rate of 1 °C/min.

Limitations to the testing included:

1. The testing was restricted to one prototype.
2. Testing was restricted to ~1200 hr.
3. Surge oxygen production rates were not tested.
4. Oxygen purity was not tested.
5. Accelerated preheating profiles were not tested. Detailed thermal models of the system could provide predictive cases for the future.

7.4 Demonstration of 20.7 MPa (3000-psig) Oxygen Production

The M-COG prototype referred to as the Two-Stage M-COG was used to demonstrate the ability to produce oxygen at 20.7 MPa (3000 psig) delivery pressure. The test article uses a single cell stack CFC configuration system similar to the Mule as the first stage. The first stage extracts oxygen from ambient pressure air and produces oxygen at an intermediate pressure, generally 0.138 to 0.344 MPa (20 to 50 psig). The intermediate pressure oxygen is fed to the second stage. The second stage receives the intermediate pressure oxygen internally and electrochemically pumps the oxygen to the outside of the wafer, where pressure increases to 20.7 MPa (3000 psig).

The pressure forces place the second-stage wafers in compression. This two-stage approach using cell stacks of planar wafers had never been built or tested. Because of the unique hardware configuration and the hazards associated with 20.7 MPa (3000 psig) oxygen, initial test conditions were restricted.

Tests were conducted at the American Oxygen facility in Salt Lake City, Utah, in October 2023.

The primary objectives of the test were:

1. Evaluate stage 1 performance.
2. Evaluate stage 1/stage 2 integration.
3. Evaluate the ability of the system to generate 3.44 MPa (500 psig) oxygen.
4. Evaluate the ability of the system to generate 10.3 MPa (1500 psig) oxygen.
5. Evaluate the ability of the system to generate 20.7 MPa (3000 psig) oxygen.

As an exercise in configuration management, Stage 1 of the system was operated independently. Stage 1 oxygen product was delivered to the interstage gas storage system and subsequently vented. Nominal pressure of the Stage 1 oxygen product was 0.207 MPa (30 psig).

Stage 1 and 2 system integration tests were conducted with the Stage 2 delivery pressure set at 50 psi. This configuration tested the leakage/pressure integrity and system integration at low system pressure.

High-pressure oxygen generation was done in increments, starting with a 3.44 MPa (500-psig) oxygen delivery pressure. Progressively higher pressures allowed for a “crawl, then walk, then run” method of testing.

Intermediate pressure testing with a 10.3 MPa (1500-psig) oxygen delivery allowed for an incremental increase in pressure vessel stresses and for thermal characterization of the second stage at three different pressures. The thermal conductivity of compressed gaseous oxygen, in a complex thermal environment with compressed oxygen and insulation, could be directly measured.

The test objective was to demonstrate the ability of the system to produce oxygen at 3000 psig without mechanical compressors or hydrogen hazards. The final step in the test was demonstration of 20.7 MPa (3000-psig) oxygen delivery.

Key test results and findings are:

1. Stage 1 operated without any upsets or anomalous behavior while producing oxygen at a 2-slpm production rate, with excess oxygen vented to the room. The majority of oxygen produced by Stage 1 was fed to an interstage reservoir and vented outside. This was the first demonstration of Stage 1 feeding an interstage reservoir.
2. Stage 1/stage 2 integration was nominal. The interstage reservoir was intentionally oversized to reduce the risk of integration anomaly.
3. High-pressure oxygen was tested incrementally. Tests initially were performed at 3.44 MPa (500 psig) delivery pressure, and performance was nominal with no upsets or anomalous behavior.
4. 10.3 MPa (1500 psig) oxygen delivery was demonstrated after the 3.44 MPa (500 psig) tests were complete. Heat transfer rates through the insulated layer inside the pressure vessel were greater than pretest analysis predicted due to increased oxygen thermal conductivity.

5. 20.7 MPa (3000 psig) oxygen was produced. The system operating temperature was reduced to limit the heat transfer from the second-stage test article to the pressure vessel wall.

Limitations to the testing included:

1. For oxygen safety reasons, the pressure vessel was prefilled with nitrogen. Oxygen was electrochemically pumped from the inside of the second stage wafers to the outside. For test safety reasons, >90% of the gas inside the pressure vessel was nitrogen rather than oxygen.
2. The duration of the 3.44-, 10.3-, and 20.7-MPa (500-, 1500-, and 3000-psig) demonstration tests were each less than 1 hr.
3. The production rate of oxygen generation was kept to <0.2 slpm to minimize thermal gradients within the second-stage cell stack. The second-stage cell stack is an untested operational environment.
4. Oxygen purity was not measured.

7.5 Operation Temperatures

The M-COG nominal operational temperature is between 650 and 800 °C. Operating temperatures are actively controlled and maintained through the use of heaters, heat exchangers, and insulation. Total energy consumption will be lower when operating in hot environments and higher when operating in cold environments, given the respective reduced or increased heater power required to maintain temperature. Because M-COG is insulated and the process air heat exchanger has high effectivity, the projected differences in energy use are assumed to be small. The heat energy needed to heat the process air from ambient to operating temperature is a function of the mass flow of the process air, the ΔT between ambient and operating temperature, and the specific heat of air ($Q = m\ c\ \Delta T$). The specific heat of air is unchanged, and the mass flow of process air is unchanged. The ΔT between 20 and 700 °C is 680 °C, while the ΔT between 45 and 700 °C is 655 °C. The projected energy savings of operating at 45 °C rather than 20 °C is 3.7% [ref. 14].

Power supply, power distribution, and system control electronics can use commercially available components. Automotive-grade electronics are commonly rated for –40 to 105 °C. M-COG systems can operate in any environment within the rated temperature range of the power and control electronics, which are the limiting factors. Power supply and control electronics used for this M-COG project were engineering laboratory grade, not production grade. Before system deployment, operational systems must be built and tested in the relevant thermal environments. These tests should be focused on the integrated system, as the ceramic wafer and cell stacks have been tested in the relevant thermal environments. Additionally, thermal cycling and/or the long-term effects of thermal cycling have not yet been demonstrated or evaluated. Given the historical concerns with thermal cycling, this should be done before the system is deployed; this could determine the magnitude of allowable, repeatable temperature excursions.

7.6 Atmospheric Pressure

Operating an M-COG system at a high elevation (i.e., <3000 m) would not affect the oxygen separation process, the overall purity of the oxygen produced, or the delivery pressure. The edges of the ion transport membrane in the M-COG wafer are hermetically sealed, and oxygen collected inside the wafer is isolated from the outside environment. Each M-COG wafer is tested at a pressure differential of 1.38 MPa (200 psig). Terrestrial environmental pressures range from 0.1 MPa (14.7 psia) at sea level to 0.05 MPa (8.1 psia) at 5400 m of elevation. Stresses caused by

environmental pressure changes are small compared with stress conditions applied during M-COG component acceptance testing. Operating an M-COG assembly at high elevation/reduced pressure reduces the peak oxygen production rate for an individual device. Process air is used to regulate internal temperatures, and air at high elevations has less thermal mass and a reduced capacity to regulate internal temperatures.

M-COG is designed to operate nominally at any altitude between sea level and 3000 m. Above 3000 m, maximum oxygen production would be restricted. An M-COG designed for 0 to 10 slpm of oxygen production at sea level would be limited to 0 to 9 slpm of oxygen production if operating between 3000 and 5000 m.

7.7 Airborne Contamination

Current M-COG configurations do not require filters to remove particles from the process air. Development testing to date has indicated that M-COG cell stacks are not damaged by particulates, and particulates do not accumulate in the cell stack area. Gas velocity is higher when passing through the cell stacks than in any other part of the process air stream. Testing has shown that sand particulates (0.625 to 2 mm diameter) accumulate at the bottom of the M-COG cabinet, which can be removed via standard maintenance approaches. Smaller particulates pass through the cell stack region without accumulating, based on more than 1200 hr of cumulative test data on the unit described in Appendix C.

Effective system performance without a particulate air filter was demonstrated when a prototype M-COG system was operated continuously for 2 years in a forward operating base in Afghanistan. The M-COG system was placed outside with direct exposure to windblown sand. After 2 years of continuous operation, the M-COG was inspected. Substantial amounts of sand and particulate (>1000 grams) had accumulated in the bottom of the cabinet, but the process air moved freely, and the system pressure drop was unaffected.

The M-COG does not require chemical filtration to remove chemical contaminants, other than gettering systems to reduce airborne sulfur content. The M-COG air separation process does not allow contaminants or poisons to enter the oxygen product, so purity is not affected.

Chemical contaminants can reduce the service life of M-COG. Testing conducted at JSC demonstrated a reduction in service life when the M-COG system was exposed to high levels (>100 parts per million by volume (ppmv)) of freons for extended lengths of time (>10 days) [ref. 15]. Testing conducted by Ceramatec demonstrated that when M-COG wafers were exposed to ambient air in Salt Lake City, Utah, oxygen production rate decreased on average 0.7% for every 1000 hr of operation [ref. 16]. Post-test inspection of the wafers identified the cause of the loss of performance to be related to sulfur exposure. M-COG systems have internal sulfur getters. There are no plans to refurbish cell stacks when they reach their end of life. These getters are sized to operate for 10 years when continuously exposed to sulfur dioxide levels of 350 micrograms per cubic meter of air ($\mu g/m^3$).[2]

7.8 Humidity

M-COG produces oxygen with a purity of >99.9% while operating in conditions ranging between 0 and 100% relative humidity. The performance of the ion transport membrane is not

[2] The annual average sulfur dioxide level in New York City in 2021 was 12 $\mu g/m^3$.

affected by the presence or absence of nitrogen, argon, carbon dioxide, or water vapor. The nitrogen, argon, and other non-oxygen constituents in the air sweep across the wafer and remove waste heat, but they are not involved in the oxygen ion transport process, and their presence or absence does not affect the rate of oxygen transport. Trace amounts of water vapor are measured in M-COG oxygen via FTIR. The maximum amount of water vapor in M-COG oxygen measured during Chassis 2 M-COG testing was 40 ppmv (Appendix B). The permissible amount of water vapor in medical grade oxygen is 67 ppmv [ref. 17].

Diagnostic testing suggests that trace water vapor is caused by permeation across cell stack seals rather than by transport through the ion transport membrane [ref. 18]. The M-COG produced >99.9% oxygen when water mist was intentionally added to the process air stream. M-COG testing is limited, and more testing is needed to understand the effects of environmental temperature and humidity on trace levels of water vapor in product oxygen and to provide full assembly service life validation. A more detailed description of water vapor permeation through the washer seal is described in Section 7.15.

7.9 Operational Scale

The main component of M-COG is the 30-wafer cell stack, which can produce 4 to 4.5 slpm of oxygen, with larger systems incorporating additional 30-wafer cell stack assemblies. Power efficiency is better for large-scale systems due to the increased thermal mass. It is assumed that single- or multi-stack systems will have comparable reliability and service life.

7.10 Packaging and Transportation

M-COG system packaging is designed to protect the ceramic stacks, and M-COG systems have been successfully transported using commercial shipping methods. The ceramic cell stack is enclosed within a stainless-steel housing, and the boxed cell stack is secured in the oxygen engine using spring mounts (see Figures 6.4-3 and 6.4-4). M-COG cell stacks are secured within a stiff structural housing, which is spring mounted to allow the system to withstand shipping vibrational and shock loads. Section 7.14 provides further discussion regarding the effects of damage on system operation. Further testing and deployment of M-COG systems will enable more robust failure modes effects analysis and system risk analyses to be performed.

M-COG systems can be shipped using standard commercial transport methods and stored in ambient environments without climate control. In May 2023, an M-COG prototype system with the CFC configuration was transported using a commercial shipping service with no special shipping requirements (Figure 7.10-1). The packaging consisted of plywood with no strict contamination- or particulate-control requirements. Future work would include reviewing aerospace processes (e.g., shipping with accelerometers and applying shipping load requirements to the hardware and packaging systems) to ensure loads are within family, prior to system initiation. The shipping demonstrated was on an older system and the applicability of the shipping and packaging processes have not been repeatably demonstrated on all generations of the M-COG assemblies.

Figure 7.10-1. M-COG with Spring Mounts for Transportation

7.11 Pressurized Oxygen Generation

It is not intuitive that a solid-state technology could produce pressurized oxygen without the use of mechanical compressors. Figure 7.11-1 provides a graphical illustration of the oxygen pressurization process. The process air region is the open-air environment where process air moves across the outside surfaces of the wafer at ambient pressure. The oxygen generation region is closed and sealed, except for the ion transport membranes that allow oxygen into the system and a delivery port that allows oxygen out of the system. The delivery port has a mechanical pressure regulator. As the feed gas enters the oxygen generation region through the ion transport membranes, the pressure increases. When the pressure exceeds the pressure regulator set point, the pressure regulator opens and delivers pressurized gas to the oxygen delivery region. The set point of the mechanical pressure regulator establishes the delivery pressure. The M-COG oxygen generation function is the same regardless of the regulator set point. Wafers and cell stacks are pressure tested at 1.38 MPa (200 psig). If the regulator pressure is set to a delivery pressure higher than 1.38 MPa (200 psig), then there is a risk that the pressure forces within the oxygen generation region could cause the wafers to crack or rupture.

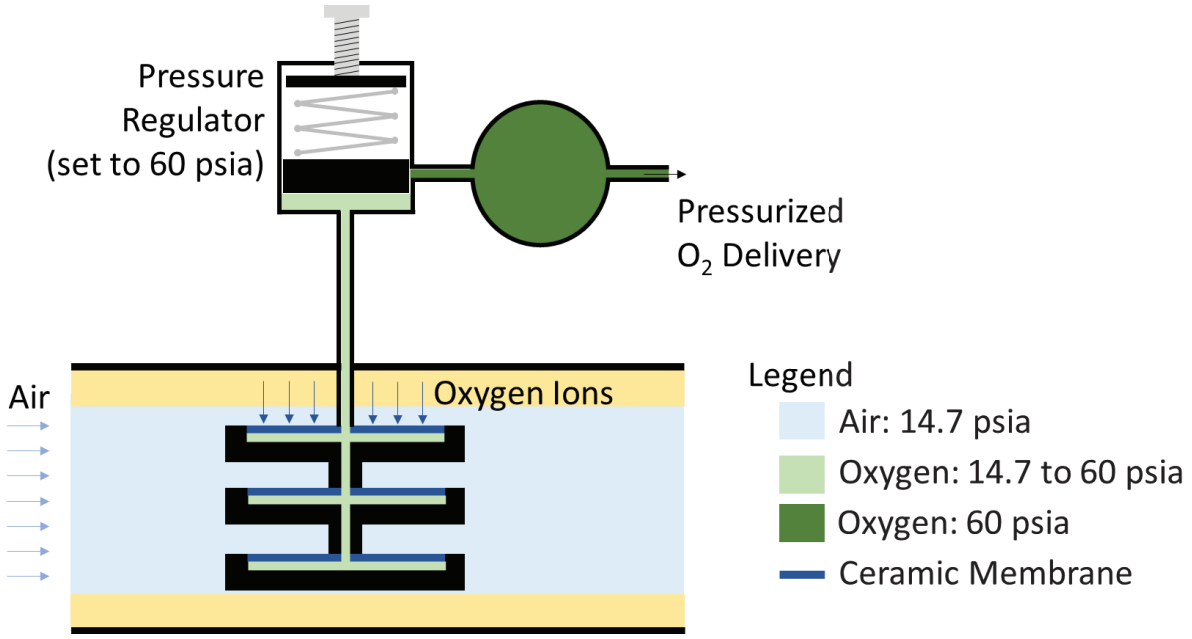

Figure 7.11-1. M-COG Oxygen Pressurization Process (pressure regulator is set to 60 psia)

7.12 Power Requirements

M-COG power use is primarily a function of heater power, cell stack power, and blower and control electronics, with the heater and cell stack power as the predominant drivers. The relative amount of heater power to cell stack power depends on the operating temperature (see Figure 7.12-1). Cell stack power requirements exponentially decrease as the operating temperature increases. For equivalent rates of oxygen production, the power consumption for the cell stack is more than 1500 W at an operating temperature of 500 °C and less than 100 W at 800 °C. Power requirements for the heater trend in the opposite direction. Heater power requirements increase substantially as operating temperature increases.

The conflicting trends of cell stack power and heater power produce the following conundrum: increasing operating temperatures to achieve more efficient cell stack performance results in M-COG systems that require substantially more insulation and larger heaters. Decreasing operating temperatures to reduce heater power consumption results in greater power use by the cell stacks. The optimum "saddle point" operating temperature with the greatest overall power efficiency depends on the thermal design. Improving heat exchanger performance and increasing the amount of thermal insulation results in a higher optimum temperature. Generally, the most efficient system-level operating temperature has been between 700 and 750 °C, per Appendix C.

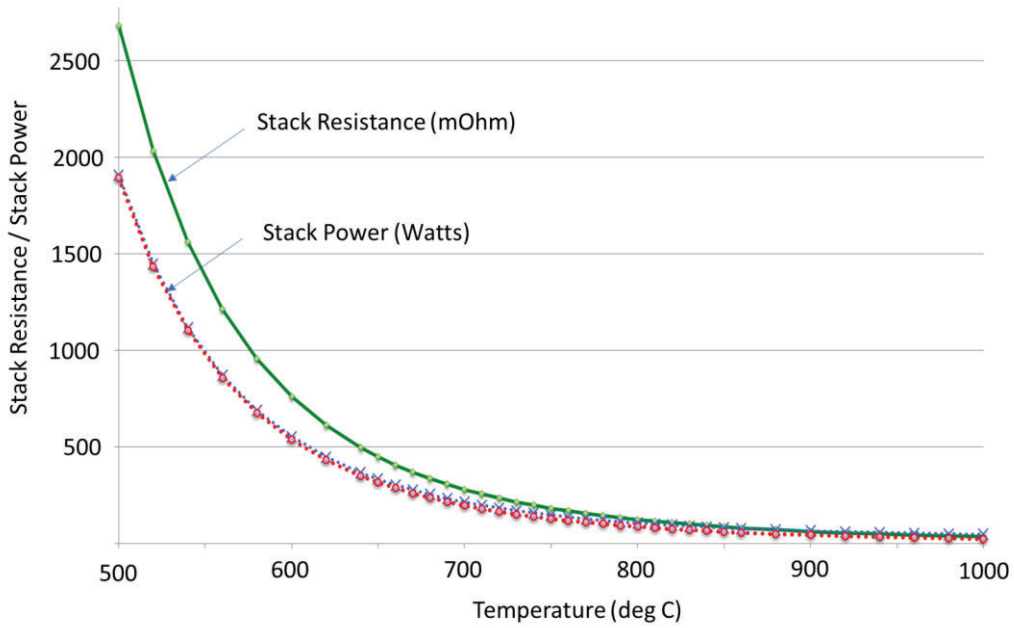

Figure 7.12-1. Cell Stack Resistance and Cell Stack Power Consumption as a Function of Temperature

A thermal management system was developed that has resulted in a substantial improvement in power efficiency. Earlier ion transport systems used a single cell stack, and the operating temperature of this cell stack was set to the optimum temperature that best balanced heater power with cell stack power. M-COG systems use multiple cell stacks, placed in series, sharing the same process flow stream. The amount of process air flow used is substantially greater than the minimum amount of process air needed to supply fresh oxygen to the cell stack. Large amounts of process air sweep across the wafer to regulate temperature. The process air leaving the first cell stack has enough oxygen to supply a second cell stack with oxygen, and the second stack operates more efficiently because it can operate at a higher temperature.

Figure 7.12-2 and Table 7.12-1 describe a simplified thermal sizing analysis comparing M-COG systems with one, two, three, and four cell stacks placed in series, with each cell stack sharing a common process air flow stream. This is a simplified thermal sizing analysis that does not account for parameters (e.g., system size, changes in the volume of process air, or changes in heat losses to the environment), but this simplified sizing calculation can demonstrate the magnitude of impact that series-segmented configuration can have on power use.

The assumptions for the thermal sizing analysis are:

- Cell stack power is 100 W for 1 slpm oxygen production.
- Cell stack production rate increases 10% for each 30 ℃ increase in operating temperature.
- Heater power is 200 W to heat process air by 80 ℃.
- Heater power use is a linear function of total heating (e.g., heating the process air by 40 ℃ requires 50% of the power to heat the process air by 80 ℃).
- Heat exchanger efficiency is 85% for all operating temperatures.

Figure 7.12-2 maps the temperatures through the process air stream for M-COG configurations with one, two, three, and four cell stacks. Notice the temperature of the hot air inlet to the heat

exchanger increases from 730, to 760, to 790, to 820 °C. The increase in hot air inlet temperature increases the cold air exit temperature from 620, to 650, to 675, to 700 °C. The resulting heater requirements change from increasing the process air stream temperature by 80 °C, to increasing by 50 °C, to increasing by 25 °C, to no need to use process heaters.

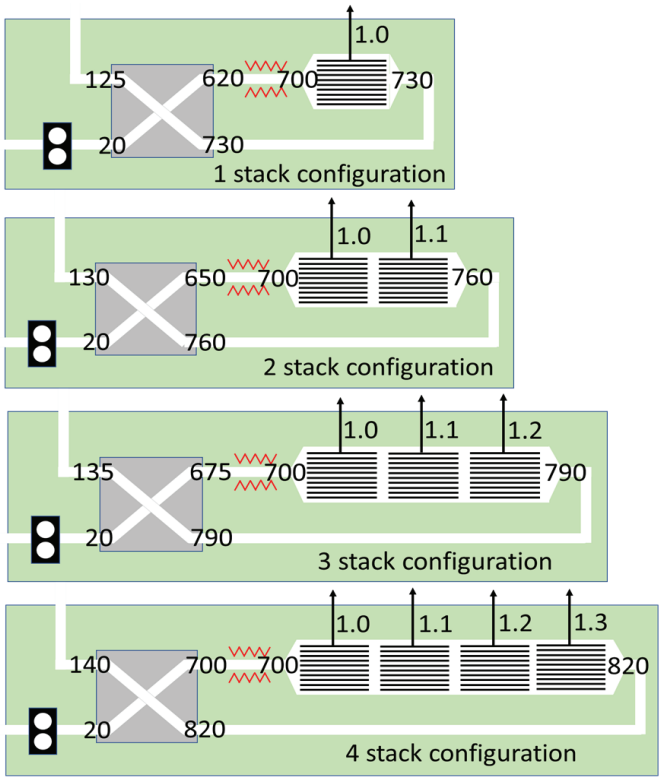

Figure 7.12-2. M-COG System Thermal Sizing Estimate Comparing Temperatures of One, Two, Three, and Four Cell Stacks

Table 7.12-1. Power Consumption for Thermal Sizing Analysis comparing M-COG System with One, Two, Three, and Four Cell Stacks

Number of Cell Stacks	Heater Power (W)	Stack Power (W)	Total Power (W)	Total O_2 (slpm)	Power Efficiency (W per slpm)
1	200	100	300	1.0	300
2	125	200	325	2.1	155
3	65	300	365	3.3	110
4	0	400	400	4.6	90

Assumptions:
Cell stack power at 700 °C is 100 W for 1 slpm oxygen production.
Each cell stack heats the process air 30 °C.
Cell stack production increases 10% for each 30 °C increase in operating temperature.
Heater power: 200 W to heat process air 80 °C (linear relationship with *dT*).
Heat exchanger thermal efficiency is 0.85.

Figure 7.12-3 shows an M-COG system with eight cell stacks in series. This system demonstrated that it is possible to develop an M-COG system that does not use heater power during steady-state operation (i.e., the temperature of the process air exiting Cell Stack 8 was sufficient to preheat the incoming air to operating temperature without additional heater power). Chassis 2 testing used an oxygen engine with four oxygen-producing cell stacks and four cell-stack surrogates, which added the appropriate amount of heat to the process air. This simplified thermal sizing exercise does not account for all aspects of thermal management but predicts that a four-cell-stack system would not require additional heater power. Any specific designs would require validation of the thermal approach with test data.

The prototype shown in Figure 7.12-3 demonstrated that, in a working system, heaters could be turned off with an eight-cell-stack system. Theoretically, a system that is self-heating is capable of thermal runaway (i.e., if cell stacks are powered on a fixed-voltage basis). M-COG cell stacks are powered on a current-controlled basis. In a current-controlled configuration, if the cell stacks increase in temperature, then they produce the same amount of oxygen (i.e., oxygen generation rate is set by current), but the cell stack power use drops because less voltage is needed to supply the specified amount of current.

The M-COG Chassis 2 prototype was tested, demonstrating that the heaters could be turned off during steady-state operations. The heat generated by the eight cell stacks was sufficient to maintain process temperature without the use of heaters. This testing demonstrated oxygen production of 4.5 slpm with 400 W of input cell stack power, resulting in a specific power of 89 W per slpm for these test conditions.

Figure 7.12-3. M-COG Prototype Chassis 2 Configured with Eight Cell Stacks in Series

7.13 Oxygen Purity

Oxygen produced by M-COG has a purity of ≥99.9%, with the main constituent of the trace material being water vapor. The water vapor is believed to enter the oxygen by permeating across the ceramic washer seals from the process air into the oxygen. Water vapor contamination observed in testing (described in Section 7.14) was limited to <50 ppmv but was limited in the range of air stream inlet water vapor.

The ion transport membrane is capable of transporting oxygen ions and is sealed off from the outside environment. The two ways for chemical constituents to get from process air to the oxygen generation region are via water vapor permeation through the washer seal and oxygen ion transport. The oxygen purity assessment assumes the M-COG system is performing nominally and has not been compromised (e.g., fractures, leaks, etc.). A specific example of operation under an off-nominal configuration is described in Section 7.14.

A limited number of ceramic materials conduct electricity via diffusion of oxygen ions through their crystalline lattice. While some of these materials can simultaneously conduct electricity via transport of electrons and/or other ionic species, for certain materials the contribution of these alternative conduction mechanisms is so negligible that the transport of oxygen ions accounts for essentially all the electrical conductivity. Materials exhibiting this exclusivity include the membrane material employed in M-COG technology, which is samarium-doped cerium oxide (CSO).

Cerium oxide (ceria) crystallizes in the fluorite structure, which consists of a cubic oxygen lattice with cerium atoms uniformly distributed. When some of the cerium atoms are replaced with a suitable lower valence dopant element (e.g., rare earth samarium or gadolinium), electroneutrality requirements require a significant number of empty oxygen sites within the crystal structure. Under the influence of an applied electrical field, these oxygen vacancies allow oxygen ions to diffuse unidirectionally through the material by hopping from one lattice site to another. As a result, a thin, dense membrane of rare-earth-doped ceria can be used as an oxygen transport membrane [refs. 4-6, 19-29]. Note that doped ceria can exhibit ionic and electronic conductivity under reducing atmosphere conditions. However, under the oxidizing conditions present in M-COG stacks, electronic conductivity is negligible [refs. 10, 30, 31]. There is an activation energy associated with the oxygen diffusion process, so the conduction of oxygen ions through the membrane is thermally activated (i.e., ionic conductivity increases with increasing temperature). Thus, to minimize the amount of electrical energy required to obtain a significant flux of oxygen through the membrane, ceria-based devices typically operate at temperatures above ~550 ℃. M-COG stacks operate in the 650 to 850 ℃ temperature range.

CSO's value as an oxygen membrane material lies in its ability to extract purified oxygen from air. To produce a highly pure oxygen stream, it is essential that other gas species in the air supply (primarily nitrogen (~78%), argon (~1%), and water vapor (~1-3%)) not be transported through the membrane. Fortunately, CSO exhibits this necessary selectivity [ref. 32].

Nitrogen: Studies on a fluorite structure solid oxide electrolyte material, yttria-stabilized zirconia (YSZ), reported solubility and conductivity of nitrogen and oxygen ions. However, while this phenomenon can occur under reducing (i.e., low oxygen partial pressure) conditions, it does not occur under the oxidizing conditions relevant to M-COG operation [refs. 33-40]. Solubility of nitrogen ions in doped ceria has been reported, but this solubility only occurred under reducing conditions [ref. 41].

Argon: Argon is chemically inert and does not form anions. Its atomic size, relative to oxygen (e.g., atomic radius of 106 versus 66 picometers (pm)), prevents argon anions from occupying vacant oxygen sites in the ceria crystalline lattice. Solid oxide membrane technology was developed to remove oxygen from impure argon gas streams. The membrane is used to remove oxygen from the gas stream, leaving the impermeable argon and other trace species. This technology was based primarily on YSZ membranes, but it was specified that doped ceria membranes could perform the same function [refs. 42, 43].

Water: Water molecules can be dissociated electrolytically into oxygen and hydrogen. However, M-COG's operating voltage (typically ~300 millivolts) is below the thermodynamic decomposition potential for water, so dissociation of water molecules would not be expected to occur under M-COG operating conditions. Cell stack power supplies have voltage limits that restrict molecular decomposition to oxygen only. Operation at significantly higher voltage could lead to localized dissociation of water molecules at or near the cathode/electrolyte interface, but due to the ~20% concentration of oxygen in air there would be a strong thermodynamic driving force for hydrogen produced to immediately react with available oxygen to reform water molecules. [ref. 44]. Note that this is an evaluation of the ability of the ion transport membrane to transport water vapor. Section 7.15 assesses water vapor transport through the washer seal.

Carbon dioxide: The same disassociation condition could apply to carbon dioxide molecules in the process air that encounter the active part of the cell, although that should require higher applied voltage than for M-COG operation. As with water, carbon monoxide produced via dissociation should react with surrounding oxygen molecules to re-form carbon dioxide.

Hydrogen: While hydrogen (protonic) conduction has been reported in doped ceria, it was only significant under reducing conditions, which are not relevant to M-COG operation. Because protons are positively charged, the direction of the applied voltage in M-COG operation would be expected to drive protons from the oxygen product side of the membrane [refs. 45, 46].

Additional analysis for other trace gas contaminants has not been pursued.

Detailed chemical analysis of M-COG purity is limited, as these analyses are expensive and time consuming. Results of the NASA chemical analyses of oxygen generated by M-COG are summarized as:

- A chemical analysis of an earlier version of an M-COG system was conducted in June 2012 [ref. 47]. Reported oxygen purity was >99.9%, which is the highest purity possible given the limitations of the chemical analysis. Combined nitrogen and argon was determined to be less than 100 ppmv (the limits of the chemical analysis), carbon dioxide was less than 1 ppmv, methane was less than 1 ppmv, and all other hydrocarbons were less than 1 ppmv. Water vapor was not evaluated due to limitations in the method of chemical analysis.
- A chemical analysis of M-COG Chassis 1 products was conducted in August 2021 (Appendix A). Reported oxygen purity was 99.97%, nitrogen levels were reported at 246 ppmv, carbon dioxide was 0.14 ppmv, and water vapor was 37 ppmv.
- Argon was below the 1-ppmv detection level, and all organic hydrocarbons were below the 1-ppmv detection level. This chemical analysis is described in Appendix B.
- A chemical analysis of M-COG Chassis 2 products was conducted in December 2022 (Appendix B). Reported oxygen purity was 99.995%. Water vapor was 40 ppmv, nitrogen

and argon levels were below the 5 ppmv detection limit, methane was below the 1 ppmv detection limit, and all other organic hydrocarbons combined were measured to be 5.7 ppmv.

Analytical assessments and chemical measurements of these three development units support the conclusion that M-COG oxygen purity met the >99% oxygen purity standard for medical oxygen listed in the United States Pharmacopeia (USP).[3]

7.14 Oxygen Purity from Off-nominal Operation

The M-COG oxygen purity assessment provided in Section 7.13 assumes an intact M-COG system with no leaks, cracks, or fractures in the system. A hazard analysis was conducted for the M-COG process and raised a specific hazard scenario [ref. 48]:

- What if an M-COG wafer was cracked? Would it be possible for an M-COG system with a crack to suffer in-leakage of outside contaminating gases, resulting in an oxygen stream with a purity less than 99.9%?

The test of Chassis 1, conducted in August 2021 (Figure 7.14-1), provided an unplanned opportunity to test this scenario. Chassis 1 used a preliminary test support fixture for the terminal plumbing assembly. The project schedule required the M-COG to be demonstrated as a working system, but the detailed design of the terminal plumbing assembly had not been developed. To support the August 2021 test, a simplified joint was used to connect the ceramic cell stack and the metal piping, but this joint fractured during shipping. Diagnostic tests determined the fracture was so severe that the system was incapable of producing oxygen at 0.007 MPa (1 psig).

WSTF personnel reconfigured the gas sampling system to allow a chemical analysis even through the oxygen product was unpressurized. The gas analysis measured the oxygen purity and determined it to be 99.97% (Appendix A). This type of leak represents the maximum potential leakage for a functional system, and the system was able to achieve oxygen purity of 99.97%. For the results above, it is important to note that this situation is valid as long as the M-COG system maintains a positive internal pressure; were that not the case, there is potential for ingress of contaminants.

[3] The USP is a compendium of drug information for the United States published annually by the more than 200-year-old United States Pharmacopeial Convention. The USP sets quality, purity, strength, and identity standards for medicines, food ingredients, and dietary supplements. The USP collects and disseminates product use information to providers and consumers and publishes revised standards every 5 years. https://www.usp.org/

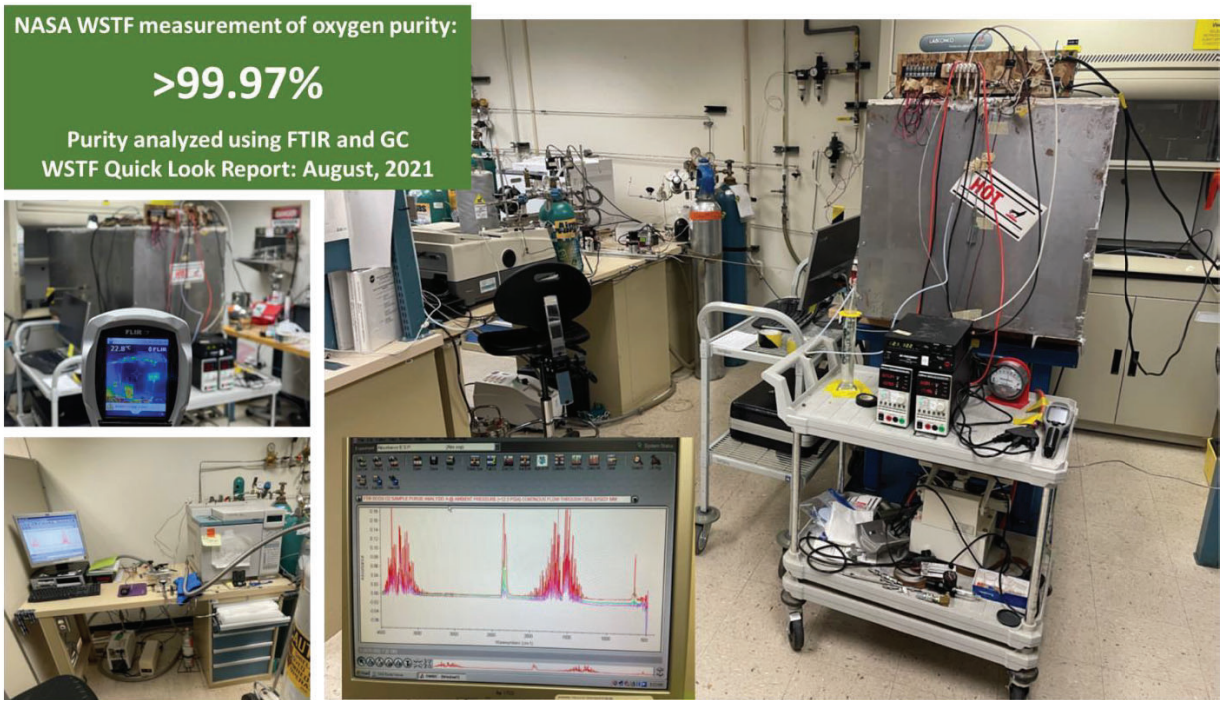

Figure 7.14-1. Images from Chassis 1 Testing

7.15 Water Vapor Transport Phenomena

Ion transport membranes are selective to oxygen and produce a pressurized product that contains oxygen with trace amounts of water vapor. The highest level of water vapor measured to date is 40 ppmv. The USP does not specify a limit for trace water vapor in >99.0% oxygen. The European Pharmacopoeia for medical oxygen [ref. 17] specifies that medical oxygen must contain less than 67 ppmv water vapor.

The suspected mechanism for water vapor transport from the air into the oxygen is through the washer seals in the cell stack. The cell stack operating temperature is nominally 700 °C; glasses and other amorphous silicate materials are permeable to water vapor at these elevated temperatures [ref. 47]. Diagnostic testing measured the effects of changes in oxygen generation rate and humidity levels in the process air on water vapor levels in product oxygen [ref. 18]. Test data trends were consistent with analytical models for permeation of water vapor across the washer seal material.

7.16 Projected Service Interval

Figure 7.16-1 shows a forward operating base in Afghanistan and a prototype M-COG system that operated continuously for 2 years, where it was operationally used as an experimental approach due to challenges with oxygen logistics specific to this location.

The M-COG system (Figure 7.16-1) includes two M-COG units in a CFC configuration and two mechanical compressors. The M-COG units operated continuously throughout the 2-year deployment. The M-COG units delivered low-pressure oxygen to a low-pressure receiver tank, which was subsequently pumped by a mechanical compressor into high-pressure cylinders. During the 2-year deployment, the compressors required scheduled service after 1 year, and one

thermocouple failed, requiring replacement. The M-COG blowers and cell stacks operated continuously without maintenance for the duration of the deployment.

Figure 7.16-1. Forward Operating Base in Afghanistan (left) and Early M-COG System with Mechanical Compressors for Cylinder Filling Operations (right)
Note: The M-COG system is shown prior to installation outside the shelters.

This unplanned field test used a M-COG engineering prototype. This system involved only two devices; no large-scale or statistically relevant data regarding maintenance needs in field use conditions are available. However, this test suggests that 2-year operability is possible with an appropriately designed inspection/maintenance cycle.

7.17 Wafer Service Life Testing

Figure 7.17-1 shows a long-term wafer test facility and test results. More than 40 wafers were tested under operating conditions, with the longest duration tests exceeding 50,000 hr (6.2 years) [ref. 49]. Some of the wafers were intentionally challenged with high levels of environmental pollutants, resulting in an accelerated life test. None of the wafers tested suffered a leak, crack, or any form of structural failure. Further, none of the wafers suffered a failure mode that affected oxygen purity.

Changes in wafer performance over time relate to area specific resistance (ASR), which is a measure of power consumption and heat generation. Operationally, as the ASR of a wafer increases over time, total system power is maintained, and the oxygen production rate decreases. The average change in ASR for the wafers tested is a 0.7% increase in ASR for each 1000 hr of operation. Post-test chemical analysis of the wafers indicates the primary cause of ASR change relates to sulfur contamination of the cathode, which was directly exposed to ambient air in the long-duration test. The M-COG design has a getter to remove sulfur from the supply air, which protects the cell stack from exposure to sulfur. This would indicate that the measured rate of 0.7% per 1000 hr is conservative, and the rate of change of ASR in operational systems should be less than 0.7%. The test data, at the time of his report, are limited to 40 total wafers, with the longest duration life test lasting 55,000 hr.

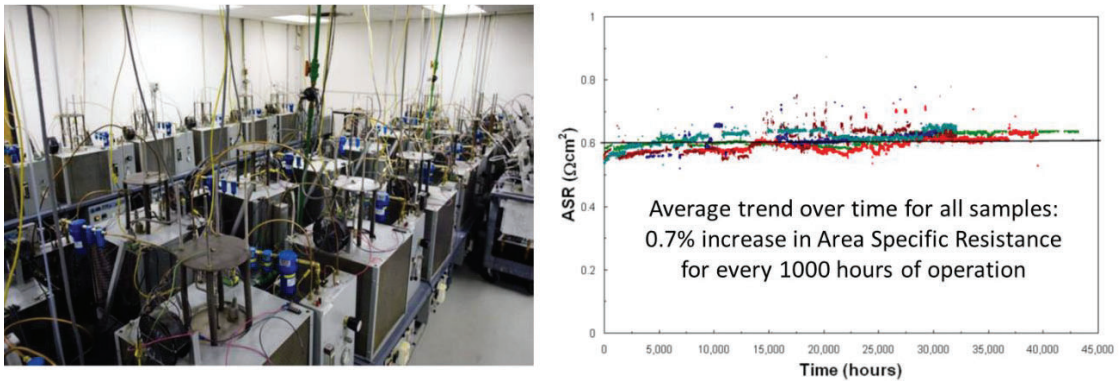

Figure 7.17-1. Long-term M-COG Wafer Test Facility (left), and Long-term Test Data (right)

7.18 Projected Storage Life

Figure 7.18-1 shows an image of an M-COG system that was received by NASA in 2011, operated until 2013, and then placed in storage from 2013 until 2021. There were no special provisions for storage, and the device was not capped, sealed, or mechanically altered. In 2021, the system was shipped from Houston, Texas, to Salt Lake City, Utah, and restarted without any modification or service to the system. Restart and operations were nominal. There was no discernable change in performance between 2013 and 2021.

This unplanned storage life test provides limited empirical data that the system offers storage and restart capability. Additional testing would more accurately define appropriate storage times and conditions for immediate restart without maintenance and inspection activities. It would be desirable for the system to have longer and less-well-defined storage conditions, as equipment that can be stored without special packaging, reconfiguration, or regularly scheduled performance tests can better serve the needs of emergency medical response. Note that direct testing of system performance after long-term storage is restricted to a single device, so no statistically relevant data regarding long-term storage is available.

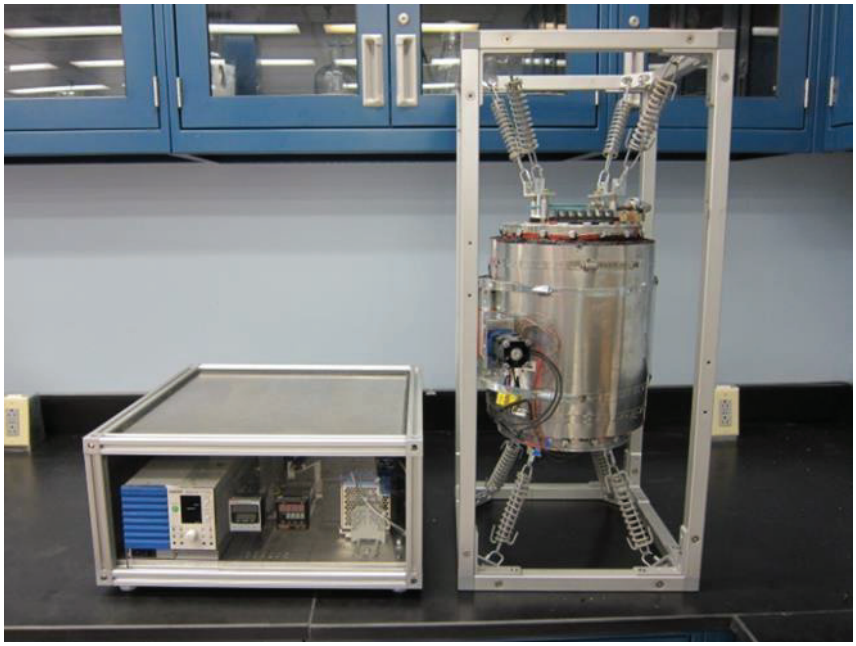

Figure 7.18-1. M-COG System Operated, Placed in Storage for 8 Years, and Successfully Operated

8.0 Current Manufacturing Status

During this assessment, a cell stack (Figure 6.4-4) was fabricated, tested, and shown to produce oxygen with a purity of >99.9 vol. % at a pressure >0.55 MPa (80 psig), with a power consumption of <100 W per slpm at a production rate of 4.5 slpm per cell stack. Testing of the ceramic wafers has been conducted, as discussed in Section 7.13.

The major remaining work is focused on life testing validation of commercial off-the-shelf components; the demonstrated reliable, continuous long-term operation of multiple M-COG systems to gain statistically anchored data and common failure and anomaly modes; and the development of repeatable and robust hardware fabrication and assembly practices that conform to regulatory requirements.

9.0 Conclusions

The NESC established the M-COG project to accelerate the pace of technology development of ion transport membrane oxygen generators, develop prototype systems, demonstrate the technology, and establish partnerships with health organizations working to improve access to medical oxygen. Results of the project are summarized in Table 9.0-1. The M-COG project met the main objectives defined at the start of the project and substantially improved the technical maturity of ceramic ion transport membrane technology. Key manufacturing risks have been reduced. Thirty-wafer cell stacks have been manufactured, tested, and shown to meet performance goals for power use, oxygen purity, production rate, and delivery pressure.

Table 9.0-1. M-COG Project Objectives and Accomplishments

Task	Status at Project Start	Status at Project Completion
Retire manufacturing risks associated with wafer and cell stack production	• Delaminated wafers • No cell stacks • No balance of plant	• First-stage cell stacks: R&D done, ready for manufacture • Second-stage wafer: 3000-psig wafers prototyped

Demonstrate large-scale medical-grade oxygen generation	• 2-slpm cell stacks (2010-2015)
	• No ability to produce oxygen in 2020
		• Plan to modularize cell stacks into larger systems
		• Demonstrated individual modules:
		  • Power: 400 W for 4.5 slpm
		  • Production: 30-wafer cell stack capable of producing 4.5 slpm
		  • Purity: 99.997%

Outline a plan for FDA certification	• No understanding of medical oxygen certification • No plan for certification	• Plans for hospital field tests • FDA/International Organization for Standardization (ISO) plan • ISO committee member advocate

Proof-of-concept cell stacks capable of withstanding a 20.7-MPa (3000-psig) pressure differential have been manufactured, tested, and shown to transport oxygen ions against a

20.7-MPa (3000-psig) pressure differential without cracking or leaking. These high-pressure wafers have not been integrated into full-scale cell stacks, but the viability of generating 20.7-MPa (3000-psig) oxygen using ceramic ion transport membrane technology has been shown.

Chassis 2 has demonstrated the ability to produce large amounts of oxygen without requiring supplemental heater power, and 30-wafer cell stacks have been shown to produce 4.5 slpm of oxygen.

M-COG is not certified for medical use, but prototype M-COG systems are available for field testing in a hospital environment. NASA is partnering with global health organizations to conduct these tests. NASA has been coordinating activities with stakeholders and communicating technical progress with global health organizations. The M-COG Technical Interchange Meeting held in Salt Lake City, Utah, in July 2021 had a special session on global health, with presentations given by:

- The Wellcome Trust
- Unitaid
- US Development Finance Corporation
- The Center for Disease Dynamics, Economics, and Policy
- The Center for Public Health & Development
- United Nations Office for Project Services
- Air Liquide Healthcare
- Sanrai International
- PCI Oxygen Solutions
- Ecole Polytechnique Federale Laussanne
- Global Health Labs
- UNICEF
- Just Actions

10.0 Findings, Observations, and NESC Recommendations

10.1 Findings

F-1. A 30-wafer M-COG cell stack was developed and tested, indicating that 4.5 slpm of purified oxygen can be produced at a pressure of 80 psig and a purity of >99.9% while consuming 400 W of power.

F-2. A two-stage ceramic oxygen generation proof-of-concept test was conducted, which suggests an ion transport membrane system is capable of producing purified oxygen with a pressure of 20.7 MPa (3000 psig).

11.0 Alternate Technical Opinion

No alternate technical opinions were identified during this assessment by the NESC assessment team or the NESC Review Board (NRB).

12.0 Other Deliverables

In addition to the final report, the M-COG project produced the following hardware assets that can be transferred to the JSC Engineering Directorate:

- Prototype M-COG oxygen generator: Chassis 1
- Prototype M-COG oxygen generator: Chassis 2
- Prototype M-COG oxygen generator: CFC-1 (the Mule)
- Prototype M-COG oxygen generator: 20.7 MPa (3000-psig) high-pressure O_2 demonstrator
- M-COG wafers: quantity, 1450

13.0 Recommendations for the NASA Lessons Learned Database

No recommendations for NASA lessons learned were identified as a result of this assessment.

14.0 Recommendations for NASA Standards, Specifications, Handbooks, and Procedures

No recommendations for NASA standards, specifications, or procedures were identified as a result of this assessment.

15.0 Definition of Terms

Finding	A relevant factual conclusion and/or issue that is within the assessment scope and that the team has rigorously based on data from their independent analyses, tests, inspections, and/or reviews of technical documentation.
Observation	A noteworthy fact, issue, and/or risk, which is not directly within the assessment scope, but could generate a separate issue or concern if not addressed. Alternatively, an observation can be a positive acknowledgement of a Center/Program/Project/Organization's operational structure, tools, and/or support.
Recommendation	A proposed measurable stakeholder action directly supported by specific Finding(s) and/or Observation(s) that will correct or mitigate an identified issue or risk.

16.0 Acronyms and Nomenclature List

°C	degrees Celsius
°F	degrees Fahrenheit
$\mu g/m^3$	micrograms per cubic meter of air
A	ampere
ASR	Area Specific Resistance
CFC	Cross Flow Cylinder
cfm	cubic feet per minute
COG	Ceramic Oxygen Generator
CSO	Samarium-doped Cerium Oxide, $Ce_{1-x}Sm_xO_2$
CTE	Coefficient of Thermal Expansion

DC	Direct Current
EVA	Extravehicular Activity
FDA	Food and Drug Administration
FTIR	Fourier Transform Infrared Spectroscopy
GC	Gas Chromatography
GRC	Glenn Research Center
GSFC	Goddard Space Flight Center
HEOMD	Human Exploration and Operations Mission Directorate
hr	hour
ISO	International Organization for Standardization
IWC	inches of water column
JPL	Jet Propulsion Laboratory
JSC	Johnson Space Center
K	kelvin
kPa	kilopascal
LaRC	Langley Research Center
m	meter
M-COG	Medical Ceramic Oxygen Generator
min	minute
mL	milliliter
mm	millimeters
MPa	megapascal
NESC	NASA Engineering and Safety Center
pm	picometer
ppmv	parts per million by volume
PSA	Pressure Swing Adsorption
psi	pounds per square inch
psia	pounds per square inch absolute
psig	pounds per square inch gauge
R&D	Research and Development
SEM	Scanning Electron Microscope
slpm	standard liters per minute
TPA	Terminal Plumbing Assembly
TRL	Technology Readiness Level
USAF	United States Air Force
USAID	United States Agency for International Development
USD	United States Dollars
USP	United States Pharmacopeia
vol. %	volume percent
W	watt
WFF	Wallops Flight Facility
WSTF	White Sands Test Facility
YSZ	Yttria-stabilized Zirconia

17.0 References

1. Graf, J. “Mapping the Capabilities and Attributes of Solid Oxide Electrochemical Systems to Human Spaceflight Needs,” 49th International Conference on Environmental Systems, ICES-2019-326 7-11, Boston, MA, July 2019.
2. Graf, J., Taylor, D., and Tylka, J. “Ceramic Oxygen Generator: A Method for Extracting High Pressure, High Purity Oxygen from Spacecraft Cabin Air,” ICES-2023-408, 52nd International Conference on Environmental Systems, Calgary Canada, July 2023.
3. Studer, D. “Demonstration of a Cylinder Fill System Based on Solid Electrolyte Oxygen Separator (SEOS) Technology: Early Field Assessment at a USAF Maintenance Facility,” AFRL-RH-BR-TR-2010-0046, Air Products and Chemicals, Inc., June 2010.
4. Skinner, S. J. and Kilner, J.A. “Oxygen Ion Conductors,” *Materials Today*, Vol. 6, Issue 3, pp. 30-37, 2003.
5. Zhang, T. S., Ma, J., Luo, L. H., and Chan, S. H. “Preparation and Properties of Dense $Ce_{0.9}Gd_{0.1}O_{2-\delta}$ Ceramics for Use as Electrolytes in IT-SOFCs,” *J. Alloys and Compounds*, Vol. 422, Issues 1-2, pp. 46-52, 2006.
6. Kuharuangrong, S. “Ionic Conductivity of Sm, Gd, Dy and Er-doped Ceria,” *J. Power Sources*, Vol. 171, Issue 2, pp. 506-510, September 2007.
7. Halley, S., Pasupathikovil-Ramaiyan, K., Tsui, L., and Garzon, F. “A Review of Zirconia Oxygen, No_x, and Mixed Potential Gas Sensors – History and Current Trends,” *Sensors and Actuators B: Chemical*, Vol. 370, 132363, November 1, 2022. doi.org/10.1016/j.snb.2022.132363
8. Straits Research. “Automotive Oxygen Sensor and Dynamic Sensor Market,” Straits Research Report Code SRAT2605DR.
9. American Oxygen, “Manufacture of 340 Wafer-Washer Assemblies,” American Oxygen Task Report #16, NASA PR# 80JSC021F016, September 2022.
10. Tuller, H. L. and Nowick, A. S. “Doped Ceria as a Solid Oxide Electrolyte,” *J. Electrochem. Soc.*, Vol. 122, No. 2, p. 255, 1975.
11. Zhang, Q., Liu, Y., Li, Z., Xiao, P., Liu, W., Yang, X., Fu, Y., Zhao, C., Yang, R. T., and Webley, P. A., “Experimental Study on Oxygen Concentrator with Wide Product Flow Rate Range: Individual Parametric Effect and Process Improvement Strategy,” *Separation and Purification Technology*, Vol. 274, November 1, 2021, 118918.
12. Ten Tips to Maximizes Heater Performance,” Watlow Engineering Tools. URL: https://www.watlow.com/resources-and-support/engineering-tools/knowledge-base/heater-performance-tips, last accessed December 11, 2023.
13. American Oxygen, “Delivery of 30 Wafer Cell Stack,” NASA PR# 80JSC021F0317, American Oxygen Task Report #21, September 2022.
14. Weislogel, M., “M-COG Thermal Assessment,” Presented at the M-COG Face-to-Face Technical Interchange Meeting, Fort Worth Texas, September 2022.
15. Broerman, C. “Memorandum for the Record (MFR) on the Freon Exposure Testing of the Ceramatec Solid Electrolyte Oxygen Separator (SEOS),” JETS-JE13-15-0512-MEMO, May 2015.
16. Taylor, D. “Solid Electrolyte Oxygen Separator (SEOS),” Presented at Oxygen Systems Coordinating Group (OSCG), San Antonio, TX, July 2010.

17. European Pharmacopoeia. Oxygen Monograph 0417, 11th Edition, effective January 1, 2023.
18. Graf, J., Taylor, D., and Martinez, J. "Determining the Source of Water Vapor in a Cerium Oxide Electrochemical Oxygen Separator to Achieve Aviator Grade Oxygen," *Microscopy and Microanalysis,* Vol. 20, Suppl 3, 2014. doi:10.1017/S1431927614011210
19. Yahiro, H., Eguchi, Y., Eguchi, K., and Arai, H. "Oxygen Ion Conductivity of the Ceria-Samarium Oxide System with Fluorite Structure," *J. Appl. Electrochemistry*, Vol. 18, pp. 527-531, 1988.
20. Inaba, H. and Tagawa, H. "Ceria-based Solid Electrolytes," *Solid State Ionics*, Vol. 83, Issues 1-2, pp. 1-16, January 1996.
21. Kilner, J. A. "Fast Oxygen Transport in Acceptor Doped Oxides," *Solid State Ionics*, Vol. 129, Issues 1-4, pp. 13-23, April 2000.
22. Jung, G.-B., Huang, T.-J., and Chang, C.-L. "Effect of Temperature and Dopant Concentration on the Conductivity of Samaria-doped Ceria Electrolyte, *J. Solid State Electrochem.*, Vol. 6, pp. 225-230, 2002.
23. Qi, X., Lin, Y. S., Holt, C. T., and Swartz, S. L. "Electric Conductivity and Oxygen Permeability of Modified Cerium Oxides," *J. Mat. Sci.*, Vol. 38, 1073-1079, 2003.
24. Lo Faro, M. and La Rosa, D., Antonucci, V., and Arico, A. S. "Intermediate Temperature Solid Oxide Fuel Cell Electrolytes," *J. Indian Institute of Science*, Vol. 89, pp. 363, 2009.
25. Kosinski, M. R. and Baker, R. T. "Preparation and Property–Performance Relationships in Samarium-doped Ceria Nanopowders for Solid Oxide Fuel Cell Electrolytes," *J. Power Sources*, Vol. 196, Issue 5, pp. 2498-2512, 2011.
26. Stojmenovic, M., Zunic, M., Gulicovski, J., Bajuk-Bogdanovic, D., Holclajtner-Antunovic, I., Dodevski, V., and Mentus, S. "Structural, Morphological, and Electrical Properties of Doped Ceria as a Solid Electrolyte for Intermediate-temperature Solid Oxide Fuel Cells," *J. Mater. Sci.*, Vol. 50, pp. 3781-3794, 2015.
27. Sharma, P., Singh, K. L., Sharma, C., and Singh, A.P. "Recent Advances in Ceria-based Electrolytes for Solid Oxide Fuel Cells," *International Journal of Innovative Research and Advanced Studies*," Vol. 3, Issue 5, 51-55, May 2016.
28. Schmitt, R., Nenning, A., Kraynis, O., Korobko, R., Frenkel, A. I., Lubomirsky, I., Haile, S. M., and Rupp, J. L. M. "A Review of Defect Structure and Chemistry in Ceria and its Solid Solutions," *Chem. Soc. Rev.*, Vol. 49, pp. 554-592, 2020.
29. Vinchhi, P., Patel, R., Mukhopadhyay, I., Ray, A., and Pati, R. "Effect of Doping Concentration on Grain Boundary Conductivity of Samaria Doped Ceria Composites," *J. Electrochem. Soc.*, Vol. 168, 124515, 2021.
30. Tuller. H. L. and Nowick, A. S. "Defect Structure and Electrical Properties of Nonstoichiometric CeO_2 Single Crystals," *J. Electrochem. Soc.*, Vol. 126, No. 2, p. 209, 1979.
31. Navarro, L., Marques, F., and Frade, J. "n-Type Conductivity in Gadolinia-Doped Ceria," *J. Electrochem. Soc.*, Vol. 144, No. 1, p. 267, 1997.
32. Meixner, D. L., Brengel, D. D., Henderson, B. T., Abrardo, J. M., Wilson, M. A., Taylor, D. M., and Cutler, R. A. "Electrohemical Oxygen Separation Using Solid Electrolyte Ion Transport Membranes," *J. Electrochem. Soc.*, Vol. 149, No. 9, D132, 2002.

33. Cheng, Y.-B. and Thompson, D. P. “Role of Anion Vacancies in Nitrogen-stabilized Zirconia,” *J. Am. Cer. Soc.*, Vol. 76, No. 3, pp. 683-688, March 1993.
34. Wendel, J., Lerch, M., and Laqua, W. “Novel Zirconia-based Superionic Conductors: The Electrical Conductivity of Y-Zr-O-N Materials,” *Journal of Solid State Chemistry*, Vol. 142, No. 1, pp. 163-167, January 1999.
35. Lee, J.-S., Chung, T.-J., and Kim, D.-Y. “Electrical and Microstructural Characterization on Nitrogen-Stabilized Zirconia,” *Solid State Ionics*, Vol. 136-137, pp. 39-44, November 2, 2000.
36. Kilo, M., Taylor, M. A., Argirusis, C., Borchardt, G., Lerch, M., Kaıtasov, O., and Lesage, B. “Nitrogen Diffusion in Nitrogen-doped Yttria Stabilised Zirconia,” *Phys. Chem. Chem. Phys.*, Vol. 6, pp. 3645-3649, 2004.
37. Reimann, C. and Bredow, T. “Adsorption of Nitrogen and Ammonia at Zirconia Surfaces,” *J. Molecular Structure*, Vol. 903, pp. 89-99, June 2009.
38. Valov, I., Rührup, V., Klein, R., Rödel, T.-C., Stork, A., Berendts, S., Dogan, M., Wiemhöfer, H.-D., Lerch, M., and Janek, J. “Ionic and Electronic Conductivity of Nitrogen-doped YSZ Single Crystals,” *Solid State Ionics*, Vol. 180, pp. 1463-1470, November 2009.
39. Lee, D.-K., Fischer, C. F., Valov, I., Reinacher, J., Stork, A., Lerch, M., and Janek, J. “An EMF Cell with a Nitrogen Solid Electrolyte—on the Transference of Nitrogen Ions in Yttria-Stabilized Zirconia,” *Phys. Chem. Chem. Phys.*, Vol. 13, pp. 1239-1242, 2011.
40. Berendts, S., Eufinger, J.-P., Valov, I., Janek, J., and Lerch, M. “Ionic Conductivity of Low Yttria-doped Cubic Zirconium Oxide Nitride Single Crystals,” *Solid State Ionics*, Vol. 296, pp. 42-46, November 2016.
41. Jorge, A. B., Fraxedas, J., Cantarero, A., Williams, A. J., Rodgers, J., Attfield, J. P., and Fuertes, A. “Nitrogen Doping of Ceria,” *Chem. Mater.*, Vol. 20, No. 5, pp. 1682-1684, February 7, 2008.
42. Chen, M. S. and Cook, P. J. “Process for Removing Oxygen from Crude Argon,” U.S. Patent 5035726 A, July 30, 1991.
43. Joshi, A. V. “Electrolyte Assembly for Oxygen Generating Device and Electrodes Therefor,” U.S. Patent 4879016, November 7, 1989.
44. Swalin, R. A. *Thermodynamics of Solids*, 2nd Edition,” Wiley & Sons, NY, p. 116, 1962.
45. Zhu, B., Albinsson, I., and Mellander, B.-E. “Electrical Properties and Proton Conduction in Gadolinium Doped Ceria,” *Ionics*, Vol. 4, pp. 261-266, May 1998.
46. Liu, R.-Q., Xie, Y.-H., Wang, J.-D., Li, Z.-J., and Wang, B.-H. “Synthesis of Ammonia at Atmospheric Pressure with $Ce_{0.8}M_{0.2}O_{2-\delta}$ (M = La, Y, Gd, Sm) and their Proton Conduction at Intermediate Temperature,” *Solid State Ionics*, Vol. 177, pp. 73-76, January 16, 2006.
47. Manohar, M. “Development and Characterization of Ceramic Membranes,” *International Journal of Modern Engineering Research*, Vol. 2, No. 4, pp 1492-1506, 2012.
48. “Cabin Air Separator for EVA Oxygen,” International Space Station CR 12209.
49. Hutchings, K. and Taylor, D. “High Pressure Low Power Ceramic Oxygen Generation System,” 2010 Annual Meeting of the Oxygen Systems Coordinating Group (OSCG), San Antonio, TX, July 2010.

17.1 Other Supporting References

Gheorghe, F. “Target Product Profile: Resilient Oxygen Concentrator,” 2nd edition, UNICEF – NEST360, April 2022.

Graf, J. “A Method of Producing Aviator Breathing Oxygen Grade High Pressure Oxygen using a Supported Monolith Ceramic Electrode,” NASA e-NTR 1392760148, submitted February 18, 2014.

Graf, J. “Medical Ceramic Oxygen Generator,” Oxygen Systems Coordinating Group Annual Meeting, Nashville TN, August 2022.

Hatch, G. “NASA VOC Analysis,” On Site Gas Analysis Report C1036395, September 2010.

Hecht, M., Hoffman, J., Rapp, D., McClean, J., SooHoo, J., Schaefer, R., Aboobaker, A., Mellstrom, J., Hartvigsen, J., Meyen, F., and Hinterman, E. “Mars Oxygen ISRU Experiment (MOXIE),” Space Science Reviews, Vol. 217, No. 1, January 6, 2021. doi:10.1007/s11214-020-00782-8

Hutchings, K. N., Bai, J., Cutler, R. A, Wilson, M. A., and Taylor, D. M. “Electrochemical Oxygen Separation and Compression Using Planar, Cosintered Ceramics,” Solid State Ionics, Vol. 179, No. 11-12, pp. 442-450, May 31, 2008.

Lopez, I., Aravena, R., Soza D., Morales, A., Riquelme, S., Calderon-Jofre, R., and Moraga, F. “Comparison Between Pressure Swing Adsorption and Liquid Oxygen Enrichment Techniques in the Atacama Large Millimeter/Submillimeter Array Facility at the Chajnantor Plateau (5,050 m),” Front. Physiol., Vol. 12, December 8, 2021. doi.org/10.3389/fphys.2021.775240

Peel, D., Neighbour, R., and Eltringham, R. J. “Evaluation of Oxygen Concentrators for Use in Countries with Limited Resources,” Anesthesia, Vol 68, No. 7, pp. 706-712, May 2013. doi.org/0.1111.anae.12260

Ross, M. and Wendel, S. K. “Oxygen Inequity in the COVID-19 Pandemic and Beyond,” Glob Health Sci Pract., Vol. 11, No. 1, February 28, 2023. doi:10.9745/GHSP-D-22-00360

United States Patent Number US 2023/02014763 A1, “Systems and Methods for Oxygen Concentration with Electrochemical Stacks in Series Gas Flow.”

Appendix A. Test Results from WSTF Testing of M-COG Oxygen Generator Prototype referred to as "Chassis 1"

National Aeronautics and
Space Administration

Document No. WSTF-IR-1268-001-21
Date September 21, 2021

Investigative Report

Medical Ceramic Oxygen Generator Demonstrator Unit

Lyndon B. Johnson Space Center
White Sands Test Facility
PO Box 20
Las Cruces, NM 88004
www.nasa.gov/centers/wstf/

Investigative Report

Medical Ceramic Oxygen Generator Demonstrator Unit

Issued By
National Aeronautics and Space Administration
Johnson Space Center
White Sands Test Facility
Materials and Components Laboratories Office

Prepared By: Steven Hornung (affiliate) Digitally signed by Steven Hornung (affiliate) Date: 2021.09.21 13:56:37 -06'00'
Steven D. Horning, Ph.D.
NASA TEST2 Contract

Reviewed By: Steven Torres (affiliate) Digitally signed by Steven Torres (affiliate) Date: 2021.09.21 14:07:05 -06'00'
Steven A. Torres
NASA TEST2 Contract

Approved By: JONATHAN TYLKA Digitally signed by JONATHAN TYLKA Date: 2021.09.24 12:40:05 -06'00'
Jonathan Tylka
NASA Materials and Components Laboratories Office

Contents

Abbreviations

FTIR	Fourier Transform Infrared
GC-TCD	Gas Chromatography with Thermal Conductivity Detection
JSC	Johnson Space Center
M-COG	Medical Ceramic Oxygen Generator
WSTF	White Sands Test Facility

1.0 Introduction

Johnson Space Center (JSC) Crew and Thermal Division (EC3) has been working with American Oxygen (Salt Lake City, UT), the developer of the Medical Ceramic Oxygen Generator (M-COG), to develop a commercial oxygen generation technology for medical use. White Sands Test Facility (WSTF) has been requested by JSC to perform an independent validation of the MCOG demonstrator unit performance by measuring the purity and flow rate of the oxygen produced under a variety of operating conditions. The M-COG is an oxygen generation system that extracts oxygen from the ambient air and produces high purity (>99.9% O_2) high pressure (>100 psig) oxygen. The test article will have four cell stacks, which will be energized separately. For this testing, the pressure will be limited to 10 psig and only one cell stack will be sampled for oxygen purity and pressure at a time.

The system uses specially formulated and manufactured ceramic plates called a cell stack to extract oxygen from the air. This unit operates at a high internal temperature (up to 750 °C). In operation, a supply of feed air is blown over the ceramic plates to selectively remove a fraction of the oxygen from the atmosphere. The feed air is then is then exhausted to the room through a heat exchanger at approximately 100 °C (212 °F).

2.0 System Description

A depiction of the M-COG is shown in Figure 1. A functional cross-section is shown in Figure 2. The unit measures 30 x 60 x 36 in. and weighs approximately 700 pounds.

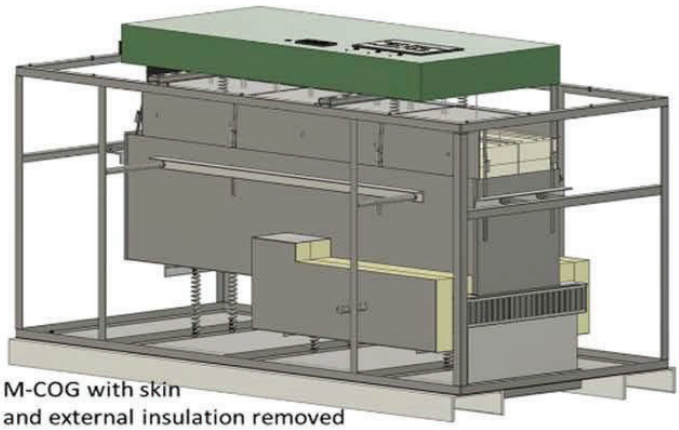

Figure 1
M-COG Demonstrator Unit with Insulation Removed

In operation, the unit is first brought up to operating temperature and then an electrical potential is applied to the cell stack, which starts the separation of oxygen from air. In operation, feed air from the room is drawn into a heat exchanger by a blower, which warms the air by heat transfer from the exhaust air. This preheated air flows through a heater then over the cell stack and is exhausted from the heat exchanger at the bottom of the unit, as shown in the cross-section diagram in Figure 2. The exhaust air is expected to be at or below a temperature of approximately 100 °C (212 °F). Surface temperatures on the unit may be as high as 60 °C (140 °F)

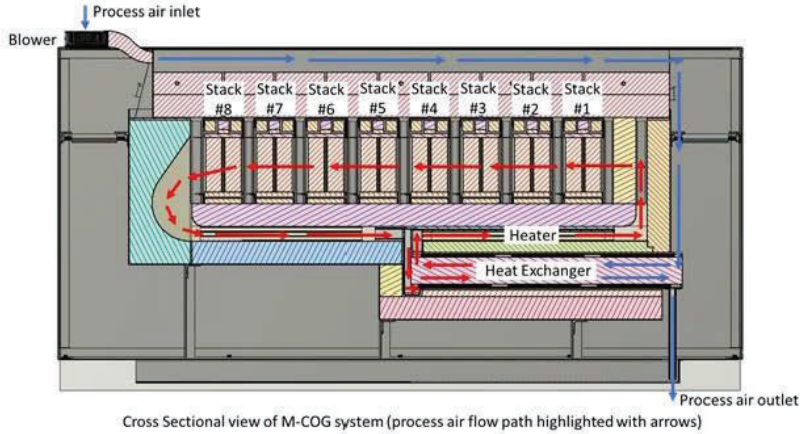

Figure 2
Functional Cross-Section of the M-COG

3.0 Analysis Methods

The contaminants present in the oxygen are determined by two different methods, Gas Chromatography with Thermal Conductivity Detection (GC-TCD) for the gases nitrogen and argon, and Fourier Transform Infrared (FTIR) spectroscopy for organics, water vapor, and carbon dioxide. For the gas chromatography analysis, a fixed-volume sample loop is filled with the gas to be analyzed. The contents of this loop are injected onto the chromatography column and a carrier gas sweeps the injected gas down the column to achieve separation of argon, oxygen, nitrogen, and any organic gases present. These components are detected by differences in their thermal conductivity and identified by the retention time on the column.

In the FTIR analysis, the analyte gas is purged through an infrared gas cell with a folded light path of 3 meters. An infrared spectrum is then acquired and from the acquired spectrum the concentrations of carbon dioxide and water can be calculated. The sum of the compound concentrations is used to determine the purity of oxygen.

4.0 Gas Handling Systems and Procedures

A manifold of 1/8th in. stainless steel tubing was fabricated to route the oxygen from the M-COG to either of the GC-TCD or FTIR and be constantly purged between analysis to exclude atmospheric contaminants from the manifold. A pressure transducer to measure back pressure is at the beginning of the manifold, followed by a back-pressure regulator with a maximum back pressure of 20 psig. A thermal mass flow meter is downstream from this to measure the output flow of the M-COG valves to route the oxygen produced to either the GC-TCD or the FTIR.

5.0 Results

The results of the analysis are given in Table 1. The sum of the contaminant concentrations is 277 ppm, resulting in a calculated oxygen concentration of 99.97 percent.

Table 1
Concentration of Detected Contaminants in MCOG Oxygen

Component	Concentration (ppm by volume)
Carbon dioxide	0.14
Moisture	37
Nitrogen	240
Argon	ND*
Organic Compounds	ND*

* ND=Not Detected

Distribution

Organization	Copies
NASA Johnson Space Center Houston Crew and Thermal Division Attn: John Graf/EC3	1
NASA Engineering Safety Center Attn: Clint Cragg/LARC-C103 Jon Haas/WSTF-C103	2
American Oxygen 2100 W Alexander St, Ste B Salt Lake City, UT Attn: Dale Taylor Tom Taylor	2
NASA Johnson Space Center White Sands Test Facility Materials and Components Laboratories Office Jonathan Tylka	1
NASA TEST2 Contract Materials and Components Laboratories Department Steven Hornung Steven Torres Technical Services Department Publications	3

Distribution will be electronic unless otherwise indicated with (HC).

Appendix B. Test Results from WSTF Testing of M-COG Oxygen Generator Prototype referred to as "Chassis 2"

National Aeronautics and
Space Administration

Document No. WSTF-IR-1268-002-23
Date January 12, 2023

Investigative Report

Evaluation of the Chassis 2
Medical Ceramic Oxygen Generator

Lyndon B. Johnson Space Center
White Sands Test Facility
PO Box 20
Las Cruces, NM 88004
www.nasa.gov/centers/wstf/

Investigative Report

Evaluation of the Chassis 2 Medical Ceramic Oxygen Generator

Issued By
National Aeronautics and Space Administration
Johnson Space Center
White Sands Test Facility
Materials and Components Laboratories Office

Prepared By: Steven Hornung (affiliate) Digitally signed by Steven Hornung (affiliate) Date: 2023.01.17 09:50:55 -07'00'

Steven D. Horning, Ph.D.
NASA TEST3 Contract

Reviewed By: Steven Torres (affiliate) Digitally signed by Steven Torres (affiliate) Date: 2023.01.17 15:23:37 -07'00'

Steven A. Torres
NASA TEST3 Contract

Approved By: JONATHAN TYLKA Digitally signed by JONATHAN TYLKA Date: 2023.01.12 16:58:51 -07'00'

Jonathan Tylka
NASA Materials and Components Laboratories Office

Contents

Abbreviations

FTIR	Fourier Transform Infrared
GC-TCD	Gas Chromatography with Thermal Conductivity Detection
JSC	Johnson Space Center
M-COG	Medical Ceramic Oxygen Generator
WSTF	White Sands Test Facility

1.0 Introduction

Johnson Space Center (JSC) Crew and Thermal Division (EC3) has been working with American Oxygen (Salt Lake City, UT), the developer of the Medical Ceramic Oxygen Generator (M-COG), to develop a commercial oxygen generation technology for medical use. White Sands Test Facility (WSTF) has been requested by JSC to perform an independent validation of the Chassis 2 M-COG unit performance by measuring the purity and flow rate of the oxygen produced under a variety of operating conditions. The M-COG is an oxygen generation system that extracts oxygen from the ambient air and produces high purity (>99.9% O_2) high pressure (>100 psig) oxygen. The test article will have four cell stacks, which will be energized separately.

The system uses specially-formulated and manufactured ceramic plates called a cell stack to extract oxygen from the air. This unit operates at a high internal temperature (approximately 750 °C). In operation, a supply of feed air is blown over the ceramic plates to selectively remove a fraction of the oxygen from the atmosphere. The feed air is then exhausted to the room through a heat exchanger at approximately 100 °C (212 °F).

2.0 System Description

A depiction of the M-COG is shown in Figure 1. A functional cross-section is shown in Figure 2. The unit measures 30 x 60 x 36 in. and weighs approximately 700 pounds.

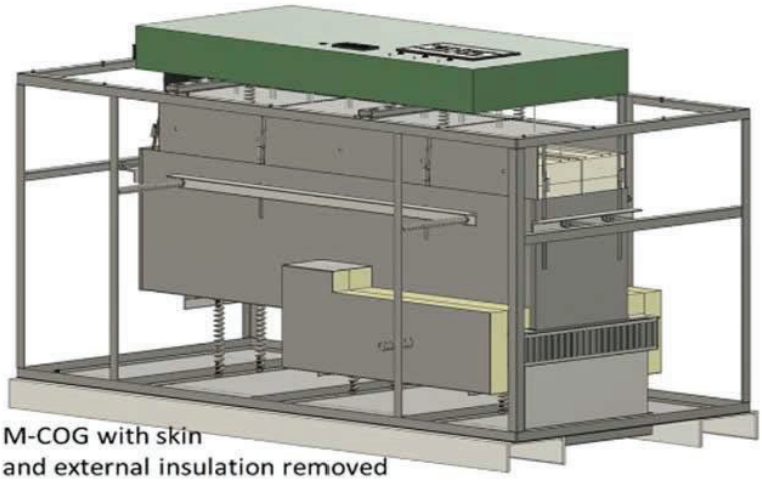

Figure 1
M-COG Demonstrator Unit with Insulation Removed

In operation, the unit is first brought up to operating temperature and then an electrical potential is applied to the cell stack, which starts the separation of oxygen from air. In operation, feed air from the room is drawn into a heat exchanger by a blower, which warms the air by heat transfer from the exhaust air. This preheated air flows through a heater then over the cell stack and is exhausted from the heat exchanger at the bottom of the unit, as shown in the cross-section diagram in Figure 2.

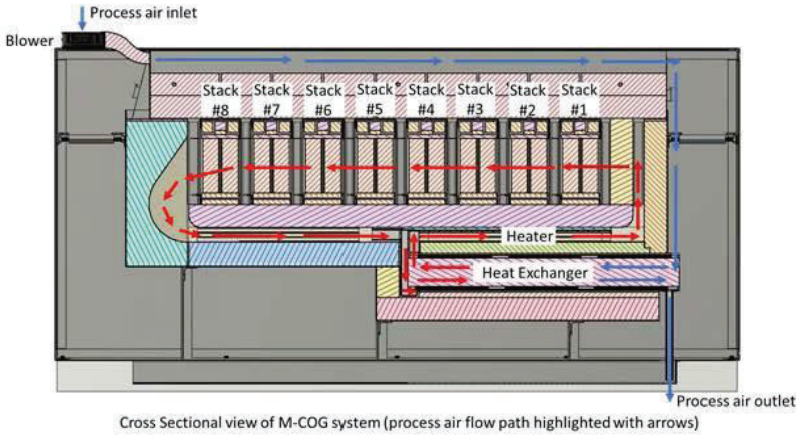

Figure 2
Functional Cross-Section of the M-COG

3.0 Analysis Methods

The contaminants present in the oxygen are determined by two different methods, Gas Chromatography with Thermal Conductivity Detection (GC-TCD) for the gases nitrogen and argon, and Fourier Transform Infrared (FTIR) spectroscopy for organics, water vapor, and carbon dioxide. For the gas chromatography analysis, a fixed-volume sample loop is filled with the gas to be analyzed. The contents of this loop are injected onto the chromatography column and a carrier gas sweeps the injected gas down the column to achieve separation of argon, oxygen, nitrogen, and any organic gases present. These components are detected by differences in their thermal conductivity and identified by the retention time on the column.

In the FTIR analysis, the analyte gas is purged through an infrared gas cell with a folded light path of 3 meters. An infrared spectrum is then acquired and from the acquired spectrum the concentrations of carbon dioxide and water can be calculated. The sum of the compound concentrations is used to determine the purity of oxygen.

4.0 Gas Handling Systems and Procedures

A manifold of 1/8th in. stainless steel tubing was fabricated to route the oxygen from the M-COG to either of the GC-TCD or FTIR and be constantly purged between analysis to exclude atmospheric contaminants from the manifold. A pressure transducer to measure back pressure is at the beginning of

the manifold, followed by an adjustable back-pressure regulator. A thermal mass flow meter is downstream from this to measure the output flow of the M-COG valves to route the oxygen produced to either the GC-TCD or the FTIR.

5.0 Results

The results of the analysis are given in Table 1. The sum of the contaminant concentrations is 45 ppm, resulting in a calculated oxygen concentration of 99.995 percent. Oxygen delivery rate was 10 liters per minute at the time of sampling. During testing, a maximum flow rate of approximately 12.5 liters per minute was recorded by the test team with four cell stacks.

Table 1
Concentration of Detected Contaminants in M-COG Oxygen

Component	Concentration (ppm by volume)
Carbon dioxide	ND*
Moisture	40
Nitrogen	ND*
Argon	ND*
Organic Compounds	5.7

* ND=Not Detected

Distribution

Organization	Copies
NASA Johnson Space Center Houston Crew and Thermal Division Attn: John Graf/EC3	1
NASA Engineering Safety Center Attn: Clint Cragg/LARC-C103 Jon Haas/WSTF-C103	2
American Oxygen 2100 W Alexander St, Ste B Salt Lake City, UT Attn: Dale Taylor Tom Taylor	2
NASA Johnson Space Center White Sands Test Facility Materials and Components Laboratories Office Jonathan Tylka	1
NASA TEST3 Contract Materials and Components Laboratories Department Steven Hornung Steven Torres Technical Services Department Publications	3

Distribution will be electronic unless otherwise indicated with (HC).

Appendix C. Test Results from American Oxygen Long-duration Performance Testing of M-COG Oxygen Generator Prototype referred to as the "Mule"

M-COG Characterization Testing and Life Testing Using SN-CFC-004

Dale Taylor

American Oxygen

January 2024

1.0 Introduction and Background

Whenever wafers or cell stacks are available, it is prudent to place the items on long term test. Long term tests can be performed with relatively little overhead, and long duration tests can track small changes in performance over time.

Wafers and cell stacks with a similar configuration but different manufacturing processes have been tested previously. These wafers and cell stacks will be referred to as Solid Electrolyte Oxygen Separator (SEOS) in this report. Material composition and configuration of SEOS and M-COG wafers are similar, but SEOS wafers were manufactured as R&D test articles while M-COG wafers are manufactured using processes that can be performed at large scale. SEOS wafers and cell stacks were tested between 2010 and 2015, with the longest duration SEOS cell tests lasting more than 55,000 hours. SEOS multi-cell stacks were operated continuously for over 35,000 hours.

SEOS wafer and cell stack test results do not directly apply to M-COG, but SEOS testing can inform expectations, and help guide test plans. SEOS wafer tests and cell stack tests did not produce any structural failure, nor were wafer or cell stacks fractured during long term testing. There was, however, a few glass seal leaks were observed in multi-cell stacks subjected to deliberately challenging operating conditions. Additionally, no wafer or cell stack tested experienced a sudden or significant change in electrochemical performance during the testing; changes in voltage / current performance were gradual. Long term testing of SEOS suggests that when operating within their design parameters of current, temperature, and process air speed, performance is steady and predictable, demonstrated by the fact that no SEOS tests had a sudden change in performance or catastrophic failure.

Long term testing of SEOS did measure slow, steady, and incremental increases in electrochemical resistance over time. These increases in resistance over time are well documented and attributed to contamination of the exposed cathode that accumulates over time. The cathode is exposed to process air and airborne contaminants contact the cathode surface. The airborne contaminants can deposit on the exposed cathode surface, thereby reducing the number of cathode sites, and causing an increase in resistance. Inspection and chemical analysis of wafers subjected to long term testing identify trace amounts of chromium and sulfur on the cathode surface. Stainless steel is the likely source of chromium, while environmental pollution is the likely source of airborne sulfur. The average rate of increase of resistance from a sample set of 40 wafers is 0.7% increase for each 1000 hours of operation.

The first full scale, production ready M-COG cell stack was manufactured in 2022. They are differentiated, in part, from SEOS cell stacks in that M-COG stack includes a recently developed advanced ceramic seal that has been shown to be much more tolerant of abusive operating conditions. Based on SEOS test data, the expectation is that M-COG wafers and cell stacks will operate in a similar fashion (i.e., no catastrophic failures) and will exhibit only minor seal leaking, which is hopefully obviated by the new sealing technology, and the gradual increase in electrochemical resistance.

In early 2023, cell stacks were placed in Cross Flow Cylinder (CFC) configuration oxygen engines. One of the CFC units was available for long term testing and CFC thermal characterization testing. Unit SN-CFC-004 was used for long term testing and thermal characterization testing. This unit was referred to as "the mule" because some of the thermal test configurations were outside the planned operating envelope. Mules have a reputation for stamina, persistence, and the ability to carry a heavy load under demanding conditions.

This report describes testing of Cross Flow Cylinder SN-CFC-004 under thermal characterization testing, and long-term testing.

2.0 System Configuration

The test article consists of an oxygen engine with a Cross Flow Cylinder configuration. The CFC contains one cell stack with 30 wafers, a set of resistive heaters, a spiral wound air-to-air heat exchanger, a blower with an external duct extendable to 18 inches to enable extra insulation around the heat exchanger, and instrumentation and system control.

The instrumentation consists of a removable anemometer to measure volume air flow through the unit, 13 thermocouples, measurement of blower power, heater power, and cell stack power (recorded as cell stack current, cell stack voltage, and total cell stack power). System control allows for changing the blower speed, heating rate, operating temperature, and cell stack current (with a cap for maximum voltage). A photograph of the system is shown in Figure 1.

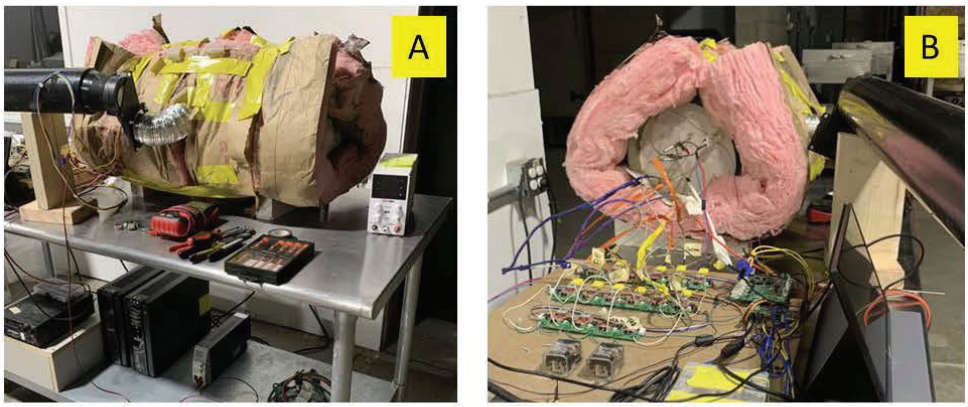

Figure 1. Mule Test Article in Run5 Configuration

The system was tested in three slightly different configurations. Figure 1 shows the system in the final configuration, referred to as "Mule Run #5". The initial test configuration was found to restrict air flow and allow too much bypass air around the stack that limited stack operating conditions. After Mule run #3, a new blower-to-CFC manifold was built and installed, and air bypass around the stack was virtually eliminated. The new configuration increases peak air flow through the system 60% more than Run #1 configuration. The air inlet duct connecting the blower to the CFC, Figure 1A, allows for additional overwrap insulation to be placed around the outside of the heat exchanger.

For Mule Run #5, a new digital power control system was installed. This digital control system enables automated system operation, has fault detection and auto-safing capability, and can integrate with production-run thermocouples. Production-run M-COG systems will use a temperature monitoring and control system that reads the unprocessed thermocouple signal and eliminates the need for a commercial signal conditioner. The system operated during Mule Run #5 is representative of what is envisioned for a production-run M-COG system.

Figure 2 provides two cross sectional views on the configuration of Cross-Flow-Cylinder. The CFC used in Mule testing has one cell stack. The cell stack contains thirty wafers, and the oxygen is ported upwards through a single delivery line projecting from the geometric center of the wafers. Immediately upstream of the cell stack, there is an air diffuser and air pre-heater. This single cell stack configuration can be expanded into a two-cell stack configuration by adding a second cell stack and diffuser/preheater in a mirror-symmetric configuration, with the base of the cell stacks touching, and one cell stack porting oxygen out the "top" of the CFC and the second cell stack porting oxygen out the "bottom" of the CFC.

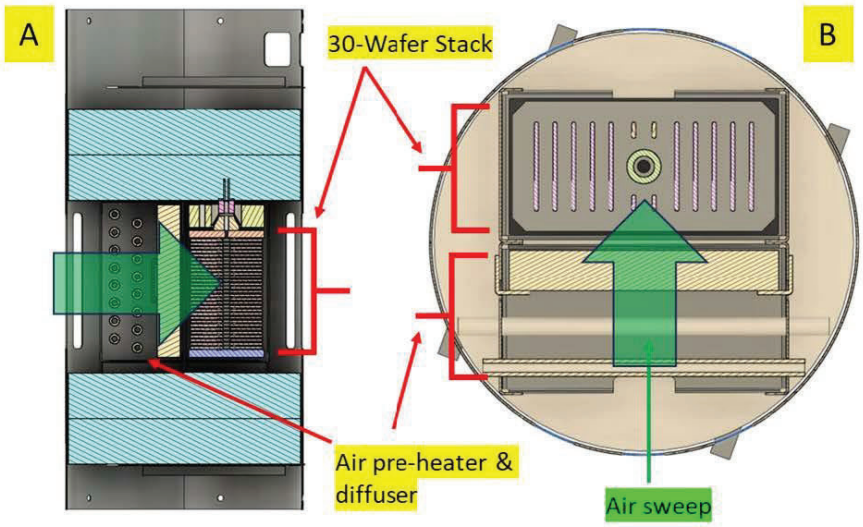

Figure 2. Single-stack Cross Flow Cylinder (CFC)
A) shows a X-section image parallel to cylinder axis. B) shows a X-section image perpendicular to cylinder axis.

3.0 Test Objectives:

Mule testing had six test objectives:

1. Understand the interactions between cell stack operating power (DC voltage and current), nominal operating temperature, heater power, and volume air flow rate.
2. Measure vertical and lateral temperature distribution in the stack as a function of operating parameters.
3. Collect as much run time as practically possible.
4. Characterize the thermal performance of a single cell CFC.
5. Integrate and check-out the instrumentation/control system with production configuration thermocouples and automated control software.
6. Understand system response to a sudden loss of electrical power.

Performance tests intended to operate under specific operating conditions can be expensive and time-consuming processes. In comparison, life tests intended to operate under steady state conditions with no oversight are simpler and less expensive to run. Between discrete characterization tests that required human supervision, the system was allowed to run under steady state conditions, as untended operations under steady state conditions can efficiently accrue run time.

Operating the CFC at different temperatures, current levels, and blower speeds was intended to characterize thermal performance. Optimal conditions for thermal performance are those that have sufficient blower power to remove heat generated by the cell stack, while maintaining thermal stresses in the cell stack within acceptable limits to avoid excessive process airflow, as heater power increases when airflow increases.

The instrumentation, power supply hardware, and control software was incrementally shifted from development systems using lab support equipment to production systems and can be manufactured at scale. Mule test sequence #1 used engineering development lab thermocouples, and manual control of the stack DC Power Supply (DCPS), and heater. Mule test sequence #5 used a production scale blower, production scale thermocouple, and automated control software. Mule testing provided the opportunity to check out new components and test component integration over a series of experiments.

In the course of long duration tests, unscheduled upsets occur, but can be informative. For example, USAF testing of SEOS at Tinker Air Force Base involved thousands of hours of continuous operations. Steady state operations resulted in nominal performance, but inclement weather resulted in a loss of power to the system. Due to the power loss, the SEOS system began to cool down, but power was returned while SEOS was in an intermediate cool down state, and system re-start from that condition caused a thermal stress fracture. It is critical to note that the USAF SEOS cell stacks used a glass sealing system that was substantially less tolerant of rapid thermal transients when compared to the M-COG stack used in Mule testing. As mentioned above, those off-nominal events can be instructive in improving overall system design and finding weaknesses exposed only by transient events.

4.0 Test Results and Performance Data

4.1 Thermal Characterization of CFC

System start-up is a dynamic event and elevates the probability of excessive thermal stresses in the cell stack. It is an engineering optimization problem: minimizing thermal stresses through slow heating rates against a desire to initiate oxygen production (i.e., up-time) as quickly as possible.

System start-up can be accelerated by powering the cell stack early, while the cell stack is at lower temperatures. The cell stack resistance is high at lower temperatures; at ambient temperature the resistance is essentially infinite, and current does not flow through the cell stack. At intermediate temperatures, 300 - 400 °C, the cell stack resistance is remains high, but a small amount of current conducts and a modest amount of stack self-heating occurs, but is constrained by the power supply voltage limit. Maximum stack self-heating occurs when cell stack resistance is high enough to produce lots of heat, but low enough to carry sufficient current under voltage limited conditions. Stack self-heating is moderate at operating conditions, where cell stack resistance is low and operating current is high. The reason for operating at high temperatures is to minimize cell stack resistance and minimize overall power use.

Figure 3 describes the temperature trends and heater power profile for a slow incremental heating of the CFC system. This incremental heating profile can inform thermal control feedback, and it can characterize the effect of cell stack self-heating on system start-up. Effects of cell stack self-heating are small, but measurable at temperatures as low as 300 °C. This is indicative of meeting manufacturing specifications with favorable Area Specific Resistance (ASR) values. Inefficient cell stacks do not produce oxygen or heat until they reach 500 °C.

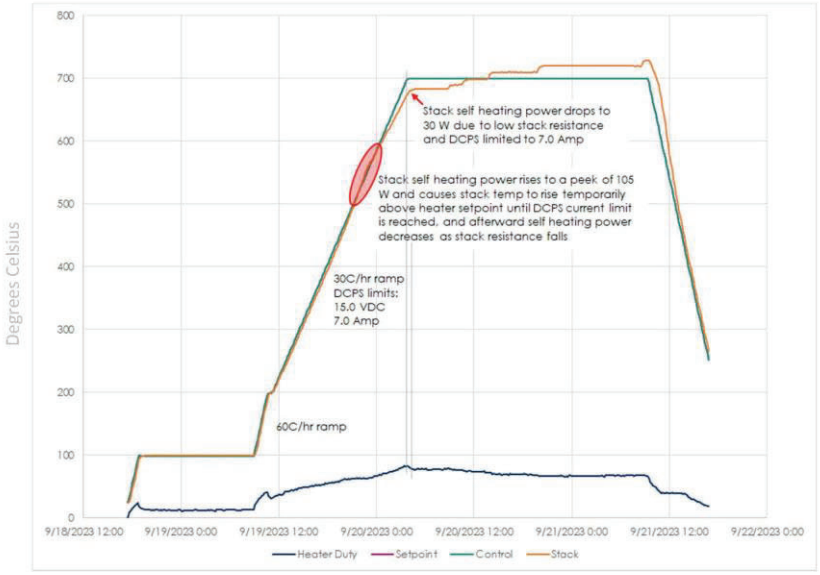

Figure 3. Thermal and Heater Profiles During Slow, Incremental Heating

Without the benefit of stack self-heating, the stack heating rate followed the heater ramp at a rate of 60 °C/h up to 200 °C at 70% blower power. There is a good chance the stack/system could be heated from room temperature to 700 °C at a rate of 60 °C/hour using heater power only.

At temperatures above 600 °C, the stack begins to lag because stack resistance drops and consequently, there is reduced cell stack self-heating. A more integrated system control strategy could facilitate faster heating by increasing power to the cell stack to 150 - 200W when the system is heating from 600 °C to 700 °C. In this temperature range, cell stack resistance is low enough to safely accommodate 150-200 W of self-heating.

Figure 4 highlights thermal profiles of different parts of the CFC system. The effects of cell stack self-heating are small, but measurable at 350 °C, and stack heating effects are substantial in the 500 – 600 °C range. An untested conjecture, based on the available data, is that if the CFC were insulated externally and kept above 300 °C during a zero-power stand by state, when the power is returned, the system could be operating at 1 slpm production rates in less than 4 hours, and 3-4 slpm production rates after 6.5 hours.

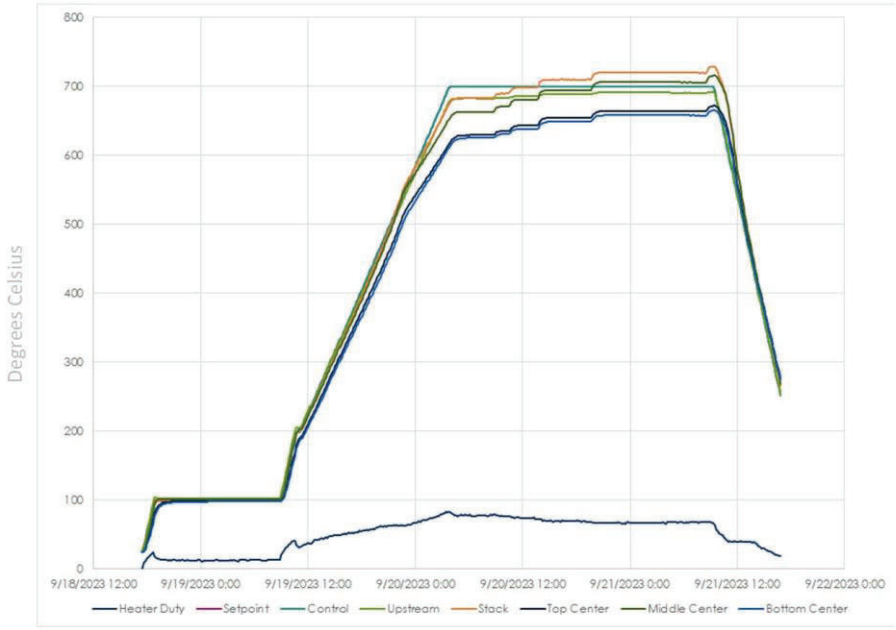

Figure 4. Thermal Profile of Different Parts of CFC During Slow, Incremental Heating

4.2 Response to High Output Operating Mode and Unscheduled System Upsets

Test article SN-CFC-004, during Test #4, had two unscheduled events that subjected the cell stack to thermal stresses far more severe than any previous test (see Figure 5).

The first unscheduled test occurred on August 29, 2023. Production scale thermocouples were being integrated with production scale system control software. Feedback from the cell stack power supply affected the thermocouple signal, which caused a spike in operating temperature while the cell stacks were powered and producing oxygen. This kind of spike is not desired, it causes thermal gradients and thermal stresses, but the cell stack was unaffected. This unplanned thermocouple upset provided a helpful diagnostic – identifying the cause of the anomaly. The anomaly has been fixed, and the fix has been tested and shown to be stable.

The second unscheduled test occurred September 2, 2023. A thermocouple spike combined with an unscheduled loss of facility power resulted in the most severe thermal stress condition imaginable: A cell stack that starts at 700 °C loses all heater power and all cell stack power, but the blower continues to operate and subjects the cell stack with a fast flow of cold air. This scenario results in the fastest cooling possible, and the greatest thermal stresses possible. It must be noted that in a production system, this condition would not be possible – the blower would be supplied by the same source of power as the heater and cell stack – it would not be possible in a production system to have blower power, but no heater power or cell stack power. This cell stack was not affected by the extreme thermal shock event.

Other things to note from Test #4: The stack was operated at 4.0 slpm, which requires 340 W. This 340W includes the ~25W needed to compress the oxygen to 1.0 atm, as this portion of stack power does not produce Joule heat. The stack was dissipating ~315W of joule heat when the core temperature is 760 °C. The cell stack is capable of operating continuously at 760 °C, but to remove 325W of heat the recommended blower speed would be 90%. This "boost mode" operating configuration would be safe and stable, and the device can run continuously under these operating conditions, but this operating configuration would not be the most energy efficient. Heater power increases when the blower speed increases to 90%.

Test 4 data suggests that the most energy efficient operating condition is 3.0 slpm (27 A), with a cell stack temperature of 740 °C, and 70% blower speed. Under this condition stack power is 230 W, 70% blower speed can remove heat and maintain temperature, with a specific power in this condition of 78 W/slpm.

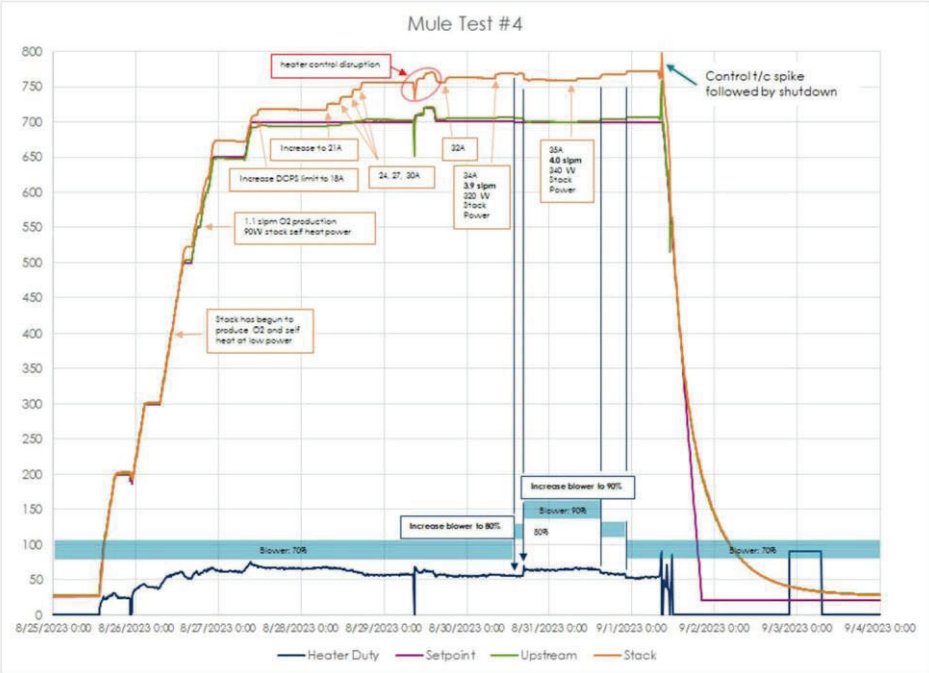

Figure 5. Thermal and Heater Power Trends During High Output Operating Mode (33% O_2 production boost relative to baseline) and Two Unscheduled System Upset Events

4.3 System Stability Over Time

System operating parameters intentionally changed during Tests 1, 2, 3, 4, and 5. These tests evaluated heat-up, cool-down, and operating under a variety of cell stack power / cell stack temperature / blower speed operating conditions.

Similar operating conditions were used for Runs #3 and #4 (see Figure 6). Stack resistance during Run #4 was within measurement error to stack resistance during Run #3. Run #4 resistance is actually slightly lower, indicating that measurement error is greater than aging effects. Testing was limited to 1248 hours, but within the limits of test duration, and the limits of system control and measurement error, there is no measurable increase in stack resistance over time. This is consistent with SEOS life test results, that average 0.7% increase in stack resistance for every 1000 hours of run time, but more than 10,000 hours of testing is needed to see a consistent and detectable trend.

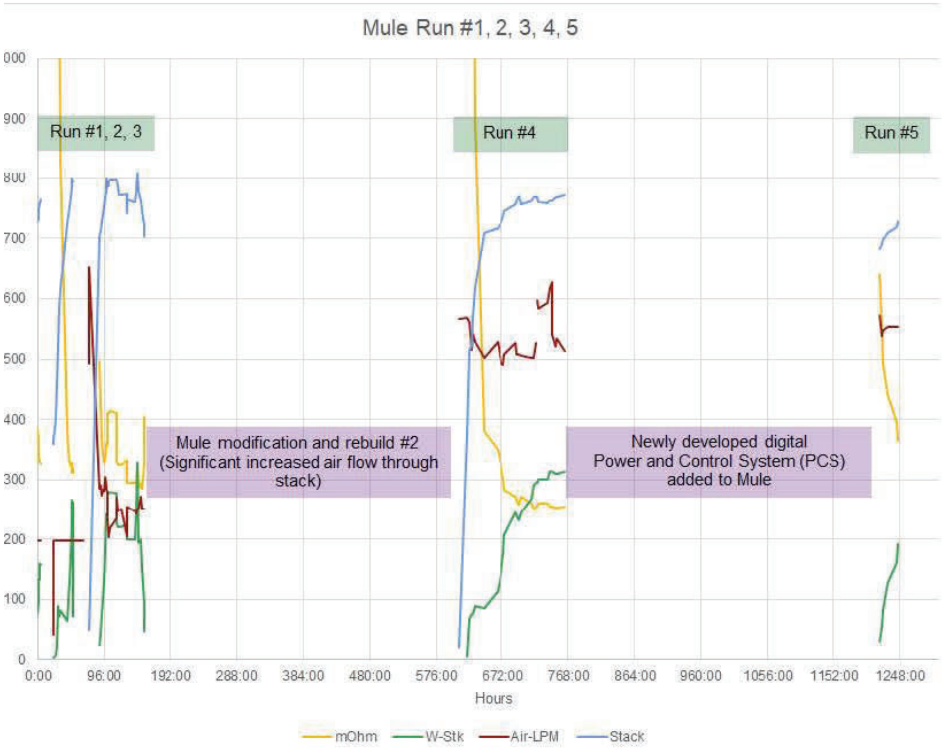

Figure 6. Current, System Power, System Performance Trends Over Time

5.0 Results

This testing proved to be helpful in characterizing system level performance, checking out system response to production level thermocouples and automated system control with fault detection. Some results from the testing are listed below:

- The cell stack and the entire system can withstand sudden, complete and extended loss of power. The cell stack was cooled from >750°C to <250 °C in five hours, without suffering any permanent damage or change in system performance, for the materials and configuration tested.
- CFC configuration M-COG systems can be safely heated at a rate of 60 °C per hour using existing system control algorithms.
- CFC configuration M-COG systems can safely produce 4 slpm in "boost mode" continuously with the existing operating conditions, but overall energy efficiency is lower compared to normal operating mode (3 slpm).

- CFC configuration M-COG system can likely produce more than 4 slpm continuously, with modification to increase process air flow. These peak production operation modes a higher specific power, but sometimes it is operationally useful to increase oxygen production.
- The conditions that are the most energy efficient operate with 3 slpm production rate and 740 °C cell stack temperature. This operating condition results in a specific power 78 W/lpm.
- SN-CFC-004 operated for more than 1200 hours, with no measurable increase in resistance.

Appendix D. Test Results from American Oxygen High-pressure Oxygen Production Tests of Two-stage M-COG Oxygen Generator

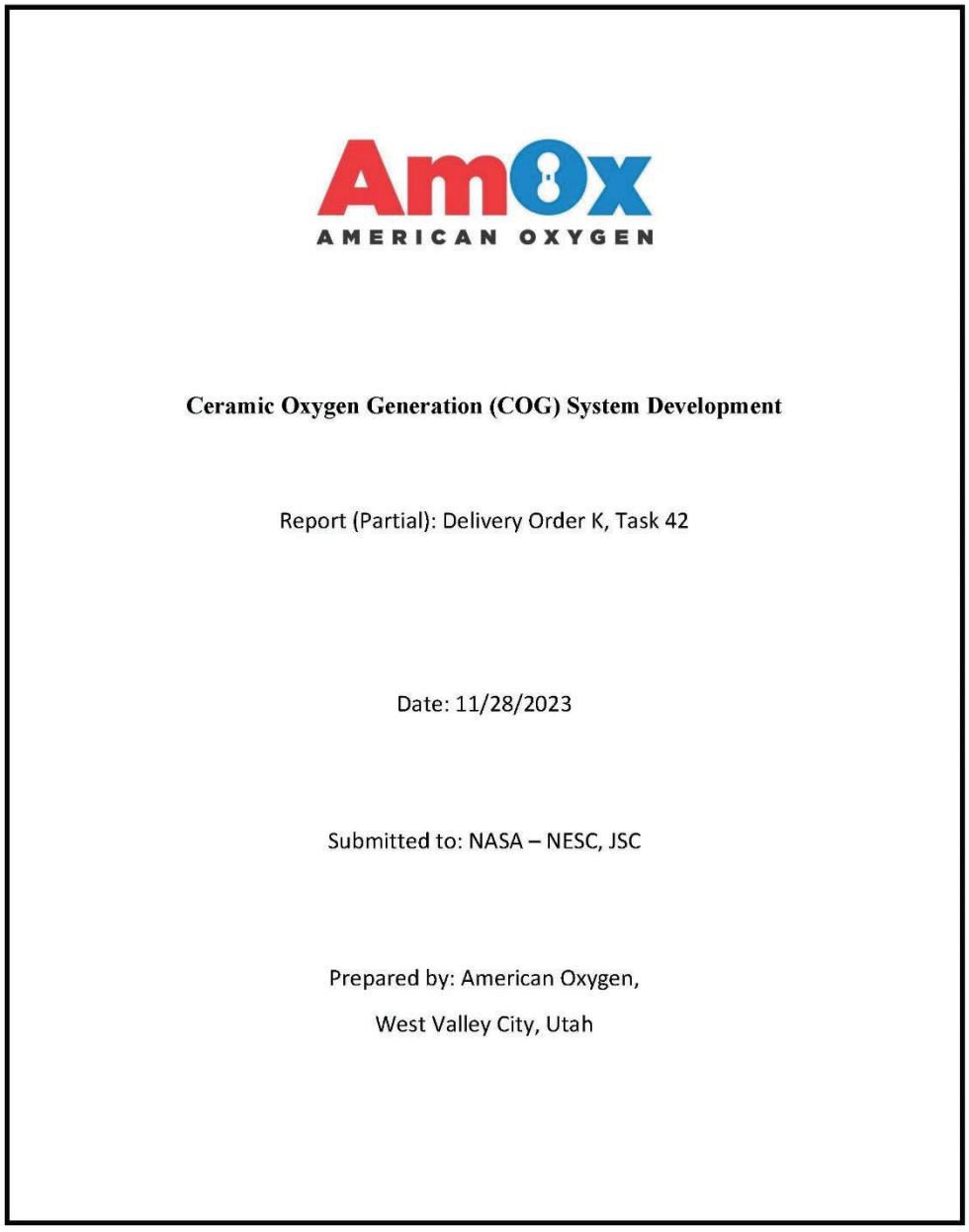

1- Introduction and Background

Task Order-K includes Tasks 42, 43, and 44 with the collective overall objective of demonstrating a first of its kind Two-Stage COG (Ceramic Oxygen Generator) system to produce ultra-pure oxygen (>99.99%) and safely compress it to 3000-psig. Order-K was a logical follow-on to previous tasks that included the design and engineering of a 3000-psig Stage-2 COG electrochemical solid-state oxygen compressor with no moving parts, and fed by a moderate pressure (up to 150-psig) Stage-1 COG ultra-pure oxygen generator. The primary objective of Task 42 is to demonstrate production of oxygen at 3000-psig back pressure using a two stage Ceramic Oxygen Generator and Compressor (COG-C) system and featuring high efficiency planar COG-C electrochemical cells (also known as "wafers"). It was the first known demonstration of its kind.

Essential parts of Task 42 was the development the following.

1- Develop a Stage-2 test vehicle featuring an internally heated and thermally insulated pressure vessel capable of containing 3000-psig oxygen depleted "air" (primarily a mix of N2 and O2, but including air-like fractions of other atmospheric gases).
2- Development of a Two-Stage COG test bay.
3- Integration of a Stage-1 COG developed under Task 43 to supply high purity oxygen to Stage-2.
4- Development of an oxygen Gas Management System (GMS) connecting Stage-1 and Stage-2, and capable of pressurizing and controlling Stage-2 pressure vessel.
5- Operation of these various subsystems in order to demonstrate solid state compression (no moving parts) of oxygen against a back pressure of 3000-psig.

High purity oxygen was supplied from a single 30-cell stack Stage-1 COG delivered under Task 42. The given COG featured a Cross-Flow Cylinder (CFC) design with a gas-to-gas multi-layer wrap around heat exchanger (HX). Models of the CFC Stage-1 COG are shown in Figures 1.1 and 1.2. Movement of process air through the Stage-1 COG was achieved with a small brushless DC blower (see Figure 1.2).

Task 42 was completed under an extremely aggressive schedule that required multiple subtasks to be executed in parallel, and the need to modify the subtasks repeatedly in order to best accomplish the overall objective of Task 42.

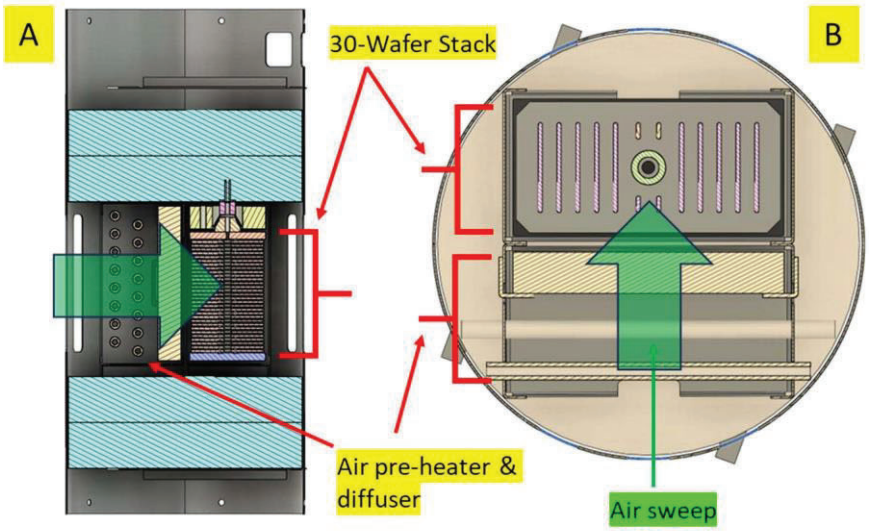

Figure 1.1: Single-stack Cross-Flow-Cylinder (CFC) design concept. A) X-section image parallel to cylinder axis. B) X-section image perpendicular to cylinder axis.

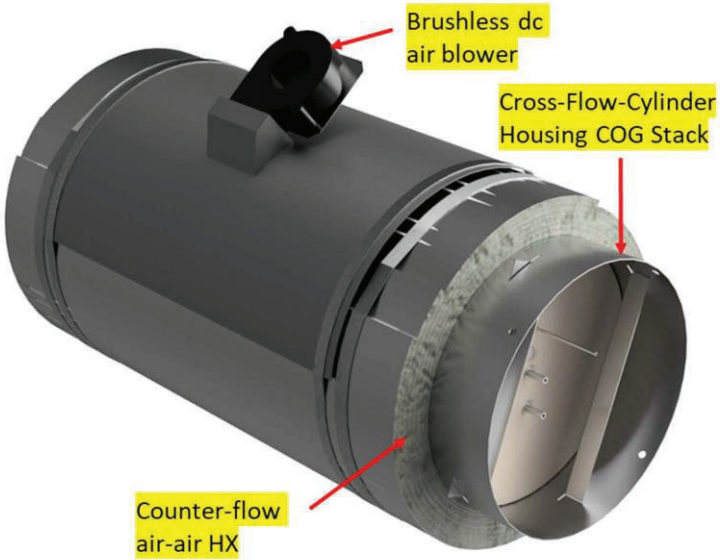

Figure 1.2: Single-stack CFC with integrated counter-flow air-air HX and low-pressure air mover.

2- Results

Subtask 41.1 - Develop a Stage-2 test vehicle featuring an internally heated and thermally insulated pressure vessel capable of containing 3000-psig oxygen depleted "air."

A "warm wall" (<450 C) pressure vessel was developed as the 3000-psig test vehicle in cooperation with Jacobs Engineering. A cross-section view of the design was shown in Figure 2.1

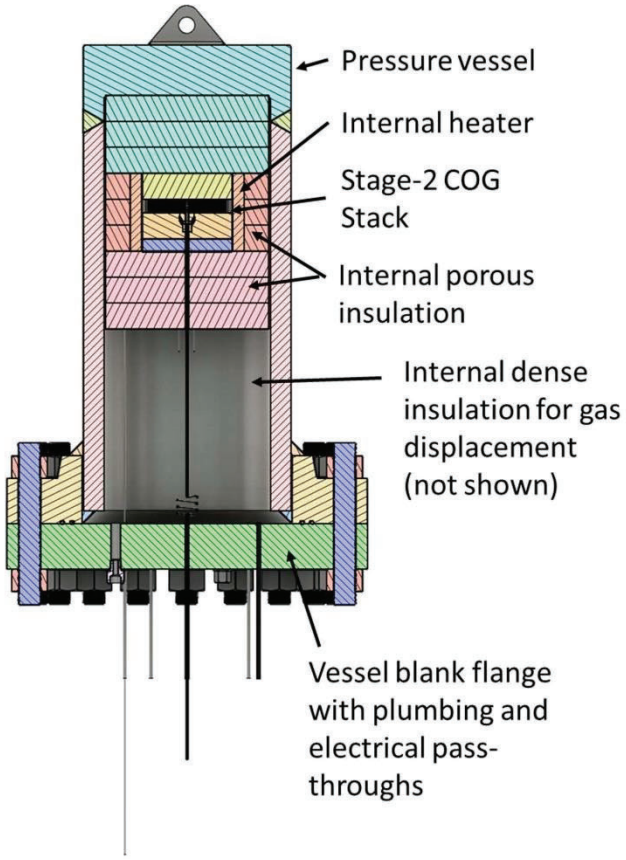

Figure 2.1: Warm-wall pressure vessel with internal heater and internal thermal insulation, and showing position of Stage-2 COG-C stack.

The 3000-psig test vehicle included two external heaters wrapped around the OD of the vessel. They were used to manage heat loss from the vessel during operation while maintaining the

maximum wall temperature below 450 C. The external heater are not shown in Figure 2.1. The vessel had an nominal OD of 18 inch, and nominal ID of 12.8 inch. The completed vessel and base flange had a combined weight of approximately 2000-lbf.

Subtask 41.2 - Development of a Two-Stage COG test bay.

A three-sided test bay was designed a built to accommodate the 3000-psig test vehicle. The working space within the bay was 8 x 8 ft with 8-ft tall walls and 4000-lbf overhead gantry with a maximum working height of 11 ft. The test bay was designed to permit forklift access from one side. Also included as part of the test bay was a raised platform with 360-deg access to

elevate the test vehicle and permit access to the various vessel penetration pass-throughs. Figure 2.2 shows a photo of the test bay and raised platform.

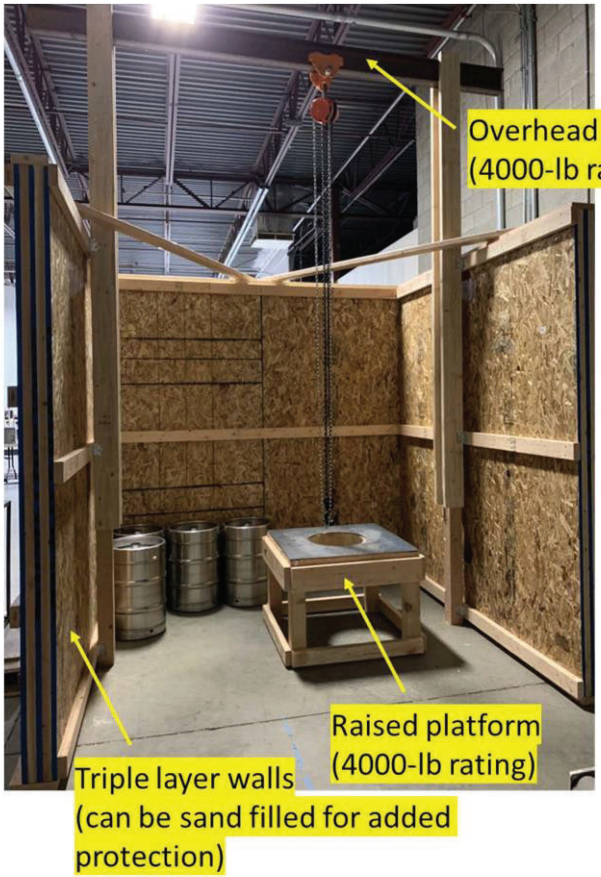

Figure 2.2: Walk-in test bay with raised platform and overhead gantry, and forklift access.

Subtask 41.3 - Integration of a Stage-1 COG developed under Task 43 to supply high purity oxygen to Stage-2.

The CFC Stage-1 COG was positioned outside the test bay in order to make it fully accessible during operational testing of Stage-2. It was connected to GMS plumbing circuit-1, and was operated at a nominal O2 supply pressure of 30-psig that was limited by an adjustable pressure

relief valve set at 50-psig. Stage-1 O2 supply pressure was managed by adjusting a 10-turn needle valved used to bleed oxygen from Stage-1 while continually supplying oxygen to Stage-2. Figure 2.3 shows the Stage-1 COG integrated into the Two-Stage COG-C system and positioned outside the test bay.

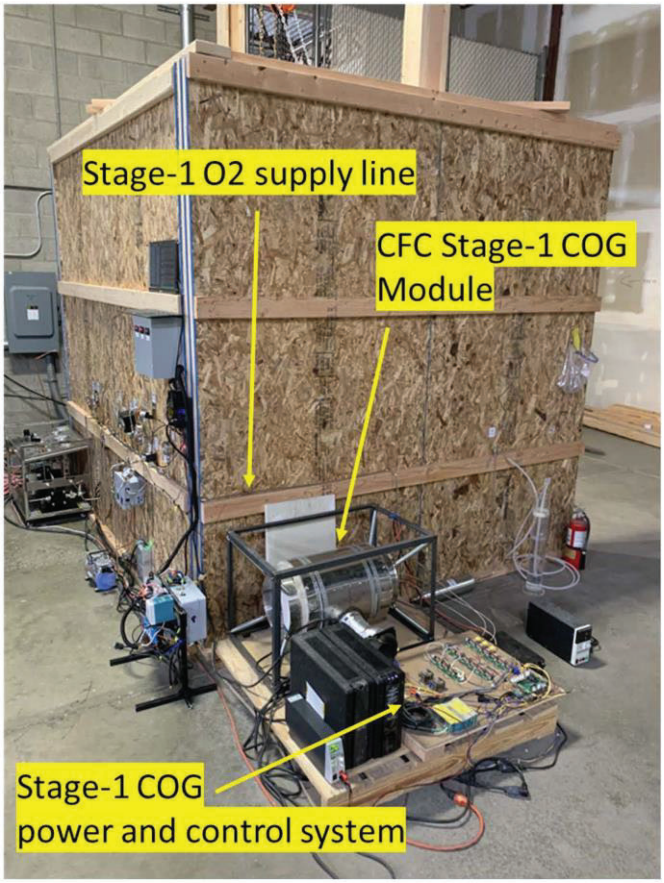

Figure 2.3: Stage-1 COG integrated into the test bay of the Two-Stage COG-C system.

Subtask 41.4 - Development of an oxygen Gas Management System (GMS) connecting Stage-1 and Stage-2, and capable of pressurizing and controlling Stage-2 pressure vessel.

A two circuit Gas Management System (GMS) was developed. Circuit-1 was the lower pressure circuit with a maximum operating pressure of 200-psig of pure oxygen (>99.99%). Circuit-2 was the higher pressure circuit with a maximum operating pressure of 3200-psig (pressure relief valve set point). Circuit-2 included the high-pressure plumbing hardware connected directly to the 3000-psig pressure vessel. This circuit was not intended for high-purity oxygen. However, all circuit-2 plumbing was cleaned for oxygen service. Circuit-2 included an oxygen booster pump capable of 2200-psig and connected to a standard commercial oxygen cylinder for pre-charging the pressure vessel, and a nitrogen booster pump capable of 4500-psig and connected to a standard commercial nitrogen cylinder for pre-charging the pressure vessel. The GMS is shown in Figure 2.4.

Circuit-1 was connected to the CFC Stage-1 COG and able to supply pure oxygen (>99.99%) to the Stage-2 stack located inside the pressure vessel. Circuit-2 included high-purity oxygen surge tank system with an array of semi-polished (minimize wetted surface area) stainless steel tanks.

All valves, gages and other parts of the GMS were labeled (see Figure 2.4) to match the associated P&ID.

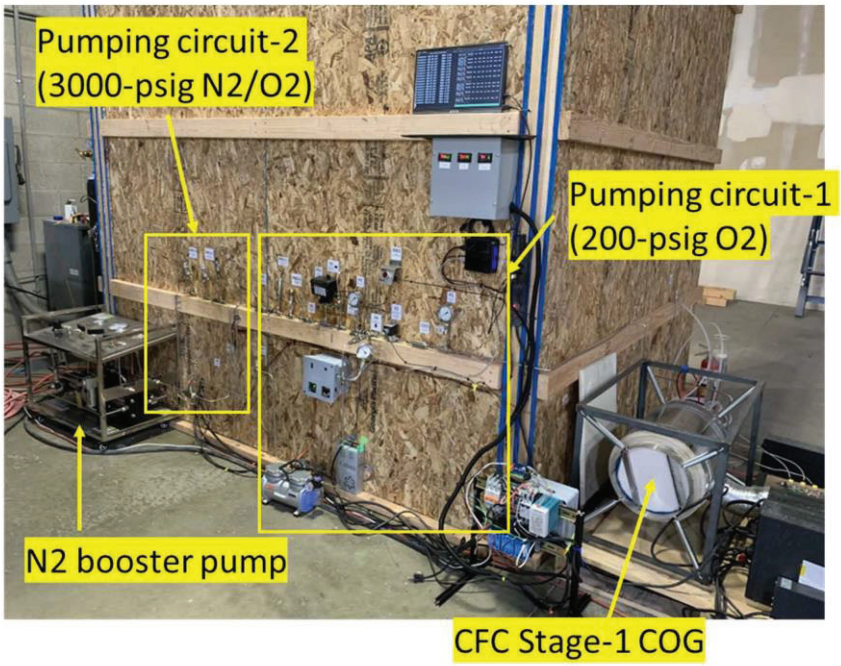

Figure 2.4: Gas Management System (GMS) showing circuit-1 (200-psig pure O2), and circuit-2 (3000-psig N2/O2 mixed gas).

Subtask 41.5 - Operation of these various subsystems in order to demonstrate solid state compression (no moving parts) of oxygen against a back pressure of 3000-psig.

Pure oxygen produced by the 30-cell Stage-1 COG-C (S1) module was supplied at a nominal pressure of 30-psig to the 1-cell Stage-2 COG-C stack (S2) positioned inside the high-pressure vessel.

A series of system shakedown tests were conducted over a period of two weeks followed by operation of the pathfinder 1-cell Stage-2 COG-C stack (S2). A plot of vessel pressure vs time for the later portion of shakedown testing and operation of the S2 pathfinder is shown in Figure 2.5. The figure does not show the entire duration of shakedown testing because a very tight schedule for Task 42 required some shakedown testing to begin before full capability to digitally record the data was complete. During the early portion of shakedown testing, data was recorded manually. Shakedown testing began 10/8/2023 that included ramping up the S2 pathfinder stack to a nominal 600C and a nominal 400-psig air in the vessel.

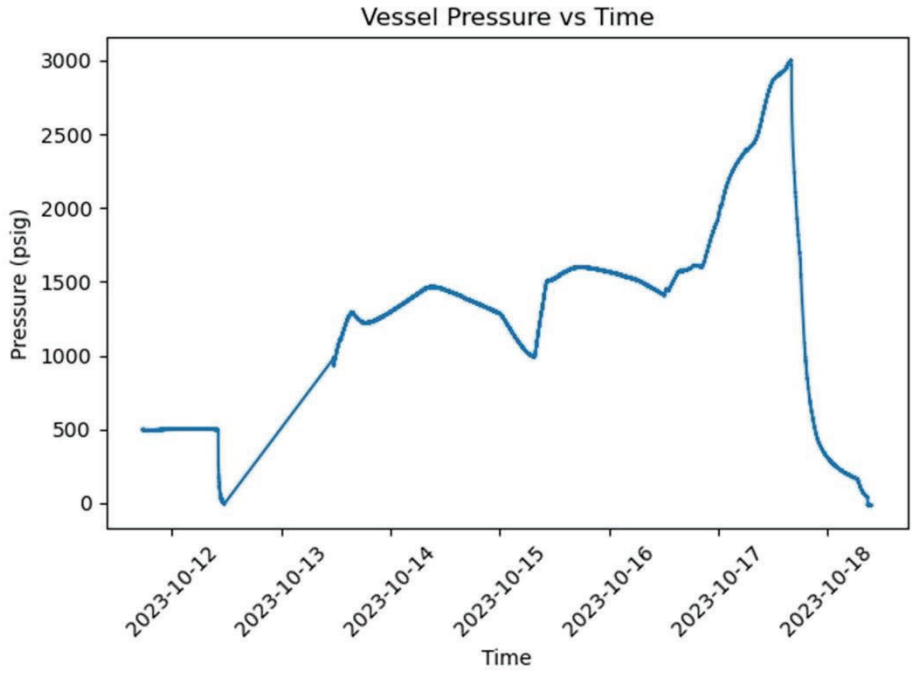

Figure 2.5: Vessel pressurization plot for the period of 10/12/2023 through 10/18/2023 and including the execution of the 3000-psig Stage-2 COG-C demonstration on 10/17/2023. Data prior to 10/12/2023 was not available because the parallel fabrication of the high-presssure plumbing circuit, including the installation of the pressure transducer, had not been completed.

Solid state compression of oxygen gas against a back pressure 3000-psig N2/O2 mixed gas was demonstrated successfully on 10/17/2023. An annotated plot of vessel pressure vs time is shown in Figure 2.6.

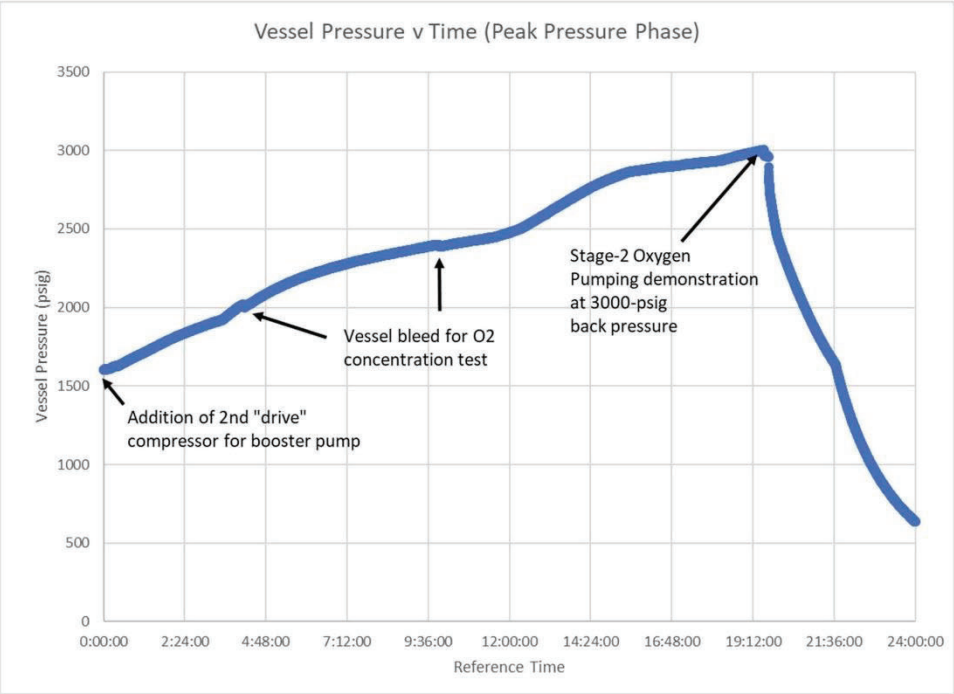

Figure 2.6: Vessel pressurization plot detail for 24-hrs surrounding the execution of the 3000-psig Stage-2 COG-C demonstration on 10/17/2023. The data begins following the installation of a second air compressor needed to drive the high-pressure boost compressor to reach the 3000-psig target.

Test Sequence (Steps):

1- Ramp vessel pressure to 3000 psig with flow to S2 shut-off. In this condition the pressure inside the S2 equals vessel pressure due to leak in S2 stack/internal-plumbing assembly
2- Operate S2 in reverse (pump O2 from vessel into S2 stack/internal-plumbing assembly) to fill the buried cell electrode (cathode in normal forward operating mode; anode in reverse operating mode) with pure O2 at a pressure equal to vessel pressure.
3- Open S1-to-S2 plumbing line. This immediately vents all gases from the interior of the S2 stack, and high-pressure (3000-psig) vessel gas begins to vent via the same plumbing path due to a leak in the S2 stack/internal-plumbing assembly. At this point, the S2 stack is submerged in mixed gas (~86% N2 + ~14% O2) at 3000-psig, and the interior of S2 stack is filled with pure O2 at ambient pressure (~12.5 psia).

4- Reverse the DC polarity applied to the S2 stack. This results in the immediate reversal of the O2 pumping direction of the S2 stack and oxygen gas inside the buried cathode (the internal electrode of the cell) was pumped from inside of the S2 to outside the cell. Video record showed the forward bias cell current (oxygen ion flux from inside the cell to outside the cell) spiked exactly as expected and then began to decay as the buried cathode (internal electrode) was quickly depleted of oxygen at low pressure. There are only two possibilities to explain forward bias current flow through the S2 cell; 1) the flow of current is the result of ionic oxygen flux through the thin ceramic membrane of the cell from the low pressure buried cathode to the high pressure external anode of the S2 cell, or 2) electronic current flow through the S2 cell in the form of an electronic short. In the case of the S2 stack/cell there two possibilities can be distinguished by observing the change in forward bias current flow as a function of time. If current flow was the result of ionic oxygen flux through the ceramic membrane, the available oxygen in the buried cathode would be quickly depleted and the cell would become "polarized" or oxygen staved at the cathode. If the current flow was due to an electronic short circuit of the S2 stack/cell, the current would remain fixed. Definitive proof that the pathfinder 1-cell S2 stack pumped oxygen in the forward bias direction (from the buried cathode at low pressure to the external anode at high pressure) was demonstrated by the rapid decrease in S2 cell current moments after reversing the polarity of the cell and pumping in the forward bias direction. This is documented by the data in Table 2.1.

Table 2.1

Ref. Time (m:ss)	Step	Vessel Press. (psig)	Vessel O2 Conc.	S2 Cell Current (mA)	S2 O2 Pumping Rate (sccm)	S2 Applied Voltage (mV)	S2 Internal Press. (psig)	S2 Internal O2 Conc.	S2 Back EMF (mV)	S2 Temp (C)
0:00	1	3000	14%	n/a	n/a	n/a	3000	90%	n/a	600
Apply DC reverse bias (pump from outside of cell to inside)										
0:01	2	3000	14%	625	2.35	-600	3000	90%	35	600
5:00	2	3000	14%	625	2.35	-600	3000	100%	37	600
Vent pressure inside S2 cell and plumbing circuit to S1										
5:01	3	3000	14%	620	2.33	-600	1000 (est)	100%	16	600
5:07	3	3000	14%	590	2.22	-600	5	100%	-60	600
Apply DC forward bias (pump from inside of cell to outside), Pump O2 into 3000 psig vessel										
5:08	4	3000	14%	691	2.6	600	5	100%	-60	600
5:09	4	3000	14%	637	2.4	600	5	90% (est)	-62	600
5:10	4	3000	14%	573	2.16	600	5	60% (est)	-70	600
5:15	4	2970	14%	531	2	600	5	20% (est)	-90	600

Test complete								

3- Conclusions & Recommendations

Task 42 was completed successfully. It was the first recorded demonstration of production and compression of oxygen at 3000-psig back pressure using solid state COG-C technology featuring a thin (<100 micron) ceramic membrane. A very important observation was the fact COG-C cell had a very thin membrane. The overall engineering of the Stage-2 COG-C cell enable this thin ceramic membrane to maintain mechanical integrity despite a 3000-psig pressure differential. The given success was achieved with a single cell Stage-2 device that was the pathfinder cell for the task. Many valuable lessons were learned under Task 42 that would enable future subsequent Stage-2 stacks to operating at higher operating conditions and it is expected the oxygen flux through the Stage-2 cell could be increase by over 10X without the need to redesign the cell.

It is recommended that Two-Stage COG-C test vehicle be used to test a multi-cell Stage-2 stack at operating current up to 20 amps, which could lead to the demonstration of a Stage-2 stack producing well over 2-slpm ultra-pure oxygen (>99.9999%) at 3000-psig.

Appendix E. Notes about Regulatory Processes and Standards for Oxygen Supply in Piped Medical Systems

Description of this Appendix:
These notes summarize a series of phone call interviews of Mark Allen, Canadian Representative to ISO Technical Committee 121 – Subcommittee 6. The most recent interview was conducted November 28, 2023. These notes were prepared by John Graf, reviewed and edited by Mark Allen.

Technical Notes:
To permit M-COG to be widely used as a production method for medical oxygen in centrally piped hospital systems, there are three main milieus to consider. The United States, the European Union and Canada, which each have a distinct regulatory process for ensuring the safety and effectiveness of medical oxygen in these systems. In all three cases, there are in two parts: the first governs the pharmaceutical "Oxygen", and the second governs the componentry, construction and operating characteristics of the source equipment.

In both the U.S. and Canada, oxygen is considered a pharmaceutical, governed by the United States Pharmacopeia (USP). The USP has two "monographs" for medical oxygen:

- "Oxygen" with a specified concentration ≥ 99.0%, conventionally produced by cryogenic air separation and;
- "Oxygen 93" with a concentration of 93.0 +/- 3.0, produced by zeolite based concentrators using Pressure Swing Adsorbtion (PSA).

Minor constituents are identical between these two and are primarily carbon monoxide and carbon dioxide.

In Canada, the system aspect is governed by the Canadian Standards Association CSA Z-7396-1:22 "*Medical gas pipeline systems — Part 1: Pipelines for medical gases, medical vacuum, medical support gases, and anesthetic gas scavenging systems*". This in turn is enforced through the Standards Council of Canada (SCC) who credentials commercial verifiers. An oxygen system in a Canadian hospital must be inspected by one of these verifiers under provincial regulation typically referenced through the building code. Health Canada (the Canadian equivalent of FDA) works with the SCC but does not involve itself with these systems.

In a centrally piped hospital system using zeolite based concentrators (PSA) oxygen but also buying oxygen in cylinders for the backup reserve (very much the typical scenario) these two monographs could mix. In this scenario, any concentration between 90 and 99 percent could be present in the pipeline. Clearly, since 90% is clinically acceptable, by definition a concentration higher than that must also be acceptable. The CSA-Z-7396-1 allows for this possibility using a concept of "90-plus" at the discretion of the facility's pharmacist.

In the United States, the physical configuration and operation of centrally piped oxygen systems is defined by the NFPA 99 2021 "*Healthcare Facilities Code*". As in Canada, the Code is largely enforced by credentialled verifiers, but there is no central credentialling agency like SCC.

The NFPA 99 does not explicitly recognize the "90 plus" concept, but also makes no special reference or prohibition to the practice of backing up a PSA concentrator with standard oxygen cylinders.

As in Canada, the FDA also has not involved itself in on site production but has historically left that aspect to regulation by the NFPA. As a result, they have never issued any formal ruling on the subject of concentrators as central sources. Producers of oxygen via cryogenic air separation processes are required to meet the USP Oxygen monograph (99.0%) and

are monitored by the FDA as pharmaceutical producers. The mixing of oxygen from the two monographs would normally be prohibited, which is likely to require FDA to undertake some action to clarify it's position on the use of zeolite based concentrators and oxygen 93 in this application.

As a spur to this action, NFPA 99 does include complete guidance for the configuration and operation of a concentrator based central supply source.

The european situation is slightly more complex. There, the pharmacopeia used is the European Pharmacopeia, and the standard for the systems is the ISO 7396-1: 2016 "*Medical gas pipeline systems — Part 1: Pipeline systems for compressed medical gases and vacuum*"

At this time, the European pharmacopeia differs from the USP in two essential aspects: it requires Oxygen be at a concentration of ≥99.5%, and it defines it as produced by cryogenic separation. It does also include a monograph for Oxygen 93 at between 90 and 96% and will soon include another for Oxygen 98% (also produced using a PSA process with two stages of separation).

As can be readily seen, the problem is the same as with USP in that there is no single monograph for the range 90-99, and the issue of mixing monographs is if anything more complex in some countries than in the U.S.

As with the NFPA and the CSA, the ISO 7396-1 includes everything required to configure and install a concentrator based central supply source in a facility. Unlike NFPA and CSA, it currently defines that supply source as producing Oxygen 93 only. Since the document is now in revision, it is expected that this limitation will disappear in the next edition.

The European Union is now in the process of converting to it's new regulatory framework for medical devices, the EU 2017/745 Medical Device Regulation (MDR). Under this regulation, oxygen concentrators in the EU are being classified as Class IIa. Therefore, they are subject to regulation as a medical device and their manufacturers as device manufacturers. As the EU MDR is being looked at and adopted around the world by medical regulators, it is important to the long term prospects of the M-COG.

This is not yet done in the U.S. by FDA or in Canada by Health Canada. Concentrators for central supply sources have not been addressed by FDA, although small domiciliary concentrators (e.g. for home care) have been. It is reasonable to expect this situation will change, but in what direction is not now clear. Health Canada appear to be content with the present regulatory situation, but would probably follow FDA in the event a ruling was issued.

Mr. Mark Allen, who sits the CSA Technical Subcommittee on medical gas systems (which writes the CSA Z7396-1), the NFPA Technical Committee on Piping Systems (which writes the NFPA 99) and serves as Canadian Representative to the ISO Technical Committee 121 / Subcommittee 6 (which writes the ISO 7396-1) has reviewed M-COG technology in light of how it might fit within these three current regulatory frameworks.

Mr. Allen's assessment must be understood to be unofficial, as he is not entitled to speak for any of these committees or regulatory bodies.

Mr. Allen's assessment is that M-COG demonstrably produces oxygen superior to the requirements of any of the pharmacopeial monographs. Therefore, with the exception of the European Pharmacopeia, there is no barrier to the use of the technology from a patient use / pharmaceutical perspective. The only limitation in the European Pharmacopeia is that the monograph also defines means of production, which in ill disposed minds could be used as an obstruction.

In the CSA Z 7396-1 and the NFPA 99 standards, an M-COG of the correct output capability could be used as a direct "drop in" replacement for a zeolite based concentrator . As the standards exist now, the M-COG would require the same monitoring and quality control devices as a PSA machine, but would be entirely functional and compliant in the context.

In the ISO standard, this would not yet be the case. Since the ISO standard defines a concentrator as a device producing Oxygen 93, the M-COG does not qualify. As mentioned, he believes this is simply a matter of carrying through changes already proposed and underway for the next edition.

In respect of the position of the M-COG or any other concentrator as a medical device, this is resolved in Europe, where it is a IIa device and the manufacturer will need to comply with all MDR rules and registrations. In the U.S., as FDA has no declared position on the matter, M-COG would neatly resolve the dilemmas facing a facility who wants on site production, which today includes the lower concentration (90% vs. 99%) the variation in concentration (90-96%) and the probability of mixing two different "oxygen" monographs. An M-COG would eliminate all of these.

Summary

- M-COG technology can be used as part of an oxygen generation system that can meet all current Canadian requirements with no changes or additions to Canadian regulatory structure. The Canadian allowance for "90-plus" would become irrelevant with M-COG technology. M-COG can exceed the purity requirements specified for USP Oxygen and properly configured, would readily fit into a source system as specified by CSA Z7396-1:22. In-line analytical chemistry systems similar to those currently used with PSA devices can verify purity. Contingency oxygen systems similar to those currently used with PSA devices can be used to meet fault tolerance requirements. Good manufacturing practice standards can be used to meet quality and reliability requirements. Canadian hospitals also have operational experience using oxygen from different sources.

- M-COG technology can be used as part of an oxygen generation system that can meet all current US requirements with no changes or additions to U.S. regulatory structure. M-COG can exceed the purity requirements specified for USP Oxygen and properly configured, would readily fit into a source system as specified by NFPA 99. M-COG can use in-line analyzers to verify that purity requirements are met.

- If it were decided by FDA to regulate M-COG as a drug manufacturing system, the technology is entirely equal to the requirement – and Good Manufacturing Practices can be cited to meet quality assurance requirements.

- M-COG technology cannot currently be used to meet EU applications that reference the oxygen 0417 monograph in the EU Pharmacopoeia. As it is currently written, 0417 specifies that the oxygen must be produced by air liquefaction.

- Certification of M-COG as a medical device, using the FDA *de novo* device submission process, while not strictly necessary at this writing, is strongly recommended, to facilitate adoption of M-COG and to facilitate acceptance under the EU MDR.

REPORT DOCUMENTATION PAGE

Form Approved
OMB No. 0704-0188

1. REPORT DATE *(DD-MM-YYYY)*	2. REPORT TYPE	3. DATES COVERED *(From - To)*
10/02/2024	Technical Memorandum	

4. TITLE AND SUBTITLE
NESC Ceramic Oxygen Generator (COG) Technology Development

5a. CONTRACT NUMBER

5b. GRANT NUMBER

5c. PROGRAM ELEMENT NUMBER

6. AUTHOR(S)
Graf, John C.; Stevenson, Jeffry W.

5d. PROJECT NUMBER

5e. TASK NUMBER

5f. WORK UNIT NUMBER
869021.01.23.01.01

7. PERFORMING ORGANIZATION NAME(S) AND ADDRESS(ES)
NASA Langley Research Center
Hampton, VA 23681-2199

8. PERFORMING ORGANIZATION REPORT NUMBER
NESC-RP-21-01639

9. SPONSORING/MONITORING AGENCY NAME(S) AND ADDRESS(ES)
National Aeronautics and Space Administration
Washington, DC 20546-0001

10. SPONSOR/MONITOR'S ACRONYM(S)
NASA

11. SPONSOR/MONITOR'S REPORT NUMBER(S)
NASA/TM-20240012679

12. DISTRIBUTION/AVAILABILITY STATEMENT
Unclassified - Unlimited
Subject Category Engineering
Availability: NASA STI Program (757) 864-9658

13. SUPPLEMENTARY NOTES

14. ABSTRACT
The NASA Engineering and Safety Center (NESC) sponsored a project to accelerate the pace of technology development of a ceramic oxygen generator (COG), for NASA and COVID related medical use. NASA applications for this technology include spacesuit oxygen tank recharge, medical applications include providing medical oxygen in remote and low resource settings. During this project, five full-scale (i.e., 30 wafer) cell stacks were built and tested in prototype systems capable of producing pressurized oxygen. System testing measured oxygen product purity, delivery pressure, production rate, and energy use. This report describes ion transport membrane mechanisms, cell stack configuration, and test results.

15. SUBJECT TERMS
Oxygen; Ion Transport Membrane; Ceramic; Oxygen Generation; Life Support Systems

16. SECURITY CLASSIFICATION OF:			17. LIMITATION OF ABSTRACT	18. NUMBER OF PAGES	19a. NAME OF RESPONSIBLE PERSON
a. REPORT	b. ABSTRACT	c. THIS PAGE			STI Help Desk (email: help@sti.nasa.gov)
					19b. TELEPHONE NUMBER *(Include area code)*
U	U	U	UU	101	(443) 757-5802